HARMONIC ANALYSIS OF A SOLAR PV INTEGRATED IEEE 9 BUS SYSTEM

THESIS

SUBMITTED IN PARTIAL FULFILLMENT OF THE REQUIREMENT FOR THE AWARD OF THE DEGREE OF

MASTER OF TECHNOLOGY
IN
ENERGY SCIENCE AND TECHNOLOGY

Submitted by
PREMJIT CHAKRABORTY
EXAM Roll No: M4ENR22006

UNDER
SUPERVISION OF
Prof. (Dr.) RATAN MANDAL

Course affiliated to
FACULTY OF ENGINNERING AND TECHNOLOGY
Under
FACULTY OF INTERDISCIPLINARY STUDIES, LAW & MANAGEMENT
JADAVPUR UNIVERSITY
KOLKATA-700032
2022

BONAFIDE CERTIFICATE

Certified that this thesis report "HARMONIC ANALYSIS OF A SOLAR PV INTEGRATED IEEE 9 BUS SYSTEM" is the bonafide work of PREMJIT CHAKRABORTY (Examination Roll No. - M4ENR22006 and Registration No. : 154599 of 2020-2021) who carried out the thesis work under my supervision. Certified further, that to the best of my knowledge the work reported herein does not form part of any other thesis report or dissertation on the basis of which a degree or award was conferred on an earlier occasion on this or any other candidate. I hereby recommend that the thesis be accepted in partial fulfilments for Post Graduate Degree of Master of Technology in Energy Science and Technology during the academic session 2020-2022.

…….
Prof. (Dr.) RATAN MANDAL

THESIS SUPERVISOR

DIRECTOR

SCHOOL OF ENERGY STUDIES

JADAVPUR UNIVERSITY

KOLKATA-700032

…….

DEAN

FACULTY COUNCIL OF INTERDISCIPLINARY STUDIES, LAW & MANAGEMENT

JADAVPUR UNIVERSITY

KOLKATA-700032

CERTIFICATE OF APPROVAL

The forgoing thesis is hereby approved as a credible study of a technological subject carried out and presented in a manner satisfactory to warrant its acceptance as a perquisite to the Post Graduate Degree of Master of Technology in Energy Science & Technology for which it has been submitted. It is understood that by this approval the undersigned person does not necessarily endorse or approve any statement made, opinion expressed or conclusion drawn therein but approve the thesis only for the purpose for which it has been submitted.

_____

_____

Committee of final examination for Evaluation of Thesis

CANDIDATE'S DECLARATION

I hereby certify that the work which is being presented in the thesis entitled "HARMONIC ANALYSIS OF A SOLAR PV INTEGRATED IEEE 9 BUS SYSTEM" by "PREMJIT CHAKRABORTY" in partial fulfilment of requirements for the award of degree of M.Tech. In Energy Science & Technology submitted in the School of Energy Studies at JADAVPUR UNIVERSITY, KOLKATA, is an authentic record of my own work carried out during a period from 2021 to 2022 under the supervision of Prof. (Dr.). Ratan Mandal and Subhajit Mukherjee. The matter presented in this thesis has not been submitted by me in any other University / Institute for the award of M.Tech Degree.

All information in this document have been obtained and presented in accordance with academic rules and ethical conduct.

I also declare that as required by these rules and conduct, I have fully cited and referenced all materials and results that are not original to these work.

NAME: PREMJIT CHAKRABORTY

EXAM ROLL NO: M4ENR22006

THESIS TITLE: HARMONIC ANALYSIS OF A SOLAR PV INTEGRATED IEEE 9 BUS SYSTEM.

SIGNATURE:

DATE:

ACKNOWLEDGEMENT

I express my sincere gratitude to Prof. (Dr.) Ratan Mandal and Subhajit Mukherjee, School of Energy Studies, Jadavpur University, Kolkata, India, for their stimulating guidance, continuous encouragement and supervision throughout the course of present work. I also wish to extend my thanks to Prof. (Dr.) Tushar Jash and other colleagues for attending my seminars and for their insightful comments and constructive suggestions to improve the quality of this research work. I would like to thank all my friend, seniors and fellow batch mates who supported me and encouraged me all time.

Last but not the least, I would like to thank my parents and my grandparents for moral encouragement and all family members for their support.

ABSTRUCT

In this project, analysis of harmonics of a Solar PV integrated IEEE 9 bus system has been done. Solar energy integration with non-renewable sources is very helpful since it lowers the rates of using non-renewable resources thus decreasing dependency on fossil fuels. Integration technology has become crucial for the world's energy requirements. Solar system attributes for integration, advantages of solar-grid integration, existing solar-grid integration methods, and impacts has also been discussed. This project will support the incorporation of solar-grid technology in future projects.

Load flow analysis has been performed by using adaptive Newton Rapson method by taking standard IEEE 9 bus system. After that Solar PV has been integrated at 3 load buses one by one and recorded the performance of the load buses due to each integration. After that harmonic load flow has been analysed and spectrums and corresponding waveforms has been captured. So, in this project the objective was to do harmonic analysis of the IEEE 9 bus system by integrating solar PV and alternator of the same rating and check the performance for each case. After examining a variety of features of solar PV grid integration from earlier works, including how it functions and how different performance factors impact the output and general effectiveness of the PV system. Numerous distortions, including VDF, THD and form factor alterations are brought on by the harmonics in the system. As a result, the system's overall effectiveness changes. Thus, working on the system's harmonic analysis component can be done. It will be based on ETAP simulation, and standard ratings can be used to improve it.

After that, minimum and maximum rating PV systems and alternators has been taken and voltage spectrum with respect to harmonic orders and harmonic waveforms with respect to time has been analyzed. For further improvement of this work, it can be implemented in large systems that means 33 buses or 66 buses can be used instead of 9 bus system. Various types of other renewable energies like wind energy, biomass etc. can be integrated to this system by analyzing performance and quality of the power to meet the load requirements based on their positions and capacity in the bus system.

List of Figures

Sl. No.	Figure No.	Description	Page No.
1	1	Energy Consumption by top 10 Energy consuming countries	13
2	2	Schematic of solar PV integration in a grid system	23
3	3	Standard IEEE 9 Bus System	25
4	4	Capability Curve of generator 1	27
5	5	Rating of generator 1	28
6	6	Impedance of generator 1	28
7	7	Capability Curve of generator 2	29
8	8	Rating of generator 2	30
9	9	Impedance of generator 2	30
10	10	Capability Curve of generator 3	31
11	11	Rating of generator 3	32
12	12	Impedance of generator 3	32
13	13	Rating of 2 winding transformer	34
14	14	Impedance of 2 winding transformer	34
15	15	Harmonic spectrum of 2 winding transformer output	35
16	16	PV Cell Working Principle	36
17	17	The ratings and P-V curve	37
18	18	Load flow analysis of an IEEE 8 bus system	45
19	19	Three Phase full Bridge Inverter	46
20	20	Rating of Inverter	48
21	21	Flowchart of the Experimental Procedure	50
22	3.1	IEEE 9 BUS system	52
23	18.1	Load Flow Analysis	53
24	22	Rating of 33 MW PV system	54
25	23	Load Flow Analysis by integrating Solar PV	55
26	24	Load Flow Analysis by integrating synchronous generator	58
27	25	Harmonics spectrum in static loads	59
28	26	Harmonic load flow by integrating solar PV	59
29	27	Harmonic load flow by integrating alternator	60
30	28.1	217.5 MW supply from PV system to BUS 8	61
31	28.2	132 MW supply from alternator to BUS 8	62
32	29.1	108.5 MW supply from solar PV to BUS 5	62
33	29.2	132 MW supply from alternator to BUS 5	63
34	30.1	108.46 MW supply from solar PV to BUS 6	63
35	30.2	132 MW supply from alternator to BUS 6	64

36	28.3	Voltage Spectrum for 33 MW PV integration at BUS 8	64
37	28.4	Voltage Spectrum for 33 MW alternator integration at BUS 8	65
38	28.5	Harmonic waveforms for 33 MW solar PV integration at BUS 8	65
39	28.6	Harmonic waveforms for 33 MW alternator integration at BUS 8	66
40	29.3	Voltage Spectrums for 33 MW solar PV integration at BUS 5	66
41	29.4	Voltage Spectrums for 33 MW alternator integration at BUS 5	67
42	29.5	Harmonic waveforms for 33 MW solar PV integration at BUS 5	67
43	29.6	Harmonic waveforms for 33 MW alternator integration at BUS 5	68
44	30.3	Voltage spectrum for 33 MW solar PV integration at BUS 6	68
45	30.4	Voltage spectrum for 33 MW alternator integration at BUS 6	69
46	30.5	Harmonic waveforms for 33 MW solar PV integration at BUS 6	69
47	30.6	Harmonic waveforms for 33 MW alternator integration at BUS 6	70

List of Tables

Sl. No.	Table No.	Description	Page No.
1	5.1	Effect of PV system and alternator integration at BUS 8	56
2	5.2	Effect of PV system and alternator integration at BUS 5	57
3	5.3	Effect of PV system and alternator integration at BUS 6	57

NOMENCLATURE:

A	Ampere
AC	Alternating Current
DC	Direct Current
KWp	Kilowatt Peak
PF	Power Factor
PV	Photovoltaic
VDF	Voltage Distortion Factor
THD	Total Harmonic Distortion
FF	Form Factor
VA	Volt- Ampere
V	Volt
W	Watt
KV	Kilo Volt
MW	Mega Watt

CONTENT

Bonafide Certificate *2*
Certificate Of Approval *3*
Candidate's Declaration *4*
Acknowledgement *5*
Abstruct *6*
List Of Figures *7*
List Of Tables *8*
Nomenclature: *9*
Chapter 1: INTRODUCTION: **12**
1.1 BACKGROUND: **12**
1.2 ENERGY SCENARIO: **12**
1.3 RENEWABLE AND NON-RENEWABLE ENERGY: **13**
1.4 NON-RENEWABLE ENERGY AND ENVIRONMENTAL ISSUES: **14**
1.5 SOLAR POWER AND ITS INTEGRATION: **14**
1.6 AIM AND OBJECTIVE OF PRESENT WORK: **15**
1.7 SCOPE OF PRESENT WORK: **15**
1.8 CONCLUSION: **15**
Chapter 2: REVIEW OF PREVIOUS WORK: **16**
2.1. INTRODUCTION: **16**
2.2. REVIEW OF EARLIER WORK: **16**
2.3. GAP OF KNOWLEDGE: **22**
2.4. POSSIBLE SOLUTIONS: **23**
2.5. SYNOPSIS OF THE WORK: **23**
2.6. CONCLUSION: **24**
Chapter 3: THEORIES ON IEEE 9 BUS SYSTEM **25**
3.1. INTRODUCTION: **25**
3.2. COMPONENTS OF IEEE 9 BUS SYSTEMS: **25**
3.3. SYNCHRONOUS GENERATOR: **26**
3.4. 2 WINDING TRANSFORMER: **33**

3.5. SOLAR PHOTOVOLTAIC SYSTEM: 35
3.6. CONCLUSION: 37
Chapter 4: PRESENT RESEARCH METHODS 38
4.1. INTRODUCTION: 38
4.2. NEWTON RAPHSON METHOD: 38
4.3. NEWTON RAPHSON METHOD FOR LOAD FLOW ANALYSIS: 38
4.4. 3 PHASE FULL BRIDGE INVERTER: 46
4.5. HARMONIC ANALYSIS: 48
4.6. CONCLUSION: 49
Chapter 5: SYSTEM DESCRIPTION AND EXPERIMENTAL PROCEDURE: 50
5.1. INTRODUCTION: 50
5.2. SYSTEM DESCRIPTION: 51
5.3. EXPERIMENTAL PROCEDURE: 51
5.4. CONCLUSION: 60
Chapter 6: RESULTS AND DISCUSSION 61
6.1. INTRODUCTION: 61
6.2. RESULTS DURING EACH STEP: 61
6.3. DISCUSSION: 70
6.4. CONCLUSION: 71
Chapter 7: CONCLUSION 72
7.1. SUMMARY OF THE WORK: 72
7.2. AVENUES OF THE FUTURE WORK: 72
7.3. CONCLUDING REMARKS: 72
REFERENCES: 73

Chapter 1: INTRODUCTION:

1.1 BACKGROUND:

A network that permits significant integration of photovoltaic (PV) power into the national utility grid is known as solar-grid integration. Now a days, non-renewable energy sources like coal, natural gas, crude oil etc. are producing greenhouse gases which are carbon dioxide, methane, nitrous oxide which are causing global warming and other climate issues. So, to reduce global warming we are trying to reduce our dependency on non-renewable sources by increasing the production of renewable sources like Solar Energy, Wind Energy, Bio Energy, Tidal Energy and these can create an huge impact towards our environment.

1.2 ENERGY SCENARIO:

There are two categories of energy sources: nonrenewable and renewable. Fossil fuels and nuclear materials are examples of nonrenewable resources that are taken from the earth and can eventually run out. The majority of energy in the modern age has been produced from these resources.

Resources that replenish as quickly as they are consumed and are always available include wind, water, solar, and geothermal energy. Some are refilled each growing season, such as biofuel made from plants and food crops. Renewable energy sources have gained in popularity in the early twenty-first century as nonrenewable resources start to run out.

Many nations, including China, the United States, Brazil, India, the United Kingdom, Japan, Spain, Germany, France, and Italy, now rely heavily on renewable energy sources. These nations are regarded as the top users of renewable energy worldwide. The top ten countries that use the most renewable energy for 2020 are depicted in Fig. 1 along with their economic performance and consumption of renewable and non-renewable energy.

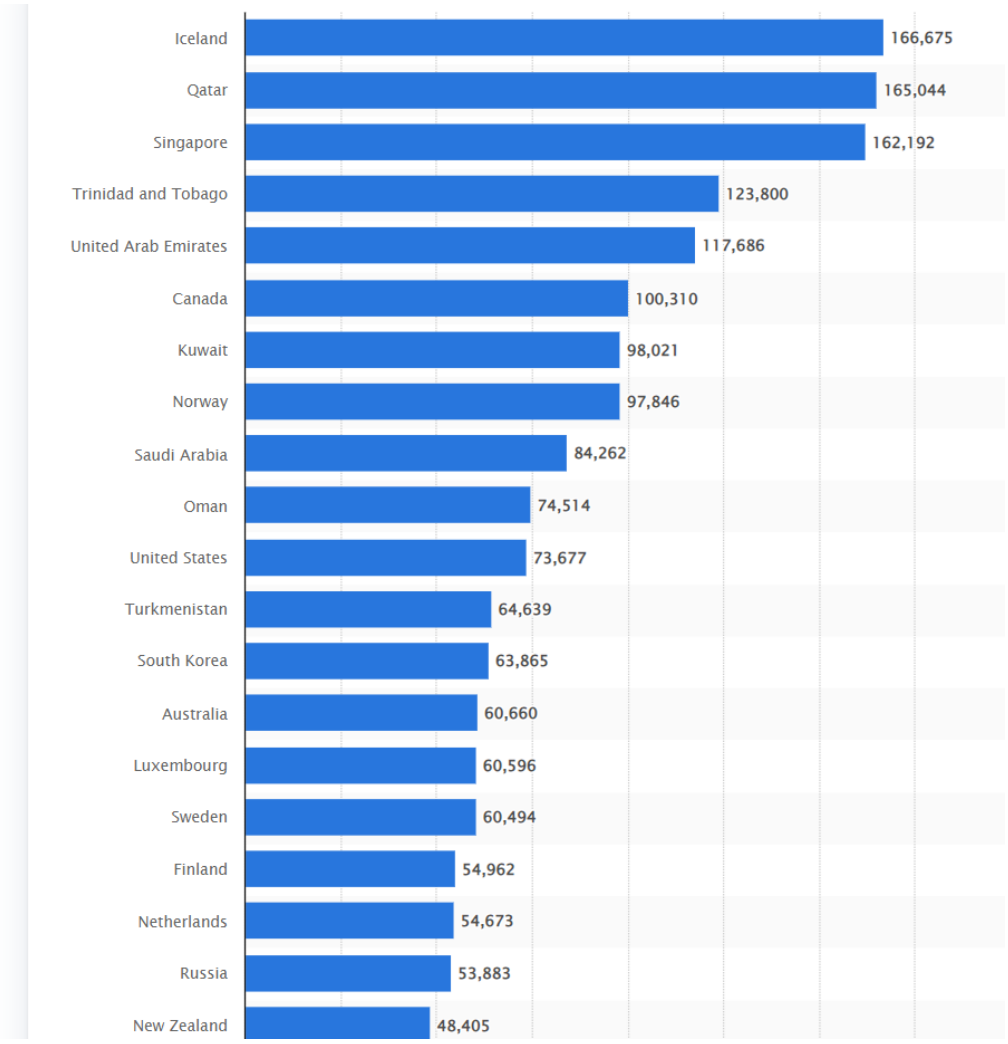

Fig. 1: Energy Consumption per Capita (KWH) By Top 10 Energy Consuming Countries [20]

1.3 RENEWABLE AND NON-RENEWABLE ENERGY:

- Energy can be divided into two main categories: renewable and non-renewable.
- Non-renewable energy sources are in short supply, typically because it takes a while for them to regenerate. These non-renewable resources have the benefit of allowing the power plants that employ them to produce additional power on demand. These are the non-renewable energy sources:
- Coal
- Nuclear
- Oil
- Natural gas

Renewable resources, on the other hand, replenish themselves. The five major renewable energy resources are:

- Solar
- Wind
- Water, also called hydro
- Biomass, or organic material from plants and animals
- Geothermal, which is naturally occurring heat from the earth

Although renewable energy sources have an endless supply in the long run, their availability at any particular time is constrained. The sun, for instance, rises every day, but when it's cloudy, it can only produce so much energy. Another drawback is that power plant operators are unable to increase the output of renewable energy when there is a spike in electricity demand, such as on a hot day when many people are operating air conditioners simultaneously.

1.4 NON-RENEWABLE ENERGY AND ENVIRONMENTAL ISSUES:

Burning fossil fuels like coal, gas, and oil releases heat-trapping gases like carbon dioxide. Climate change is caused by this heat-trapping mechanism, and the current climate crisis is being sparked by the inability to address this issue. Fossil fuels are hydrocarbon-containing substances, such as coal or gas that are present in the Earth's crust and were created from the remains of living things during the Earth's geological history. The vast bulk of greenhouse gas emissions worldwide are caused by these energy sources. According to the most recent study from the Intergovernmental Panel on Climate Change, a group of international scientists empowered by the United Nations, if emissions are left unchecked, the atmosphere might warm by as much as 2.7 degrees Fahrenheit above preindustrial levels by the year 2040.

1.5 SOLAR POWER AND ITS INTEGRATION:

From the calculator powered by a single solar cell to rural dwellings powered by an off-grid rooftop PV system, photovoltaics were initially only employed as a source of electricity for small and medium-sized applications. In the 1980s, the first commercial concentrated solar power facilities were created.

A solar cell, also known as a photovoltaic cell, is a type of electrical appliance that uses the photovoltaic effect, a natural physical and chemical phenomenon, to convert light energy directly into electricity. It is a particular type of photoelectric cell, which is characterised as a device whose electrical properties, such as current, voltage, or resistance, change when exposed to light. The electrical building blocks of photovoltaic modules, also referred to as solar panels, are frequently individual sun cell devices. Whether the source is sunshine or a man-made light, solar cells are referred to as photovoltaic. They are capable of creating energy as well as acting as photodetectors (such as infrared detectors), which may detect light or other electromagnetic radiation in the visible range or measure the intensity of light.

Since that time, grid-connected solar PV installations have increased roughly exponentially as the price of solar electricity has decreased. Gigawatt-scale solar power plants and millions of

installations have both been and are being constructed. The most affordable source of electricity in history will be provided by solar photovoltaic technology by 2020.

1.6 AIM AND OBJECTIVE OF PRESENT WORK:

A standard IEEE 9 Bus system was taken. The system consists of

- 3 synchronous alternators with swing modes
- 3 transformers
- 3 static load

In this project, the reports which has been recorded are:

1 Load flow of the IEEE 9 BUS system.
2 Effect of each PV integration at the load buses.
3 Harmonic analysis for each integration whether it is solar PV or synchronous alternator.

Load flow analysis has been performed by using adaptive Newton Rapson method. After that Solar PV has been integrated at 3 load buses one by one and recorded the performance of the load buses due to each integration. After that harmonic load flow has been analysed and spectrums and corresponding waveforms has been captured. So, in this project the objective was to do harmonic analysis of the IEEE 9 bus system by integrating solar PV and alternator of the same rating and check the performance for each case.

1.7 SCOPE OF PRESENT WORK:

Reading the aforementioned papers, I noticed that grid-connected photovoltaic (PV) systems have emerged as a competitive alternative in low-voltage (LV) networks as a result of the introduction of lucrative policy frameworks like metering and a significant decrease in the cost of PV system installation. As a result, it is anticipated that many rooftop solar PV systems will be linked to utility grids in the upcoming years. However, there is a lack of understanding regarding harmonic analysis of solar PV. As much as possible from the papers and other resources, I have read about the performance parameters and developing techniques. I want to work on the solar PV system's harmonic analysis while it is linked to the grid.

1.8 CONCLUSION:

Grid-connected home PV systems typically range in size from small to medium (1 to 15 kWp) compared to the distribution grid's high short-circuit levels. Therefore, when a single PV system is connected to the grid, voltage distortion in the system is essentially nonexistent. Harmonic analysis makes it easier to incorporate grid-connected solar PV into the power system for efficient operation. Several studies have been conducted over the past few years to evaluate the harmonic affects caused by grid-connected solar PV installations. I have therefore chosen to focus on the harmonic analysis of the solar PV grid integration. The potential for clean energy in the near future is greatly increased by this section.

Chapter 2: REVIEW OF PREVIOUS WORK:

2.1. INTRODUCTION:

Solar energy integration into non-renewable sources is important as it lowers the rates of consuming non-renewable resources thus reduces dependence on fossil fuels, the world's energy requirements have imposed significant need for different methods by which energy can be produced or integrated.

PV technology can also be employed for small-scale generation systems. It is mostly used for household solar water heating. However, the majority of African nations receive a significant amount of intense sunlight each year, which may be used to generate power. Africa is therefore exceptionally abundant in solar radiation. The deserts of North and West Africa, including Egypt, Nigeria, and some regions of Southern and East Africa, are notable regions because they receive extended periods of sunshine with a very high intensity of irradiation. [18]

2.2. REVIEW OF EARLIER WORK:

K.N. Nwaigwe et al. described in the paper "An overview of solar power (PV systems) integration into electricity grids" that In addition to the fact that solar energy integration into non-renewable sources is important as it lowers the rates of consuming non-renewable resources thus reduces dependence on fossil fuels, the world's energy requirements have imposed significant need for different methods by which energy can be produced or integrated. Both the solar system side and the utility side handle integration concerns and interoperability between the two systems (solar and grid generating). This review will assist in implementing solar-grid integration in future projects without duplicating the obvious difficulties faced in existing projects and provide information on the viability of solar-grid integration for academics and scientists. [1]

Amine Allouhi et al. described in the paper " A novel grid-connected solar PV-thermal/wind integrated system for simultaneous electricity and heat generation in single family buildings" that It is crucial to create new integrated renewable energy systems that are grid-connected for use in sustainable home construction. This study aims to evaluate the energy, financial, and environmental performance of an unique grid-connected renewable energy system made up of wind turbine, sensible heat storage, and solar hybrid PV-Thermal collectors. The economic analysis of the suggested configuration showed that its Net Present Cost (NPC) is lower by 20.7 percent, 10.7 percent, and 11.5 percent compared to grid only, PV-T only, and wind only scenarios, respectively, than three other power supply scenarios. As a result, the new method offers encouraging development prospects, particularly because it also enables a reduction of up to 54% in annual CO2 emissions when compared to the traditional energy supply mode that solely relies on the electric grid.

The rise of industry and the improvement of living standards are expected to result in a major increase in energy needs. The global energy system is still dependent on fossil fuels, which are in

large part to blame for the substantial volumes of greenhouse gases that are causing environmental deterioration. This is true despite all the progress made to transition towards cleaner energy generation technologies. In addition to harming the environment, the energy expenses associated with these traditional power production methods strain the budgets of all nations, but especially those with limited fuel sources. Resources for producing energy from renewable sources are thought to be excellent alternatives to conventional energy sources. Top among the currently developed renewable energy sources are solar and wind energy. Both technologies have bright futures, especially given the notable reductions in production costs, better reliability. A constant and irregular flow of energy is mandated by the contemporary power industry. Alternatives like solar and wind are characterized by their sporadic nature, which makes production and consumption incompatible. The problem makes it extremely difficult to integrate these sources into the existing electrical networks. [2]

Eltawil et al. describes in this paper "Modelling and analysis of grid integration for high shares of solar PV in small isolated systems -A case of Kiribati" that Pacific island nation Kiribati is working to integrate more solar PV energy into its national system in order to lessen its unsustainable reliance on imported fossil fuel. However, this can present technological difficulties for the small, isolated system's dependable performance. A technical analysis was done in this work to look into the effects the pipeline of grid-connected PV systems will have on Kiribati's Tarawa power system. Variations in PV production and the necessary spinning reserves to make up the lost power were examined. The PowerFactory programmer was used to model the utility network. [3]

Fu Wang et al. describes in this paper "Performance of solar PV micro grid systems: A comparison study" that the power conditioning system, energy storage, loads, and energy management and control system are the main components of the micro-grid. These micro-grid systems are designed to promote the use of renewable energy while lowering running expenses in accordance with demand response and market electricity prices. We initially described the layout, parts, and structures of the micro-grid systems in this essay. To evaluate their performance, a thorough comparison of the PV systems and a streamlined operation plan were carried out. [4]

Alanazi et al. describes in the paper "Co-optimization generation and transmission planning for maximizing large scale solar PV integration" that Solar photovoltaic (PV) systems have had exceptional growth at both the household and utility sectors in recent years, making them the renewable energy source with the fastest growth in the United States. Some states plan to meet a target renewables portfolio standard (RPS) in the near future, which would require utilities to guarantee that a portion of the electricity they sell comes from renewable energy sources. Planning for the growth of generation and transmission systems has some similarities to the idea of capacity expansion models. With assumptions about future power demand, fuel prices, technology cost and performance, policy and regulation, and technology, capacity expansion models try to simulate generating and transmission capacity investment. [5]

Almakhles et al. describes in the paper “Solar PV network installation standards and cost estimation guidelines for smart cities” that the PV market has experienced substantial expansion as a result of the increased concern over climatic changes and alternate energy sources. China and Japan are the Asian nations that have the largest worldwide PV market share. The increase in the use of PV for electric generation on both a large and small scale was sparked by the subsidies, incentives, and low lending rates offered by several countries, like as India. Additionally, this has encouraged significant investment in PV installations. The solar PV installation can be split into two types, Low power and High power. Rooftop and microgrid installations of low power PV systems are typical, with the consumer investing mostly for self-consumption and maybe feeding any extra power back to the grid. The main goal is to maintain a steady supply of electricity or make a concerted attempt to switch to green energy. Large PV farms, on the other hand, are largely for profit and are financed by private investors, venture capitalists, and other corporate entities. The American Society of Testing and Materials, or ASTM, has created more than 12,000 international standards to raise product quality and safety. Around 135 different countries' technical and business professionals work together to create ASTM Standards. [6]

Azapagic et al. describes in the paper “Energy self-sufficiency, grid demand variability and consumer costs Integrating solar PV, Stirling engine CHP and battery storage” that in the last ten years, there has been a substantial rise in the market for solar PV in residential buildings, with 138 GW of installed capacity by 2013. Government incentives like Feed-in Tariffs (FITs) and the quick decline in manufacturing costs have been the driving forces behind this. The ramping demands of variable load power plants, like combined cycle gas plants, are increased by the intermittent and nocturnal nature of PV generation. [7]

Yagli et al. describes in the paper “Operational solar forecasting for grid integration: Standards, challenges, and outlook” that with the increased penetration of renewable energy, solar irradiance and photovoltaic (PV) power forecasting—or solar forecasting—have become crucial components of grid functioning. As a result, over the past ten years, the volume of literature on solar forecasting has grown tremendously. In terms of publications, solar forecasting, the newest and previously smallest subdomain of energy forecasting, has now surpassed price forecasting and is quickly catching up to wind and load forecasting in that regard. [8]

Qiang et al. describes in the paper “Achieving grid parity of solar PV power in China- The role of Tradable Green Certificate” that the development of renewable energy is essential for China's energy transformation and climate change mitigation. Currently, solar photovoltaic (PV) plays a significant role in many nations to replace fossil fuel energy as a major renewable energy source. Solar PV generation capacity in China has significantly increased since the implementation of the feed-in tariffs (FIT) regulation in 2011. By the end of 2018, the cumulative installed capacity of solar PV power had reached 175.03 GW, and the power generation was 177.50 TWh, accounting for 28 percent of China's total renewable energy power. During the years 2009 to 2013, the cumulative capacity of PV power doubled.

Realizing grid parity for Chinese solar PV power has significant implications for the future growth of the energy system and is crucial to meeting the Paris Agreement's National Determined Contribution (NDC) objective for carbon abatement. In this study, we estimate the adoption rate

of solar PV technology in China using empirical data from 541 solar PV power projects between 2010 and 2016. The LCOEs of solar PV power are then computed from 2018 to 2030. Additionally, it is determined whether and when grid parity may be reached in China based on a comparison of the projected LCOEs and the on-grid price of coal-fired power.

The learning rate of solar PV power from 2010 to 2016 is 12.60 percent, per our estimation results. According to this hypothesis, solar PV power could attain grid parity between 2023 and 2025. We determine that the learning rate should be between 17.5 and 20.3% depending on the price of coal-fired power in order to attain grid parity for solar PV power in 2020. However, it is challenging to increase the learning rate in the short term due to the lag effect of technological learning for solar PV generation. Therefore, promoting grid parity before 2020 may still require additional policy instruments. [9]

Bowen et al. describes in the paper "Potential economic value of integrating concentrating solar power into power grids" that the reduction of greenhouse gas emissions is now a worldwide initiative among nations. To address the potential threats that climate change poses to the entire planet, more aggressive emission-reduction objectives are being recommended. In recent years, many nations or economies, including the US, the EU, and Japan in particular, have made the objective of carbon neutrality (net zero carbon emissions) a part of their long-term plans. China declared that it would reach its target of carbon neutrality by 2060, with emissions peaked by 2030, at the UN General Assembly in September 2020. (NDRC, 2021). This will surely be a very difficult goal that will lead to huge adjustments in all spheres of life given that China currently makes up about 28.8% of global emissions (BP, 2019).

To examine the potential economic benefit of CSP integration in power grids, an economic dispatch model of a power system integrating CSP is provided in this work. In order to depict the unpredictability of fluctuating renewables while taking the correlation of wind and solar resources into continuous time, a modified scenario tree approach is used. The model is applied to three distinct energy-profiled Chinese provinces, and the results show that incorporating CSP into the current power grid has a significant economic benefit. [10]

Fujii et al. describes in the paper "Optimal integration assessment of solar PV in Japan's electric power grid" that the third-largest PV installed capacity in the world is in Japan, and the nation's power system is greatly impacted by the quick PV deployment. The installation of the FIT (feed-in-tariff) in 2012 specifically encourages the penetration of solar PV, and the total PV capacity is over 40 GW, an increase of almost 10 times before the FIT enforcement. Due to the shutdown following the Fukushima nuclear accident, the percentage of solar PV only climbed to 4.7 percent in FY2016, while that of nuclear held just 1.6 percent.

Because the Japanese power grid is compared to a straight-line power grid, which has significant bottlenecks in interregional power transmission and struggles to consolidate national power resources to integrate renewables, power grid planning has focused on effectively securing enough grid security and adequacy to accommodate renewable energy. Therefore, good PV integration

would help to keep power supply costs reasonable under the expanding use of PV systems in Japan. With the use of scenario reduction techniques or Monte Carlo simulation over PV outputs, for instance, the consideration of PV output uncertainty is seen as a significant future research issue. [11]

Yang et al. describes in the paper "BESS-Sizing Optimization for Solar PV System Integration in Distribution Grid" that renewable energy sources can reduce carbon emissions, but because they are erratic, the distribution grid may experience problems with power delivery. Additionally, several power pricing are contrasted to talk about how they affect the investment in BESS. The sizing and scheduling improvements are combined in the suggested strategy, increasing the dimension and complexity of the optimization problem. To enhance the effectiveness of the procedure, a revised electrons drifting algorithm (e-DA) is suggested and used to the suggested optimization issue.

In this research, a dual-loop optimization technique is proposed for PV system BESS and SI sizing and scheduling optimization. The suggested approach can optimize the active/reactive power scheduling of battery sets and SI in addition to identifying the appropriate capacities for both. The computational outcomes demonstrate that the suggested approach, solved by e-DA, can significantly enhance the quality of the solutions with a longer but still manageable computing time. Both the hosting capacity for green energy and the reliability of the power supply would be significantly increased in the future with the development of BESS and reactive-power regulation technologies. The investment in modernizing power facilities might also be put off properly for the industries that provide electricity. [12]

Jain et al. describes in the paper "Towards better performances for a novel rooftop solar PV system" that one of the most accessible energy sources is solar energy, which can be transformed into electric power in a fairly clean way utilising photovoltaic systems. The engineering community is being increasingly pushed by environmental concerns like global warming and greenhouse gas emissions to look for additional renewable energy sources or to create new technologies that could employ clean energy sources. In Northern nations like Sweden and Norway, who are now almost entirely dependent on renewable energy sources for their electricity, the renewable energy sector has grown significantly over the past ten years. Only a few nations, like Sweden and Norway, have the goal of producing all of their energy from renewable sources within the next five to ten years.

In order to increase the effectiveness of an existing PV plant situated on the rooftop of the G.D. Naidu Block at Vellore Institute of Technology, a novel design for a 248 kW PV system was given in this study (Vellore, India). to design the innovative photovoltaic system with the highest energy efficiency possible. The outcomes of numerical simulations performed in a PV system demonstrated that the newly developed Design 2 provides the grid with the most energy while exhibiting the fewest energy losses. Additionally, this led to a sizable decrease in CO2/SO2/NO emissions. According to the economic comparison of the two designs, Design 2 is superior to Design 1. However, it appears that there is very little incident solar energy being converted to electrical energy. [13]

Q. Guan et al. describes in the paper “Adaptive current harmonics suppression strategy for grid-tie inverters” that grid-connected inverters are becoming the most vital piece of interface gear for distributed power generation systems due to the ever-stricter standards in power quality. Even though the inverters may produce sinusoidal grid current and unity power factor, conventional voltage-oriented proportional integral (PI) controllers are limited in their ability to counteract the current ripples brought on by the modulation and/or dead time of power switches. The grid-side current harmonics have been reduced using a variety of control techniques. The precision of the system parameters has a significant impact on the predictive current control in and the dead-time compensation in. Therefore, fine-tuning the controller's parameters is challenging.

For three-phase grid-tie inverters, this article has suggested an adaptive current harmonics suppression technique. In order to make the algorithm less model-dependent and facilitate the design of a practical controller, the proposed method modelled the voltage errors caused by the switching modulation and the dead-time effect in the synchronous rotating frame and fitted the unmeasurable voltage errors with a truncated Fourier series expansion. By incorporating the voltage errors' adaptive compensation term in the current control loop as an equivalent disturbance compensation, the current harmonics are reduced. The tracking errors of the d and q-axis currents and the amplitude errors of the adaptive compensation term have been shown to be confined using the stability analysis in the sense of Lyapunov. [15]

Y. Zhang, et al. describes in the paper “Symmetric-component decoupled control of grid-connected inverters for voltage unbalance correction and harmonic compensation” that unbalanced voltages have a negative impact on electrical loads and power distribution networks, such as overloading transformers and limiting the capacity of distribution lines, increasing induction motor temperatures and overloading, and decreasing the efficiency of power electronic rectifiers. Unbalanced voltages have a negative impact on electrical loads and power distribution networks, such as overloading transformers and limiting the capacity of distribution lines, increasing induction motor temperatures and overloading, and decreasing the efficiency of power electronic rectifiers.

In this study, a sequence impedance model is created to help with controller design and to show how the control architecture functions. The αβγ-components are first separated into αβ- and γ-quantities. Asymmetrical control is made possible by decoupling the regulation of the zero-sequence component from the regulation of the positive- and negative-sequence component. Second, the αβ-quantities may be analysed using a simple frequency-domain-based analytical method because they are combined into a complex quantity. As a result, the frequency domain decoupling of the fundamental positive-sequence component's control and the other components' compensation can be achieved. [15]

A.E. Labrador Rivas et al. describes in the paper ” Adaptive current harmonic estimation under fault conditions for smart grid systems” that data sensing is required for smart transmission and distribution networks to keep an eye on transformers, substations, and power lines. For smart features to function on a particular platform, adaptive communication networks must permit open-standardized communication protocols. The notion of a micro-grid (mG) combines distributed generation (DG), loads, control, and storage elements to operate as a unit in an islanded or grid-connected mode. Advanced technology, control, sensors, and dependable data transfer systems are

all part of the mG. It entails the introduction of the big data idea using several data sources in the systems of the next power grid. By improving system security and reliability and maximising the use of grid assets, real-time control based on swift and reliable information interchange across many platforms would increase system resilience.

This research shows that harmonic estimation in non-stationary conditions is a difficult task. Estimation filters add a delay that might interfere with the minimal specifications for SG monitoring and control systems. In this work, a larger numerical comparison framework has been used to identify the optimum harmonic estimation approach. As a result, the effectiveness and efficiency of the used estimate algorithms have been examined primarily in light of three separate factors: amplitude error estimation, time-delay introduction, and computational complexity. Under stationary settings and Gaussian noise, all five of the harmonic estimating algorithms that were examined demonstrated a substantial performance in single and multiple amplitude harmonic estimations. However, with non-gaussian noise, merit metrics like the NMSE have suffered. [16]

2.3. GAP OF KNOWLEDGE:

Integrating PV systems into national networks can minimise generating costs, boost grid resilience, decrease transmission and distribution line losses and lesser the need to invest in additional utility generation capacity.
New ideas like combining PV-T collectors and small wind turbines for residential use may result in more compact yet effective power generation systems for the production of both electricity and heat.
Through the use of an energy management system, micro-grid systems have the ability to match the load profiles of local or residential structures with the power production profiles. The micro-operating system's plan allows for large profitability, and the majority of the electricity used during peak hours is generated by PV panels or battery discharge.
PV systems, both low power and high power, have experienced phenomenal growth on a global scale. In order to assist the stakeholder in choosing the type of PV system to be installed such as one with or without a battery, a single inverter or a string of inverters a thorough market investigation was undertaken to assess the cost breakdown of the various subsystems.
A battery system with a higher capacity offers greater advantages in terms of lowering grid demand fluctuation and boosting residential self-sufficiency. Grants and low-interest loans are anticipated to spur global manufacture and boost demand for battery storage. A number of interest groups predict that battery prices will fall sharply in the near future, which may cause the energy sector to decentralise.
An innovative rooftop solar PV system is a very profitable way to meet the industrial unit's power needs. The Indian government only permits 50% of the permitted load to be put on an industrial unit (to prevent unlawful energy trading), which is the sole drawback to the system installation. Generally speaking, solar panels have a lifespan of 25 to 30 years. However, this does not imply that they cease to produce power after 25 years; it just indicates that energy output has decreased by an amount that manufacturers deem to be meaningful. It has been demonstrated by performance data from several sources that the PV system can operate effectively for 25–30 years.
The primary difficulties in integrating solar PV into industrial microgrids under reliability restrictions. High availability of electrical generation is required for the ongoing operation of industrial power plants. However, compared to big grids or household systems with electrical

demands that are likely to be shed or postponed, the electrical system is more prone due to its low inertia and poor flexibility.

2.4. POSSIBLE SOLUTIONS:

Solutions can be done by using more precise forecasting software to enable earlier forecasts of the potential drop of solar power to the minimal penetration capacity, and installing solar over a vast region to lessen the effects of generation unpredictability brought on by local cloud cover Changing the source of the electricity and storing extra energy for later usage encouraging consumers to use power during times when it is more easily accessible will change the demand for electricity.

2.5. SYNOPSIS OF THE WORK:

After examining a variety of features of solar PV grid integration from earlier works, including how it functions and how different performance factors impact the output and general effectiveness of the PV system. Numerous distortions, including VDF, THD and form factor alterations are brought on by the harmonics in the system. As a result, the system's overall effectiveness changes. Thus, working on the system's harmonic analysis component can be done. It will be based on ETAP simulation, and standard ratings can be used to improve it.

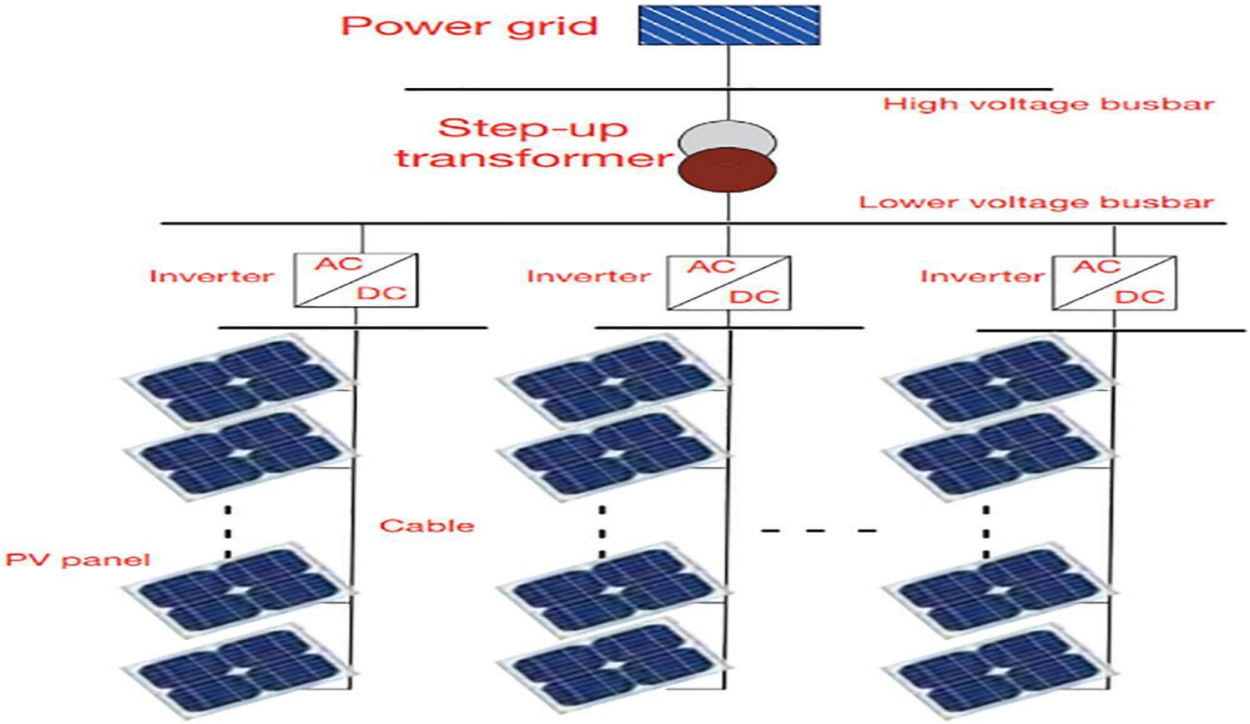

Fig 2: Schematic of solar PV integration [1]

2.6. CONCLUSION:

As I have described, the articles I read to learn more about solar PV grid integration and the power quality generated by the process have given me some fundamental understandings of how solar PV integration actually operates, as well as its constituent parts and performance criteria. In contrast to the high short-circuit levels of the distribution grid, grid connected residential PV systems are typically small to medium sized (1 to 15 kWp). As a result, when a single PV system is linked to the grid, system voltage distortion is essentially non-existent.

Chapter 3: THEORIES ON IEEE 9 BUS SYSTEM

3.1. INTRODUCTION:

In the previous chapters, various kinds of research work that has been done has been discussed. Corresponding problems and their respective solutions has also been discussed. In this chapter, IEEE 9 bus system components and their significance in this research work will be discussed.

3.2. COMPONENTS OF IEEE 9 BUS SYSTEMS:

Three synchronous generators, nine buses, six transmission lines, three transformers, and three P-Q loads make up the IEEE 9 bus system. In this project, we have used standard IEEE 9 BUS system to analyse the load flow of the system by integrating solar PV and alternator so that we can observe the harmonic analysis for each cases. We have got the harmonic orders responsible and corresponding spectrum for each cases. Figure 3 shows how various devices are connected to one another.

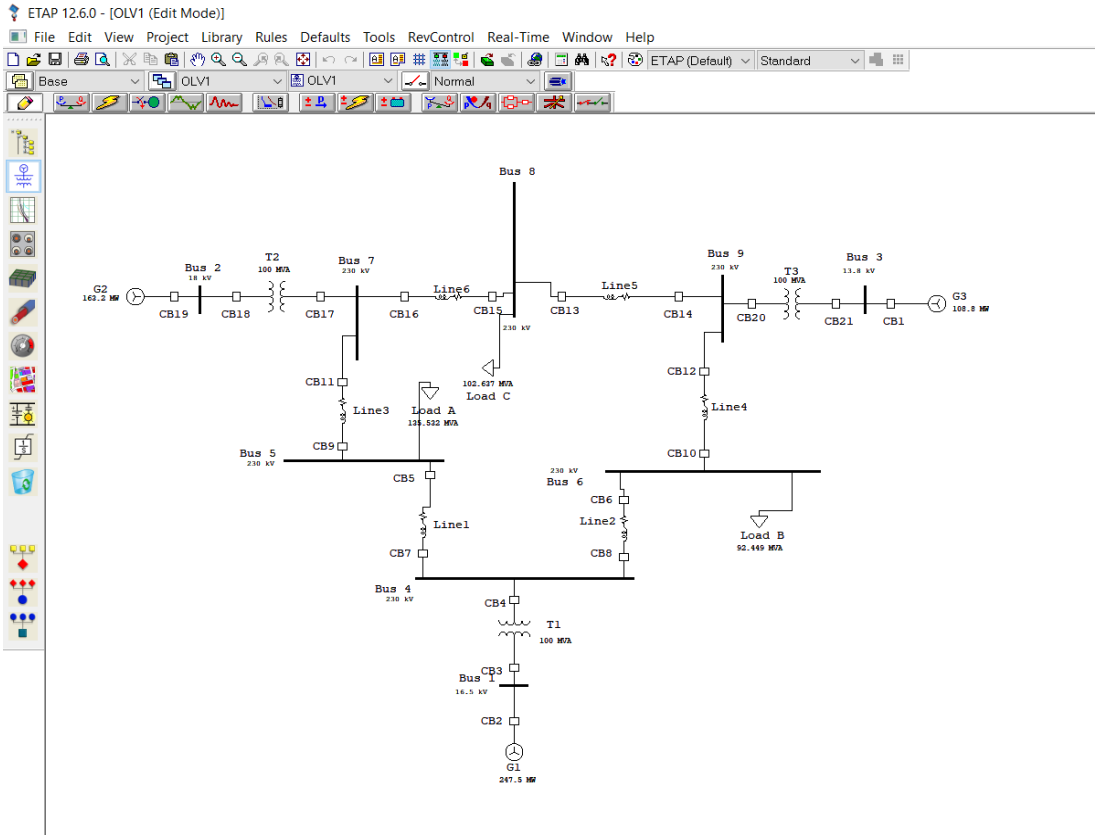

Fig 3: Standard IEEE 9 Bus System

3.3. SYNCHRONOUS GENERATOR:

A synchronous generator is a device that uses electromagnetic induction to transform mechanical power into alternating current (AC) electricity. Alternators or AC generators are other names for synchronous generators. Since it generates AC power, it is referred to as an "alternator." Because it needs to be run at synchronous speed in order to generate AC electricity at the desired frequency, this generator is known as a synchronous generator.

CONSTRUCTION OF SYNCHRONOUS GENERATOR:

Alternator has two main parts:

- **Stator** – The alternator's stator is its stationary component. The armature winding, which is where the voltage is produced, is carried by it. The stator serves as the alternator's output.
- **Rotor** – The alternator's revolving component is known as the rotor. The primary field flux is created by the rotor.

WORKING PRINCIPLE OF SYNCHRONOUS GENERATOR:

An electromagnetic field (EMF) is created in a conductor when the flux connecting it changes. This is how an alternator operates. When the alternator's armature winding is exposed to a revolving magnetic field, the winding will produce voltage. The alternate north and south poles develop on the rotor when the alternator's rotor field winding is stimulated by a DC exciter. The RMF of the rotor poles cuts the armature conductors mounted on the stator as the rotor is turned counter clockwise by a primary mover. As a result, electromagnetic induction induces the EMF in the armature conductors.

The Fleming's right hand rule can be used to determine the polarity of the EMF and the frequency is provided by equation 1 that is:

$$\boldsymbol{f = \frac{PNs}{120}} \ldots\ldots\ldots (\mathbf{1})$$

Where,

- Ns is the synchronous speed in RP
- P is the number of rotor poles.

In this project, we have used 3 synchronous generator. Generator 1 is connected at BUS 1 which has rating of 16.5 KV. We have used operating mode as swing mode and salient pole rotor structure has been used. We also considered that the output of the alternator do not consist any harmonic spectrum.

Salient Pole Rotor:

The significance of the word salient is nothing but projection. Consequently, salient pole rotor is made up of poles that extend from the rotor core's surface. In order for the adjacent poles to have opposite polarities when the field winding is activated by the DC exciter, each field winding is connected to the others in series. Salient pole type rotors cannot be built with a robust enough structure to survive the mechanical forces that may be placed on them at greater speeds. High speed operation of salient pole rotor would result in windage loss and a propensity for noise production.

Capability curve: The generator's capability curve specifies the range of temperatures at which it can continuously supply reactive power without overheating. The apparent power of a generator are specified at a specific terminal voltage. Only the turbine's ability to distribute power can place a cap on the amount of active power a generator can produce. Three constraints, however the Armature Current Limit, the Field Current Limit, and the End Part Heating Limit regulate the amount of reactive power that a generator may continually produce without overheating.

The ratings and impedances that we have used in simulation purpose results a capability curve and we have projected it by ETAP system. The ratings, impedances and capability curve of Generator 1 is shown in the figure 4 to 6.

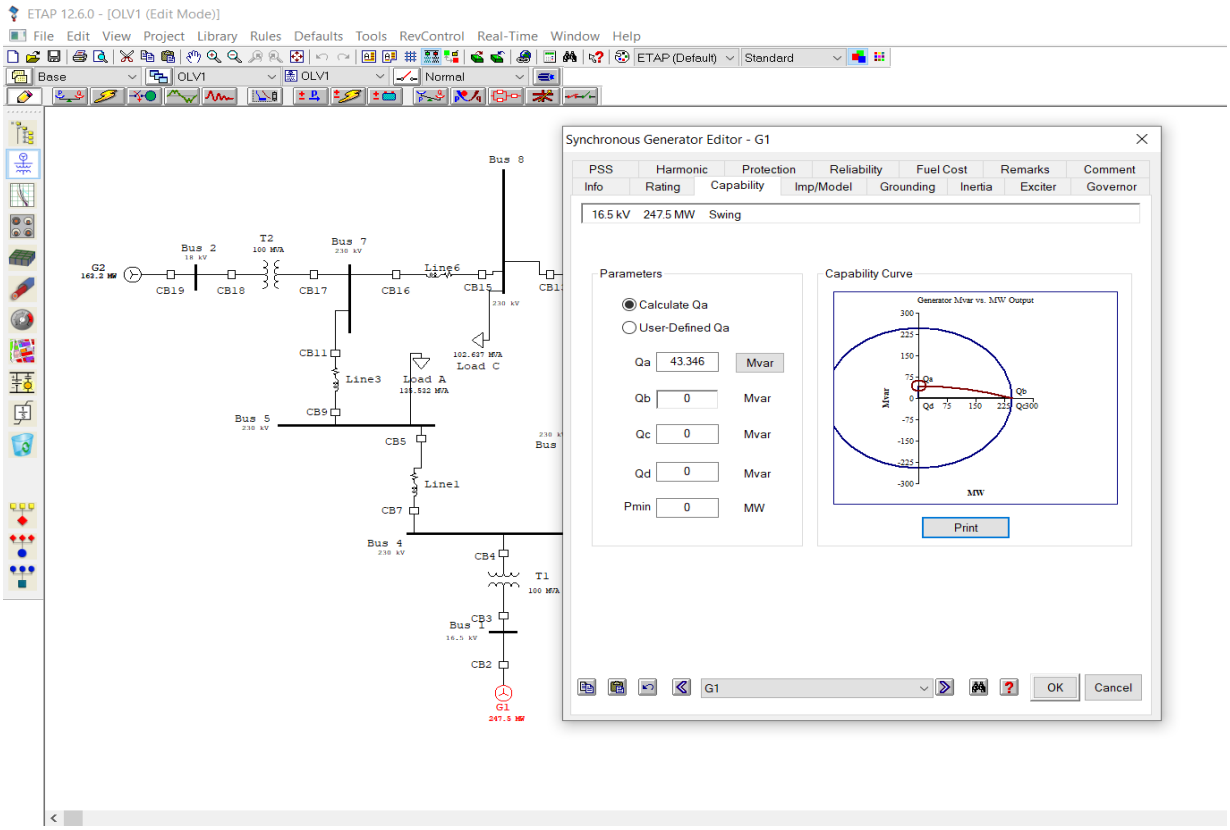

Fig 4: Capability Curve of generator 1

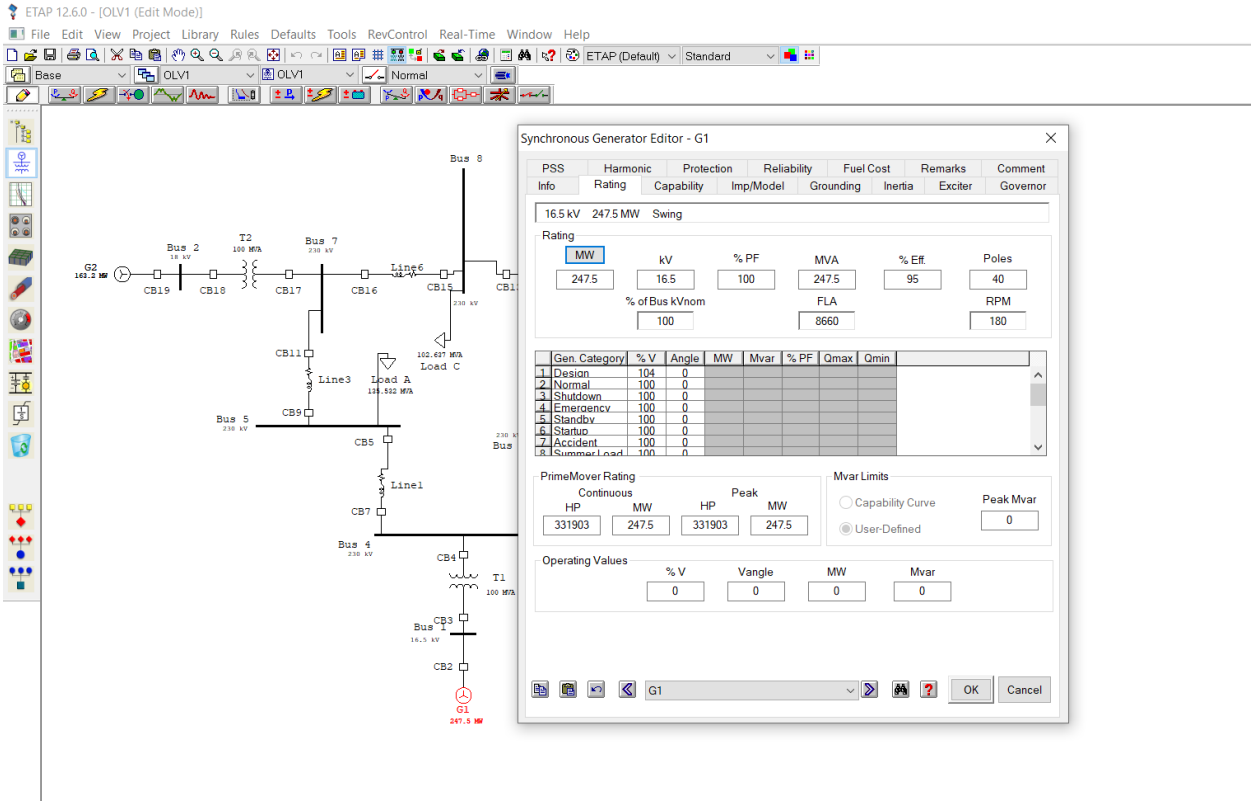

Fig 5: Rating of Generator 1

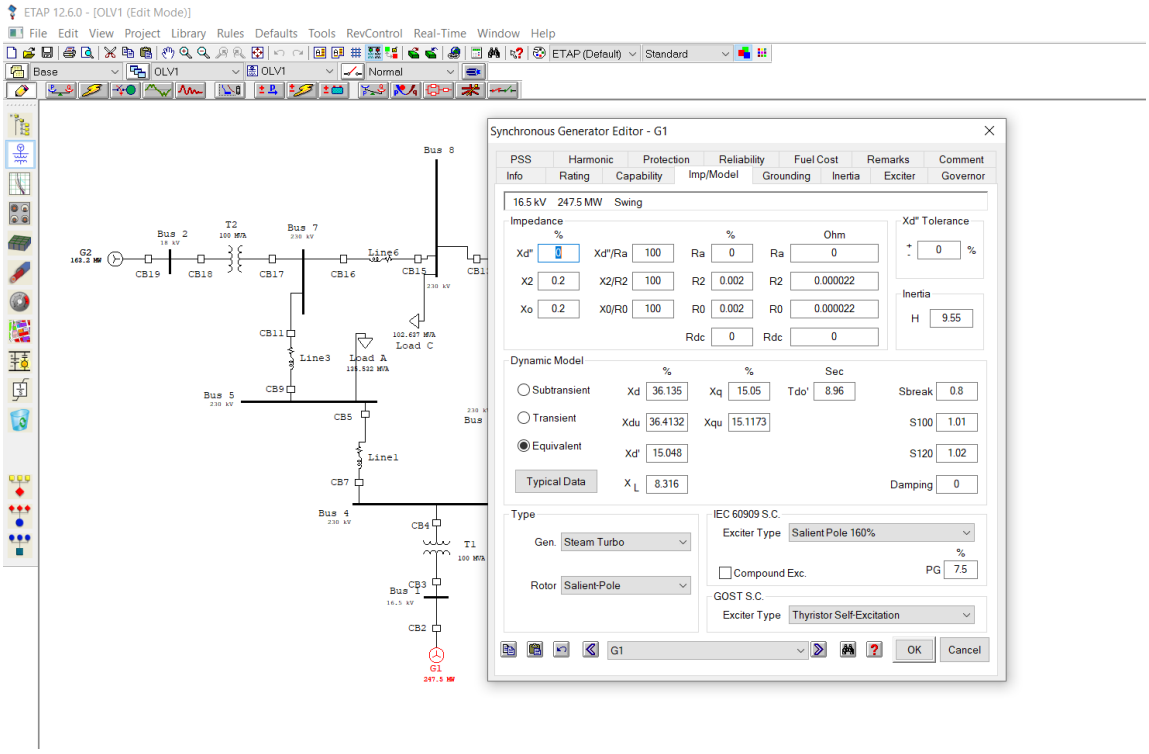

Fig 6: Impedance of Generator 1

Generator 2 is connected at BUS 2 which has rating of 18 KV. We have used operating mode as voltage control mode and round rotor (cylindrical) structure has been used. We also considered that the output of the alternator do not consist any harmonic spectrum.

CYLINDRICAL ROTOR:

The cylindrical rotor's design prevents physical poles from being visible, unlike with a salient pole rotor. Slots of the rotor shaft are divided into equal intervals in about two-thirds of the cylindrical rotor's outer perimeter. These slots contain the field windings, which are activated by the DC supply. The type of the field winding is dispersed. The pole faces are formed by the rotor's unslotted section. The cylindrical rotor's figure makes it obvious that the generated poles are non-salient, or that they don't protrude from the rotor surface.

Similarly, the ratings and impedances that we have used in simulation purpose results a capability curve and we have projected it by ETAP system. The ratings, impedances and capability curve of Generator 2 is shown in the figure 7 to 9. The ratings and capability curve of Generator 2 is shown below.

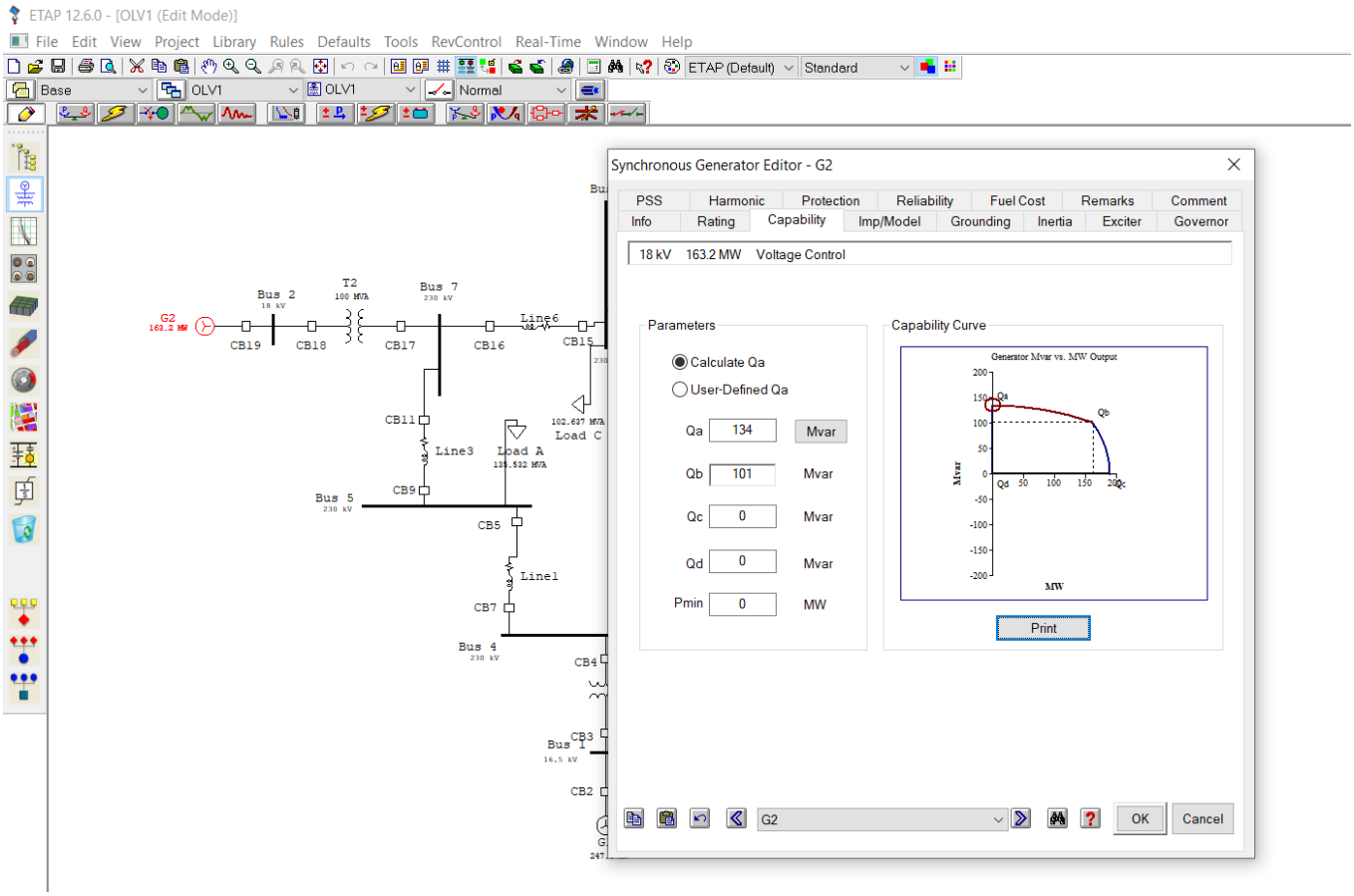

Fig 7: Capability Curve of generator 2

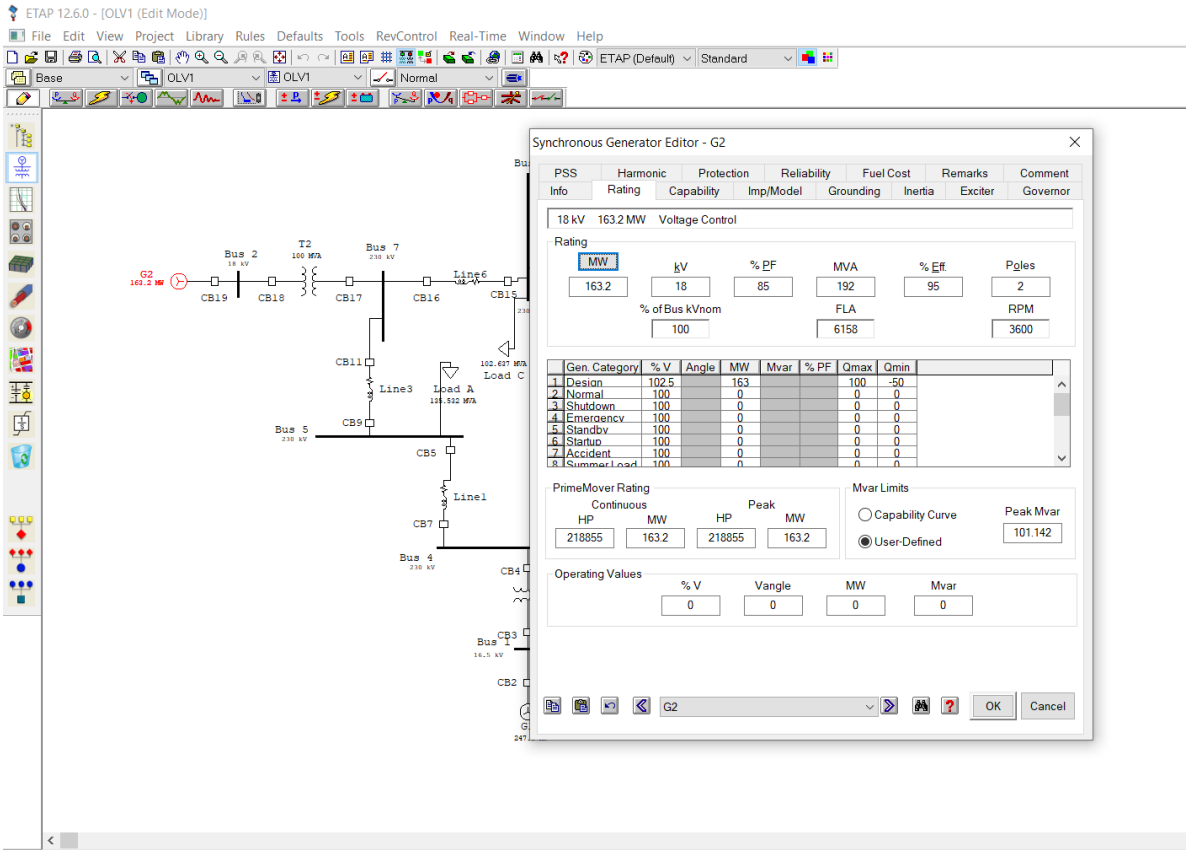

Fig 8: rating of generator 2

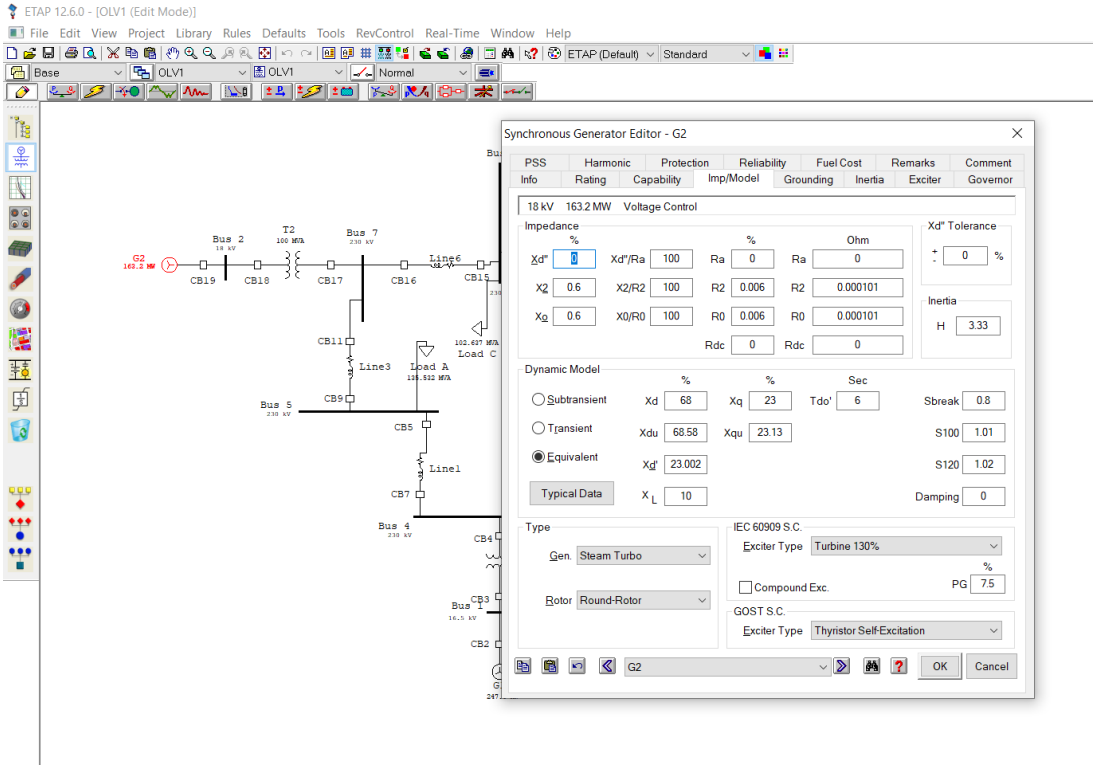

Fig 9: Impedance of generator 2

Generator 3 is connected at BUS 3 which has rating of 13.8 KV. We have used operating mode as voltage control mode and round rotor (cylindrical) structure has been used. We also considered that the output of the alternator do not consist any harmonic spectrum.

Similarly for Generator 3, the ratings and impedances that we have used in simulation purpose results a capability curve and we have projected it by ETAP system. The ratings, impedances and capability curve of Generator 3 is shown in the figure 10 to 12. The ratings and capability curve of Generator 3 is shown below.

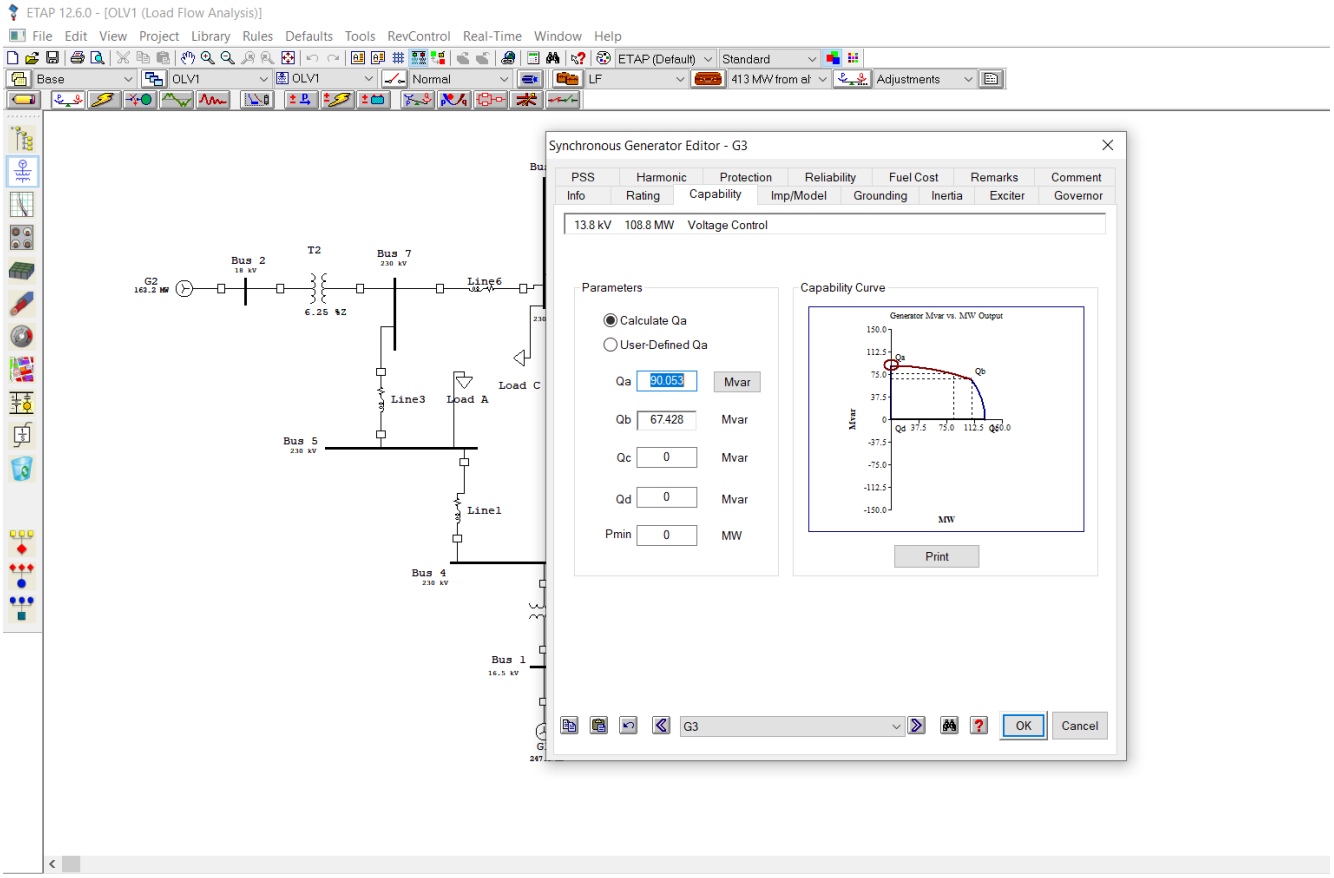

Fig 10: Capability Curve of generator 3

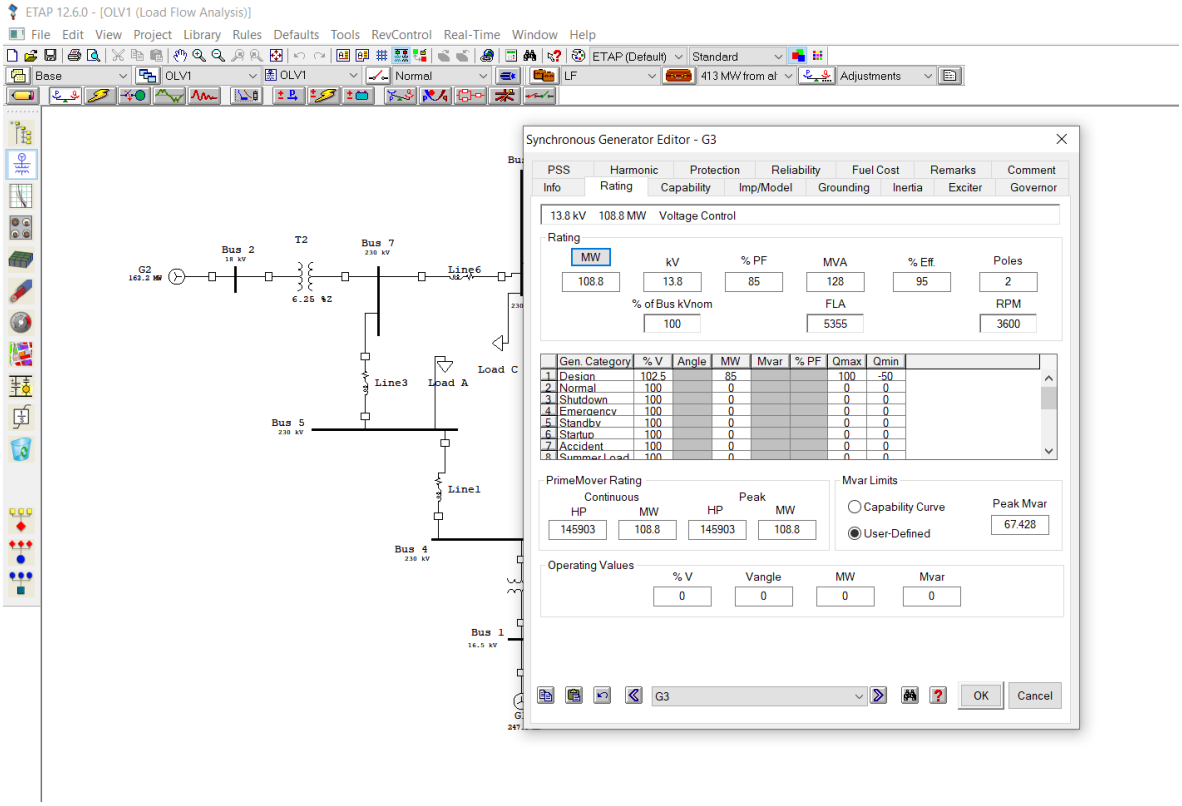

Fig 11: Rating of Generator 3

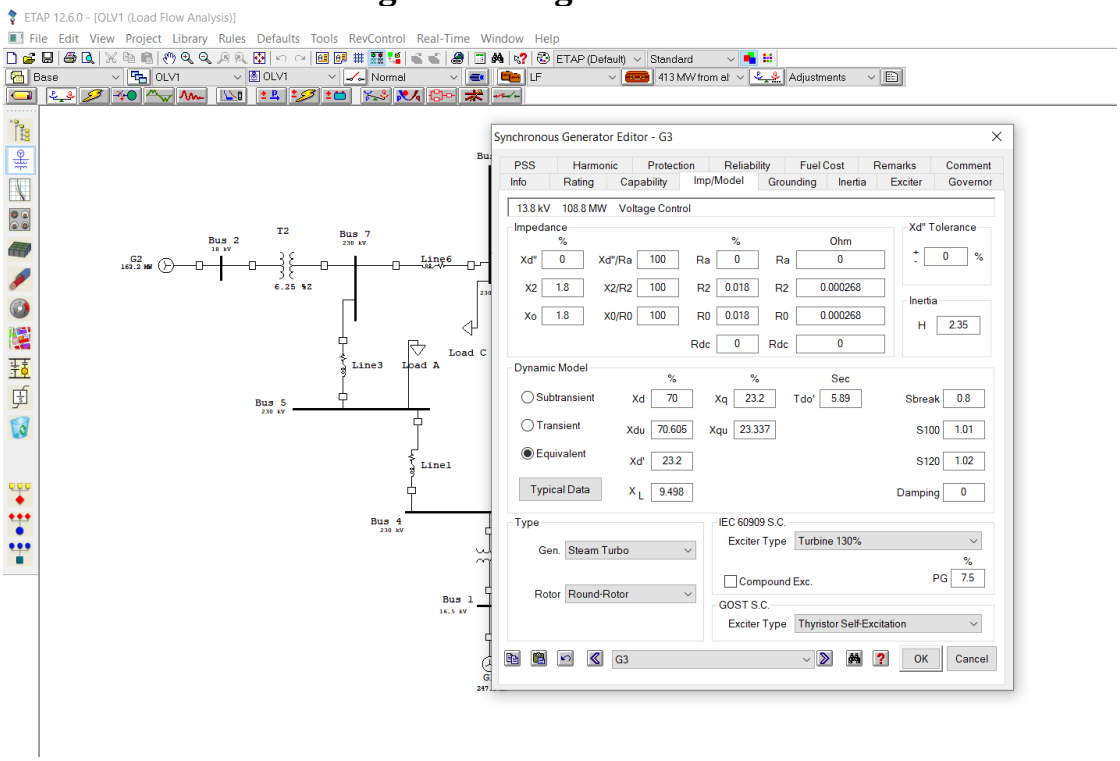

Fig 12: Impedance of Generator 3

3.4. 2 WINDING TRANSFORMER:

A transformer with two windings is one where the magnetic flux between the windings is linked throughout time. One of these winding, known as the primary, receives electricity from a source at a specific voltage, while another winding, known as secondary, sends power to the load, typically at a voltage that differs from the source. Two winding can switch off in their functions. The exciting current will become excessive if a given winding in an iron-core transformer operates at a voltage that is higher than its rated value at the specified frequency.

Although some flux, known as leakage flux, creates it's path through air and it does not link to the other winding, the core typically provides the primary path for the magnetic flux in conventional iron-core transformers. Iron-core transformers essentially contain all of the flux inside the core when there is no load and the circumstances are constant, as well as the leakage flux is often little. The no-load voltage induced in each turn of the windings is referred in equation 2 that is:

$$E_{turn} = -\int_A^{\infty} \frac{d(B\cos\alpha)}{dt} dA = -\frac{d\phi}{dt} \dots\dots\dots (2)$$

The rms value of induced emf caused by a sinusoidal flux of amplitude m in an N-turn winding is given by equation 3 that is:

$$E = 4.44 f \phi_m N \dots\dots\dots (3)$$

There are 2 types of transformers:

1. **Core type transformers:** The magnetic core of the core type transformer is built using laminations, which results in a frame with a rectangular shape. As shown in the image below, these laminations are shaped like L strips. The other layer is layered differently to eliminate continuous junctions, which helps to prevent the high amount of resistance.

2. **Shell type transformers:** The core of a single phase shell type transformer is constructed with of three limbs. The core's mechanical strength is increased by this design. Additionally, it enhances the safety of windings against outside mechanical shocks. The middle limb is wrapped in both the HV and LV windings. The lateral limbs only carry half of the flux, whereas the centre limb carries the full flux. As a result, the centre limb's cross-section is twice as large as the side limbs' to account for the flux.

   The magnetic flux travels over two closed magnetic pathways, reducing core losses and boosting transformer efficiency. As a result, a transformer of the shell type produces greater output than a transformer of the core type. One of the key advantages of shell-type capacitors is that the core provides strong resistance to the electromagnetic forces that can develop between the current-carrying conductors in the event of a short circuit.

The ratings, impedances and harmonic spectrums of transformers are shown in the figure 13 to 15.

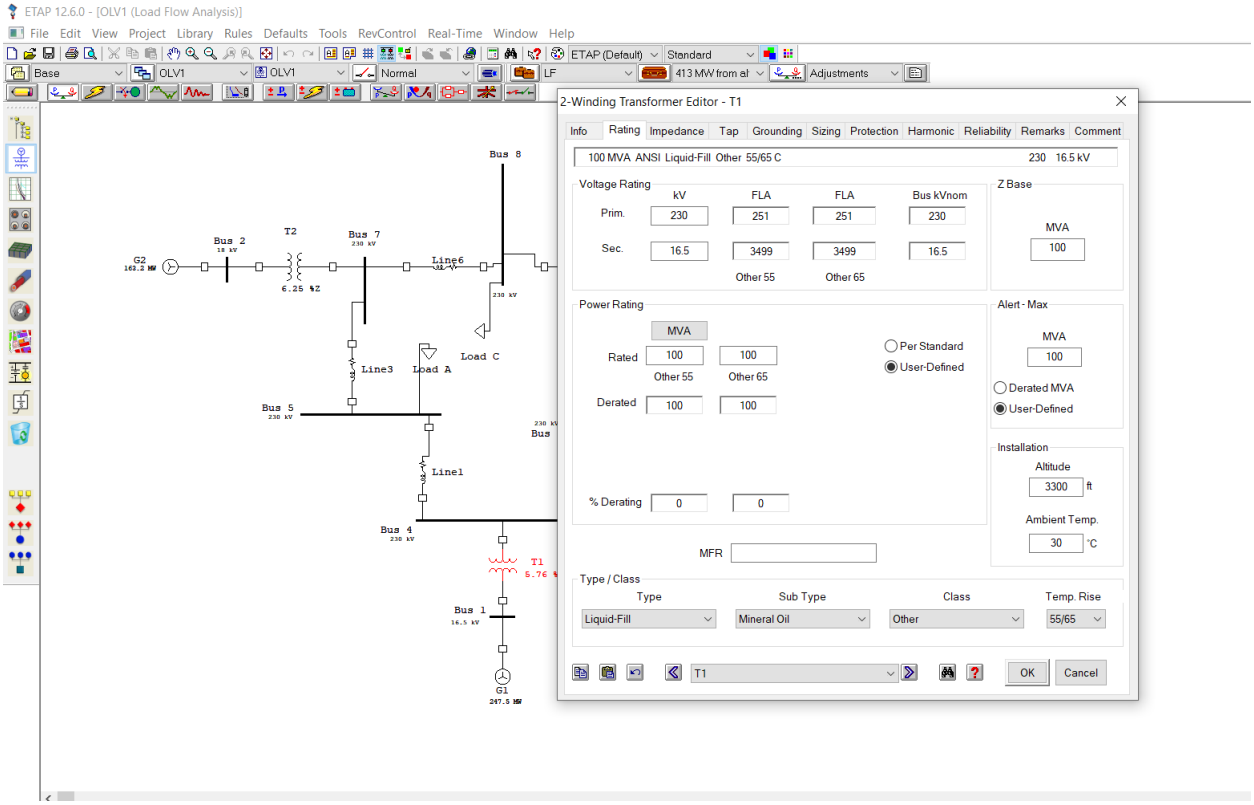

Fig 13: Rating of 2 Winding Transformer

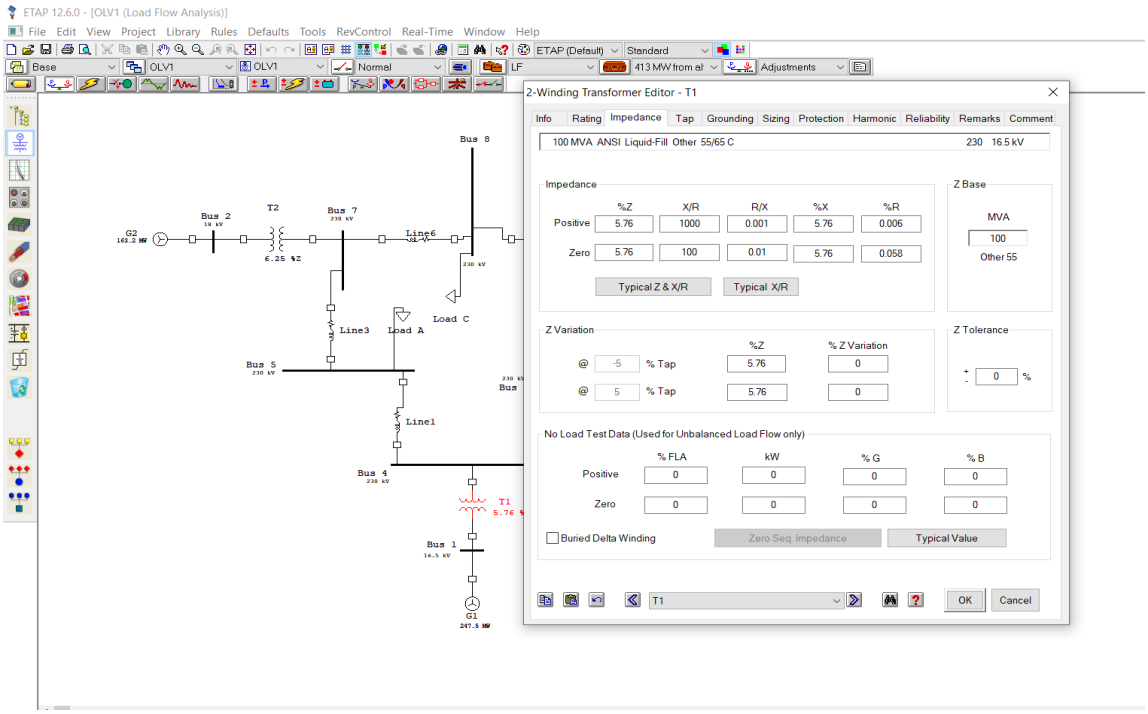

Fig 14: Impedance of 2 Winding Transformer

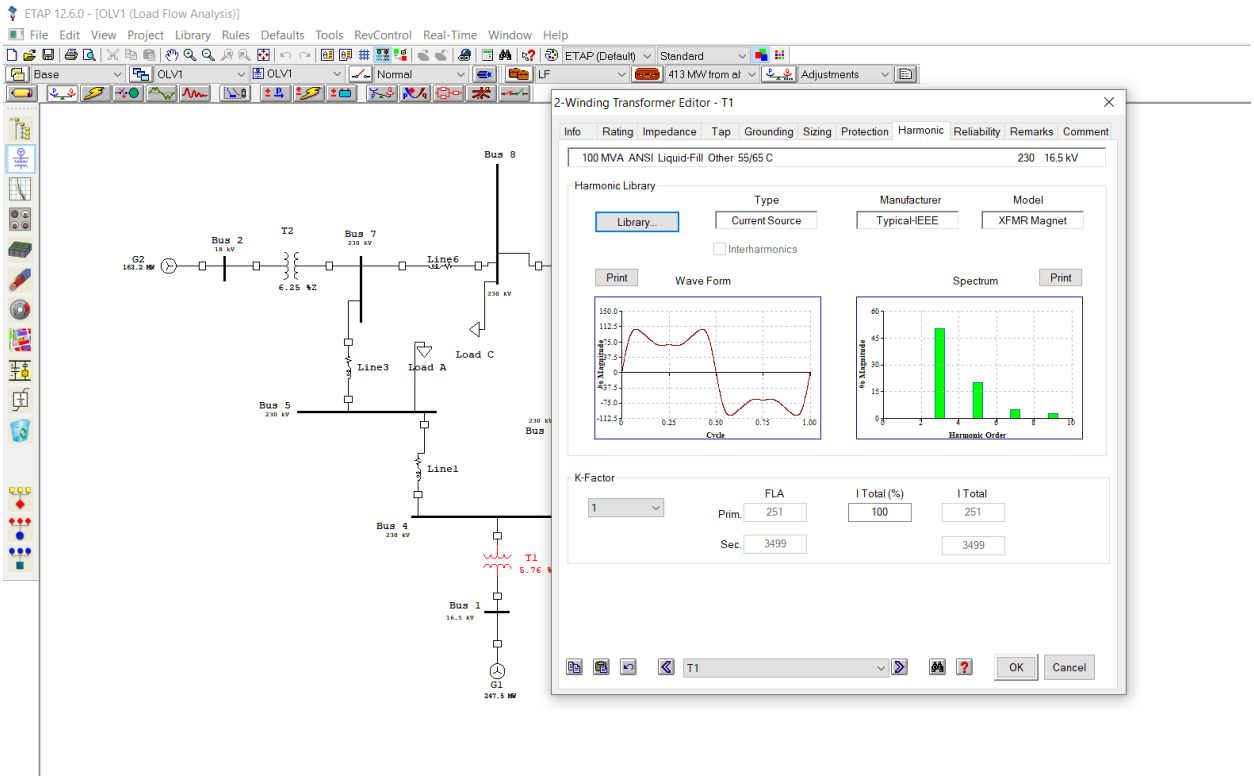

Fig 15: Harmonic Spectrum of 2 Winding Transformer Output

3.5. SOLAR PHOTOVOLTAIC SYSTEM:

A photovoltaic (PV), often known as a solar cell, cell may reflect, absorb, or pass through light that strikes it. The semiconductor material that makes up the PV cell can conduct electricity more effectively than an insulator but not as effectively as a good conductor like a metal. In PV cells, a variety of semiconductor materials are employed. When a semiconductor is exposed to light, the light's energy is absorbed and transferred to the semiconductor's negatively charged electrons. The additional energy enables the electrons to conduct an electrical current through the material. a PV cell's efficiency may be calculated as the ratio of the electrical power it produces to the energy from the sunlight . This ratio shows how well the cell converts energy from one form to another. The qualities of the available light (such as its intensity and wavelengths) and a number of cell performance factors determine how much power is generated by PV cells.

The bandgap, which describes what wavelengths of light the substance can absorb and convert to electrical energy, is a crucial characteristic of PV semiconductors. The PV cell can effectively utilise all of the available energy if the semiconductor's bandgap matches the wavelengths of light absorbed by the cell.

WORKING PRINCIPLE:

Solar cells transform solar energy into electrical energy. A substance that absorbs light energy is found in solar cells, such as silicon. The energy causes an electric potential energy difference, or voltage, by knocking electrons loose so they may flow freely. Electric current is produced when electrons or negatively charged particles flow. Similar to the terminals of a battery, solar cells contain positive and negative connections. Current flows from the negative to positive contact if a conductive wire is used to connect the contacts. A PV cell's mechanism for producing energy is depicted in the figure below.

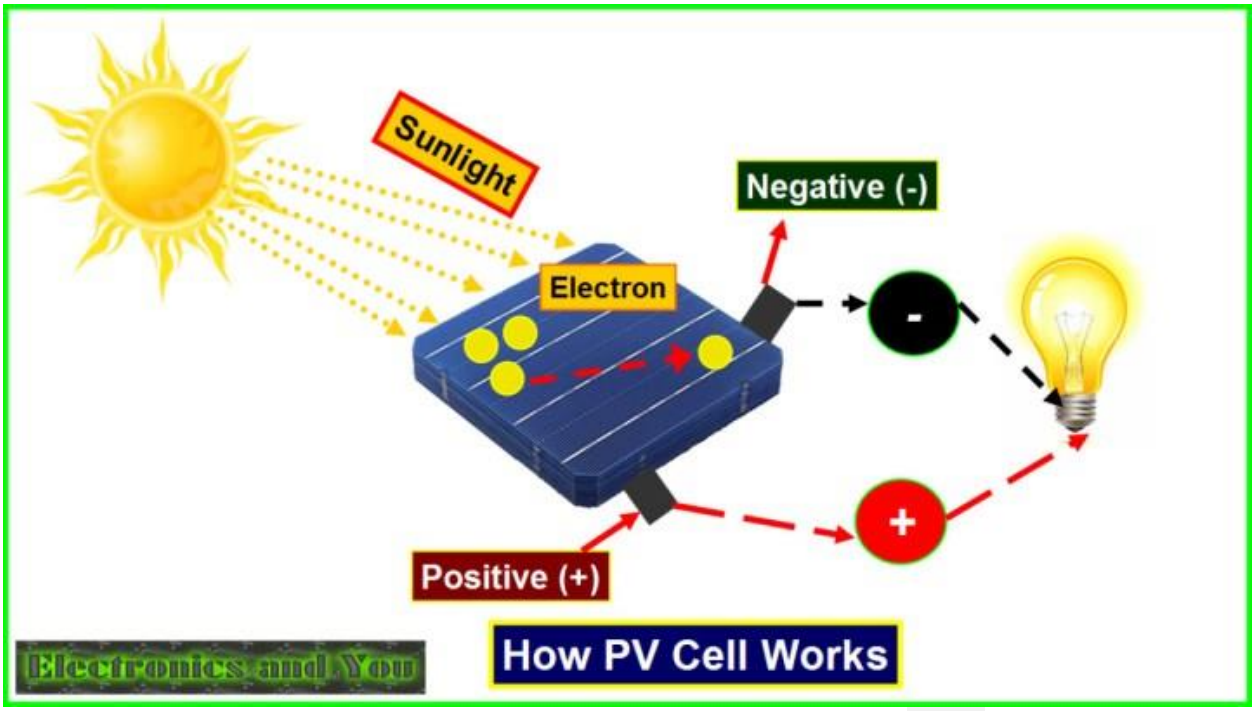

Fig 16: PV Cell Working Principle [18]

The ratings and P-V curve of the PV panel are shown below.

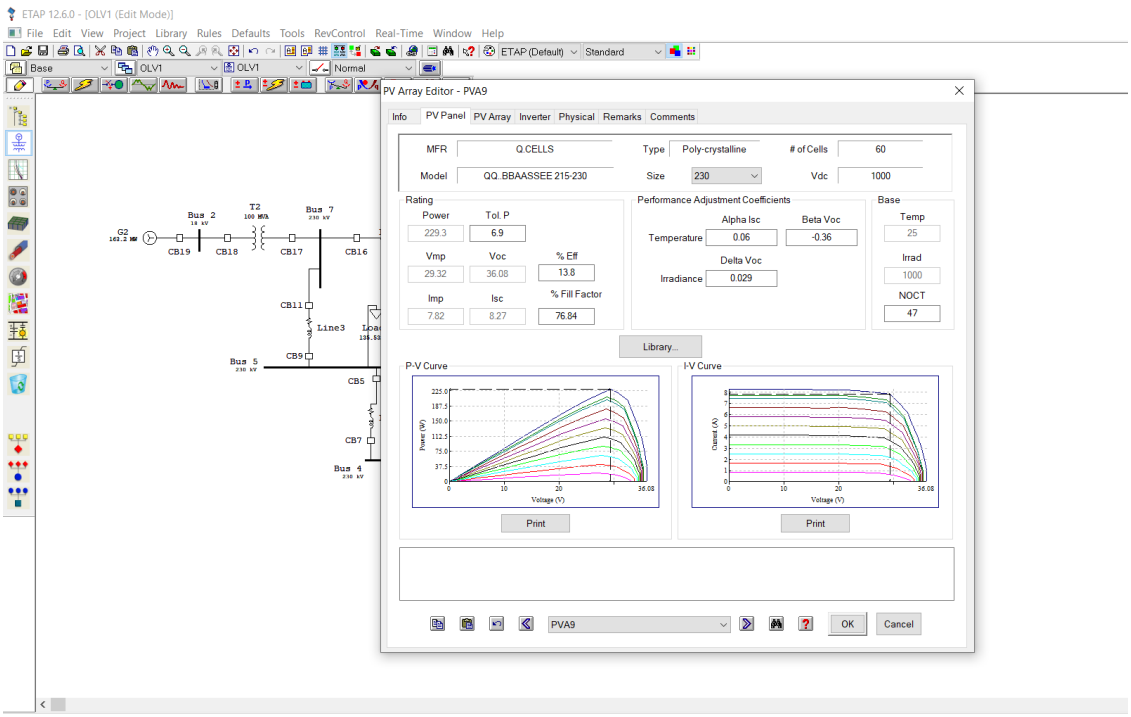

Fig 17: The ratings and P-V curve

3.6. CONCLUSION:

These concepts which I have discussed in the previous sections are very important aspects and they are playing a crucial role to build the basics of this project. I have studied lot of thesis papers to gather these concepts and these concepts has helped me to do this project. When compared to the high short-circuit levels of the distribution grid, the size of grid-connected house PV systems generally ranges from small to medium. As a result, voltage distortion when a single PV system is linked to the grid is almost non-existent.

Chapter 4: PRESENT RESEARCH METHODS

4.1. INTRODUCTION:

In the previous section, various sections of the system has been discussed that is alternator and its components, solar PV, two winding transformer. In this section, various technologies and their applications are explained. NR method and load flow analysis by using NR methods has been explained. Load flow algorithm for NR method has also discussed.

4.2. NEWTON RAPHSON METHOD:

A real-valued function with the root f(x) = 0 can be easily approximated using the Newton-Raphson technique, sometimes referred to as Newton's method. It makes advantage of the notion that a straight line tangent can serve as an approximation for a continuous and differentiable function.

Suppose you need to find the root of a continuous, differentiable function f(x), and you know the root you are looking for is near the point $x = x_0$.

Then Newton's method in equation 4 tells us that a better approximation for the root is

$$x_1 = x_0 - \frac{f(x0)}{f'(x0)} \dots\dots\dots\dots\dots\dots (4)$$

This process may be repeated as many times as necessary to get the desired accuracy. In general, for any x-value x_n, the next value is given by equation 5 that is:

$$x_{n+1} = x_n - \frac{f(xn)}{f'(xn)} \dots\dots\dots\dots\dots (5)$$

4.3. NEWTON RAPHSON METHOD FOR LOAD FLOW ANALYSIS:

For the solution of non-linear algebraic equations, the NR Method for Load Flow Analysis is a potent technique. In comparison to the GS approach, it is more efficient and will converge in the majority of circumstances. It is, in fact, a viable approach to solving the load flow problem in big power networks. It is one flaw is that a huge amount of computer memory is needed, however this has been fixed with a compact storage system. By completing the first iteration using the GS approach and using the values so acquired for beginning the NR iterations, convergence may be significantly sped up. It is helpful to go over the NR approach in its general form before describing how it is used to address the load flow problem.

Think about a collection of n non-linear algebraic equations.

$$f_i(x_1, x_2, \dots, x_n) = 0; \quad i = 1, 2, \dots, n \qquad (6.53)$$

Assume that the unknown's starting values are x^0_1, x^0_2... x^0_n.

Let Δx^0_1, Δx^0_2… Δx^0_n represent the corrections, which, when combined with the starting hypothesis, result in the correct answer. Therefore

$$f_i(x_1^0 + \Delta x_1^0,\ x_2^0 + \Delta x_2^0,\ \ldots,\ x_n^0 + \Delta x_n^0) = 0; \quad i = 1, 2, \ldots, n \tag{6.54}$$

By extending these Taylor series equations around the original hunch, we obtain

$$f_i(x_1^0,\ x_2^0,\ \ldots,\ x_n^0) + \left[\left(\frac{\partial f_i}{\partial x_1}\right)^0 \Delta x_1^0 + \left(\frac{\partial f_i}{\partial x_2}\right)^0 \Delta x_2^0 + \ldots + \left(\frac{\partial f_i}{\partial x_n}\right)^0 \Delta x_n^0\right] + \text{higher order terms} = 0 \tag{6.55}$$

where

$$\left(\frac{\partial f_i}{\partial x_1}\right)^0, \left(\frac{\partial f_i}{\partial x_2}\right)^0, \ldots, \left(\frac{\partial f_i}{\partial x_n}\right)^0$$

are the derivatives of f_i evaluated at (x01, x02,..., x0n) with regard to x1, x2,..., xn.

When higher order terms are ignored, Eq. (6.55) may be written in matrix form.

$$\begin{bmatrix} f_1^0 \\ f_2^0 \\ \vdots \\ f_n^0 \end{bmatrix} + \begin{bmatrix} \left(\frac{\partial f_1}{\partial x_1}\right)^0 & \left(\frac{\partial f_1}{\partial x_2}\right)^0 & \cdots & \left(\frac{\partial f_1}{\partial x_n}\right)^0 \\ \left(\frac{\partial f_2}{\partial x_1}\right)^0 & \left(\frac{\partial f_2}{\partial x_2}\right)^0 & \cdots & \left(\frac{\partial f_2}{\partial x_n}\right)^0 \\ \vdots & \vdots & & \vdots \\ \left(\frac{\partial f_n}{\partial x_1}\right)^0 & \left(\frac{\partial f_n}{\partial x_2}\right)^0 & \cdots & \left(\frac{\partial f_n}{\partial x_n}\right)^0 \end{bmatrix} \begin{bmatrix} \Delta x_1^0 \\ \Delta x_2^0 \\ \vdots \\ \Delta x_n^0 \end{bmatrix} \simeq \begin{bmatrix} 0 \\ 0 \\ \vdots \\ 0 \end{bmatrix} \tag{6.56a}$$

or in vector matrix form

$$f^0 + J^0 \Delta x^0 \simeq 0 \tag{6.56b}$$

The Jacobian matrix is referred to as J^0 . Equation (6.56b) is denoted by

$$f^0 \simeq [-J^0]\ \Delta x^0 \tag{6.57}$$

$$f^0 \simeq [-J^0]\ \Delta x^0 \tag{6.57}$$

Eq. provides approximate values of the adjustments x^0 (6.57). Since they are a collection of linear algebraic equations, triangularization and back substitution may be used to solve them quickly.

Then, updated x values are

$$x^1 = x^0 + \Delta x^0$$

or, for the (r + 1)th iteration, generally

$$x^{(r+1)} = x^{(r)} + \Delta x^{(r)} \tag{6.58}$$

In other words, until Eq. (6.53) is satisfied to the appropriate precision, iterations are performed.

$$|f_i(x^{(r)})| < \varepsilon \text{ (a specified value)}; \quad i = 1, 2, \ldots, n \tag{6.59}$$

NR Algorithm for Load flow Solution:

First, let's suppose that every bus is a PQ bus. The following non-linear algebraic equations must be satisfied by the load flow solution at any PQ bus.

$$f_{iP}(|V|, \delta) = P_i \text{ (specified)} - P_i = 0 \tag{6.60a}$$

$$f_{iQ}(|V|, \delta) = Q_i \text{ (specified)} - Q_i = 0 \tag{6.60b}$$

where Eqs. (6.27) and provide equations for Pi and Qi, respectively (6.28). The vector of residuals in equation (6.57) for a test set of variables |Vi|, I equates to

$$f_{iP} = P_i \text{ (specified)} - P_i \text{ (calculated)} = \Delta P_i \tag{6.61a}$$

$$f_{iQ} = Q_i \text{ (specified)} - Q_i \text{ (calculated)} = \Delta Q_i \tag{6.61b}$$

While the corrections vector, x0, is equivalent to

$$\Delta|V_i|, \ \Delta\delta_i$$

For the load flow example, equation (6.57) for

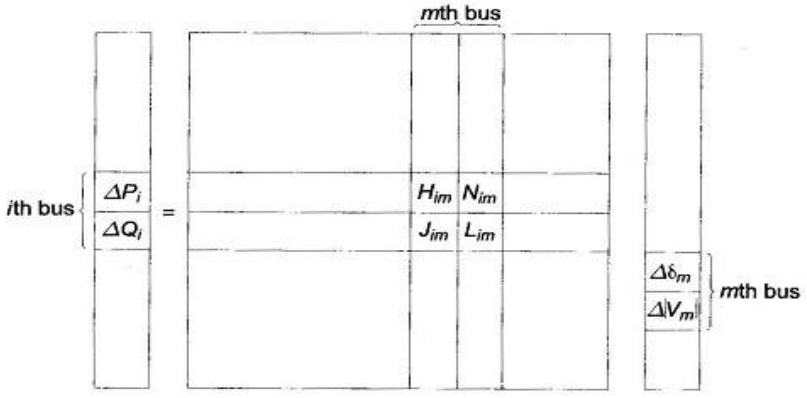

(6.62a)

finding the estimated corrections vector may be expressed as where

$$H_{im} = \frac{\partial P_i}{\partial \delta_m}$$

$$N_{im} = \frac{\partial P_i}{\partial |V_m|}$$

$$J_{im} = \frac{\partial Q_i}{\partial \delta_m} \qquad (6.63a)$$

$$L_{im} = \frac{\partial Q_i}{\partial |V_m|}$$

The Jacobian components for the ith bus residuals and mth bus corrections are instantly apparent as a 2 x 2 matrix contained in the box in Eq. (6.62a), where I and m are both PQ buses.

There are no equations that match Eq. (6.60) at the slack bus (bus number 1) since P1 and Q1 are undetermined and |V1|, 1 are fixed. As a result, in Eq, the slack bus does not enter the Jacobian (6.62a).

Now that PV buses are there, think about the Newton-Raphson Method for Load Flow Analysis Formula. If the ith bus is a PV bus, Q_i is undetermined, which means that Eq. (6.60b) does not apply to this bus.

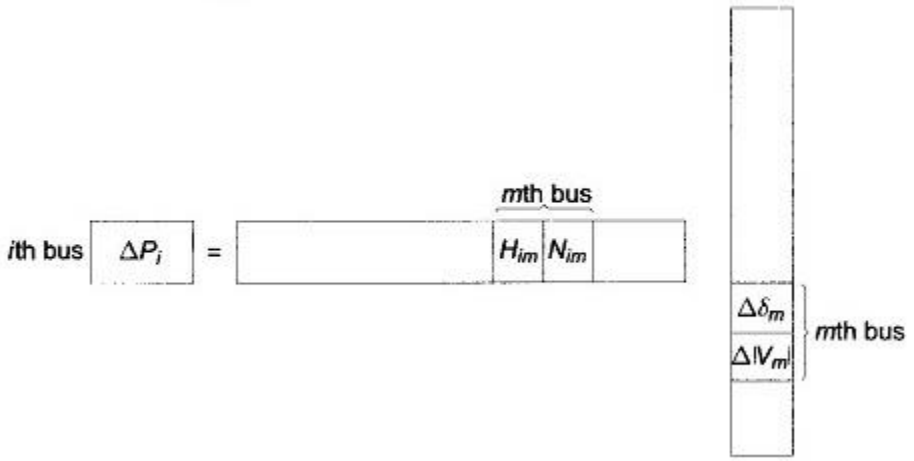

(6.62b)

If the mth bus is likewise a PV bus, then |Vm| is fixed, making |Vm| equal to 0. Now we can write

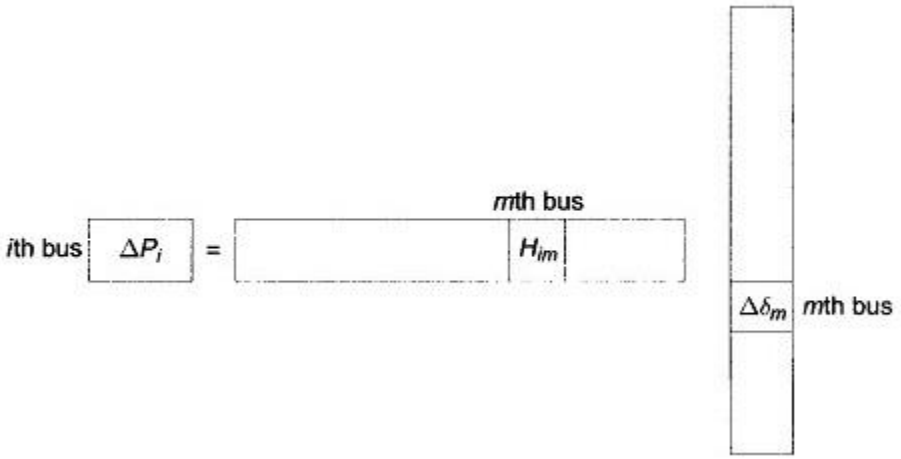

(6.62c)

Additionally, we may write if the mth bus is a PV bus and the ith bus is a PQ bus.

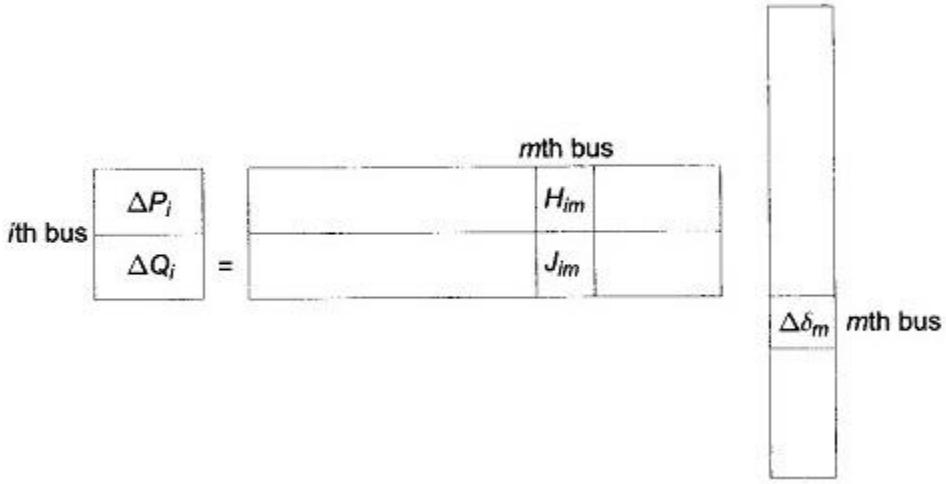

(6.62d)

The voltage adjustments may easily be normalised for numerical solutions.

$$\frac{\Delta|V_m|}{|V_m|}$$

The associated Jacobian components as a result become

$$N_{im} = \frac{\partial P_i}{\partial|V_m|}|V_m|$$

$$L_{im} = \frac{\partial Q_i}{\partial|V_m|}|V_m| \qquad (6.63b)$$

The following expressions are provided for the Jacobian's (in normalised form) components in the load flow equations (6.60a and b):

Case 1:

$$m \neq i$$

$$H_{im} = L_{im} = a_m f_i - b_m e_i \tag{6.64}$$

$$N_{im} = -J_{im} = a_m e_i + b_m f_i$$

where

$$Y_{im} = G_{im} + jB_{im}$$

$$V_i = e_i + jf_i$$

$$(a_m + jb_m) = (G_{im} + jB_{im})\ (e_m + jf_m)$$

Case 2:

$$m = i$$

$$H_{ii} = -Q_i - B_{ii}|V_i|^2$$

$$N_{ii} = P_i + G_{ii}|V_i|^2 \tag{6.65}$$

$$J_{ii} = P_i - G_{ii}|V_i|^2$$

$$L_{ii} = Q_i - B_{ii}|V_i|^2$$

By looking at the YBUS matrix, a significant observation about the Jacobian may be made. Without a connection between buses I and m, Yim = 0 (Gim = Bim = 0). Therefore, we may write using Eqs. (6.63) and (6.64).

$$H_{im} = H_{mi} = 0$$

$$N_{im} = N_{mi} = 0$$

$$J_{im} = J_{mi} = 0 \tag{6.66}$$

$$L_{im} = L_{mi} = 0$$

The Jacobian is therefore equally sparse to the YBUS matrix.

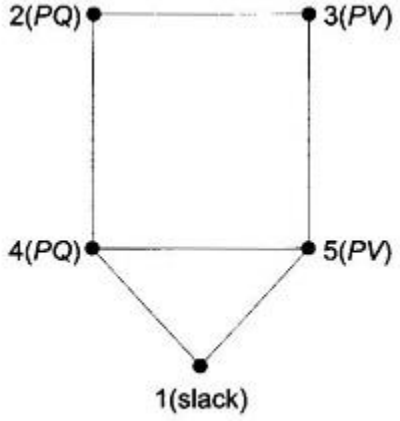

Fig. 6.10 Sample five-bus network

The finest example of how to create Eq. (6.62) of the NR technique is a problem. A five-bus power network with different bus types is shown in Figure 6.10. The following matrix equation may be used to get the vector of corrections from the vector of residuals.

The Jacobian (6 x 6 in this case) and the vector of residuals [ΔP2 ΔQ2 ΔP3 ΔP4 ΔQ4 ΔP5]T are computed according to a specific vector of variables [δ2|V2|δ3δ4|V4|δ5]T. The vector of adjustments is then obtained by triangularizing and back substituting the solution to equation (6.67).

$$\left[\Delta\delta_2 \; \frac{\Delta|V_2|}{|V_2|} \; \Delta\delta_3 \Delta\delta_4 \; \frac{\Delta|V_4|}{|V_4|} \; \Delta\delta_5\right]^T$$

The vector of variables is then updated by the addition of corrections.

$$\begin{array}{c|c|c|cccccc|c|}
 & & \longrightarrow \text{Bus No.} & & 2 & 3 & 4 & 5 & & \\
 & & & & & & & & & \\
\text{Bus No.} & & & \Delta P_2 & H_{22} & N_{22} & H_{23} & H_{24} & N_{24} & & \Delta\delta_2 \\
\downarrow & 2 & & \Delta Q_2 & J_{22} & L_{22} & J_{23} & J_{24} & L_{24} & & \frac{\Delta|V_2|}{|V_2|} \\
 & 3 & & \Delta P_3 & H_{32} & N_{32} & H_{33} & & & H_{35} & \Delta\delta_3 \\
 & & & \Delta P_4 & H_{42} & N_{42} & & H_{44} & N_{44} & H_{45} & \Delta\delta_4 \\
 & 4 & = & \Delta Q_4 & J_{42} & L_{42} & & J_{44} & L_{44} & J_{45} & \frac{\Delta|V_4|}{|V_4|} \\
 & 5 & & \Delta P_5 & & & H_{53} & H_{54} & N_{54} & H_{55} & \Delta\delta_5 \\
 & & & \uparrow & & & \uparrow & & & & \uparrow \\
 & & & \text{Residuals} & & & \text{Jacobian} & & & & \text{Corrections} \\
 & & & & & & \text{(Evaluated at trial values of variables)} & & & & \text{in variables}
\end{array} \qquad (6.67)$$

Iterative Algorithm:

The following is the iterative procedure for the NR method's solution to the load flow problem:
1. Assume |V|, δ at all PQ buses, and δ at all PV buses, with voltage and angle at slack bus fixed (typically δ = 0). Without any other information, flat voltage starting is advised.
2. Calculate ΔQi, (for all PQ buses) and ΔPi, (for PV and PQ buses) (6.60a and b). Stop the iterations, compute P1 and Q1, and display the whole solution, including line flows, if all values are below the specified tolerance.
3. If the convergence requirement is not met, use Eqs. (6.64) and (6.65) to assess the Jacobian's components (6.65).
4. To compensate for voltage angles and magnitudes, solve Eq. (6.67). **[17]**

Load flow analysis of an IEEE 9 bus system by using NR method is shown below:

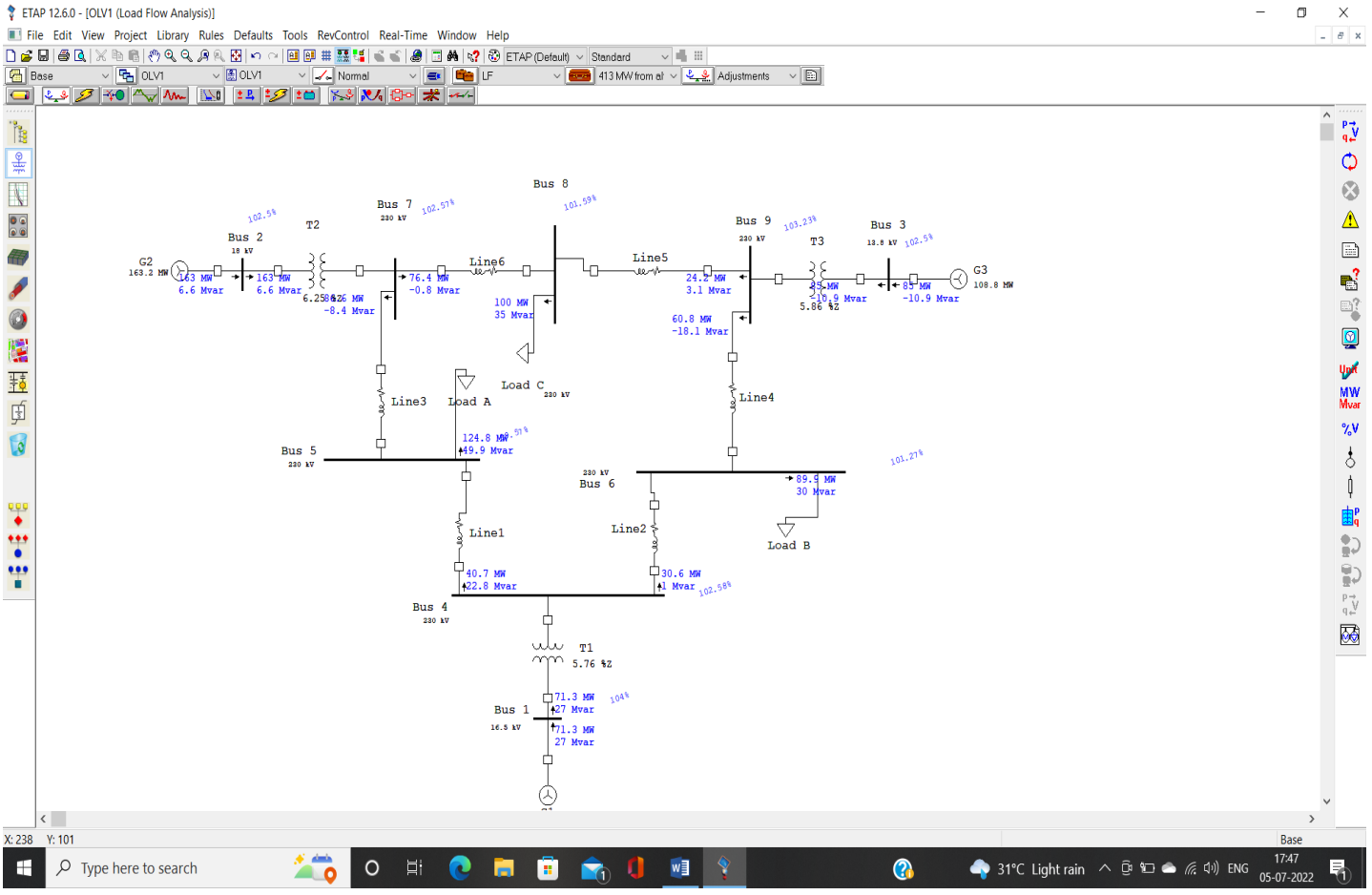

Fig 18: Load flow analysis of an IEEE 9 bus system

4.4. 3 PHASE FULL BRIDGE INVERTER:

A device called a three phase bridge inverter transforms a DC power input into a three phase AC output. It gets its DC power from a battery or, more frequently, a rectifier, just like a single phase inverter. Bridge inverters with six steps are the simplest three phase inverters. Six thyristors are used as a minimum. A step, in the context of inverters, is the shift in firing from one thyristor to the next in a sequential manner. Each step is at a 60° interval to obtain a 360° cycle. This implies that thyristors will be properly sequenced and gated at regular intervals of 60 degrees to produce three phase AC output voltage at their output.

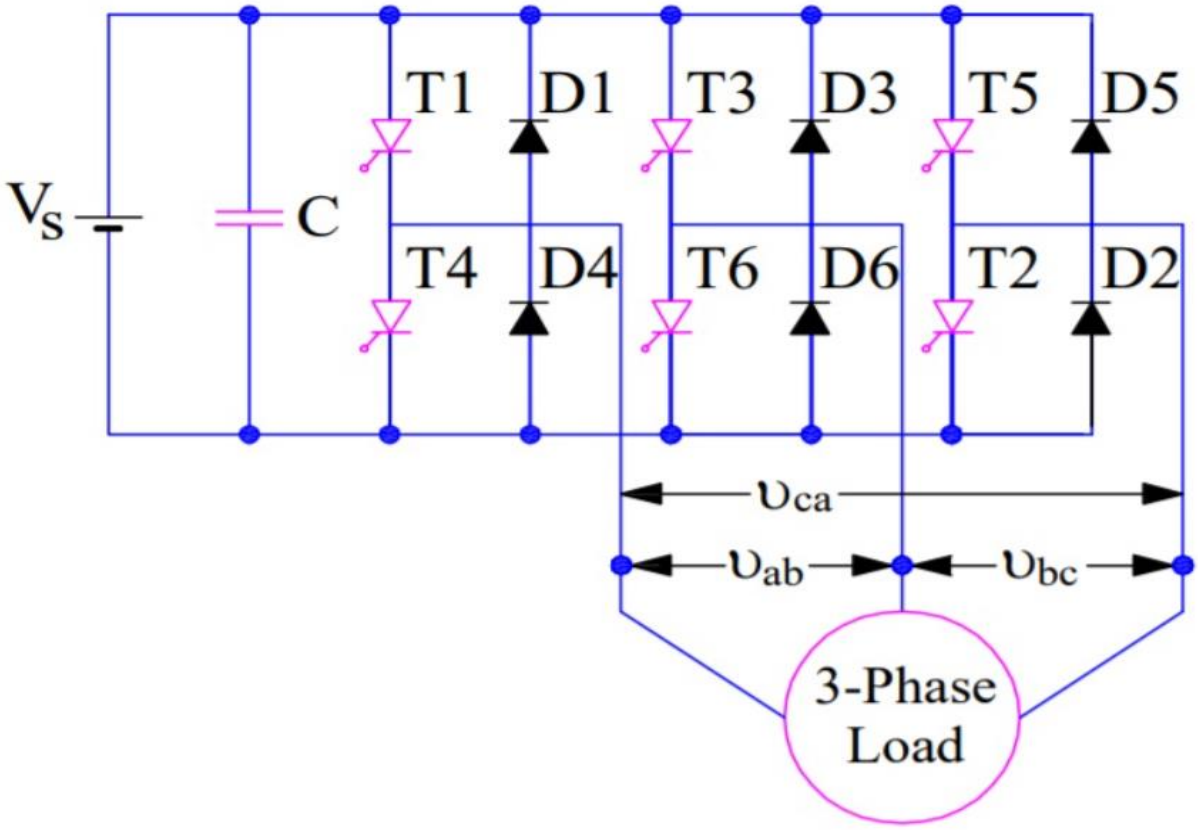

Fig 19: Three Phase full Bridge Inverter [19]

Working Principle of Three Phase Bridge Inverter:

There are two possible patterns of gating the thyristors. In one pattern, each thyristor conducts for 180° and in other, each thyristor conducts for 120°. But in both these patters the gating signals are applied and removed at 60° interval of the output voltage waveform. Therefore, both these models require a six step bridge inverter.

180° Conduction Mode of Three Phase Inverter:

Each thyristor conducts for 180 degrees when the three phase inverter is operating in 180° conduction mode. Thyristor pair (T1, T4), (T3, T6), and (T5, T2) are switched on in each arm with a 180° time interval. It denotes that T1 stays on for 180 degrees and T4 conducts for the next 180 degrees in a cycle. Thyristors in the top group, T1, T3, and T5, conduct at a 120° angle. It indicates that if T1 is shot at wt = 0°, T3 and T5 will follow at 120° and 240°, respectively. Additionally, lower group thyristors, i.e. (T4, T6 & T2).

120° Conduction Mode of Three Phase Inverter:

Each thyristor conducts for 120° of a cycle in an inverter with a 120° mode. Similar to an inverter operating in 180° mode, a 120° mode inverter similarly needs six steps, each lasting 60°, to complete an output AC voltage cycle. Here, it should be remembered that a step is nothing more than the transition from firing one thyristor to the next in the appropriate order. T1 is demonstrated to conduct for 120° before ceasing to conduct for the next 60°. At wt=180°, T4 is switched ON and conducts for the next 120°, or until t = 300°. This simply indicates that neither T1 nor T4 conducts during a 60° interval, or from t=300° to 360°. In actuality, T4 is tuned OFF at t = 300° and is tuned ON again at t = 360°. At t = 120°, T3 is switched ON and conducts for the next 120°. After then, there is a 60° break during which neither T3 nor T6 conduct. T6 is switched ON when t = 300°. Additionally, it continues for the following 120°, after which a 60° gap follows, and T3 is switched ON once more. The third row is finished in a similar way.

The minimum rating of the inverter that has been used to analyze the power flow analysis of the BUS system is shown below.

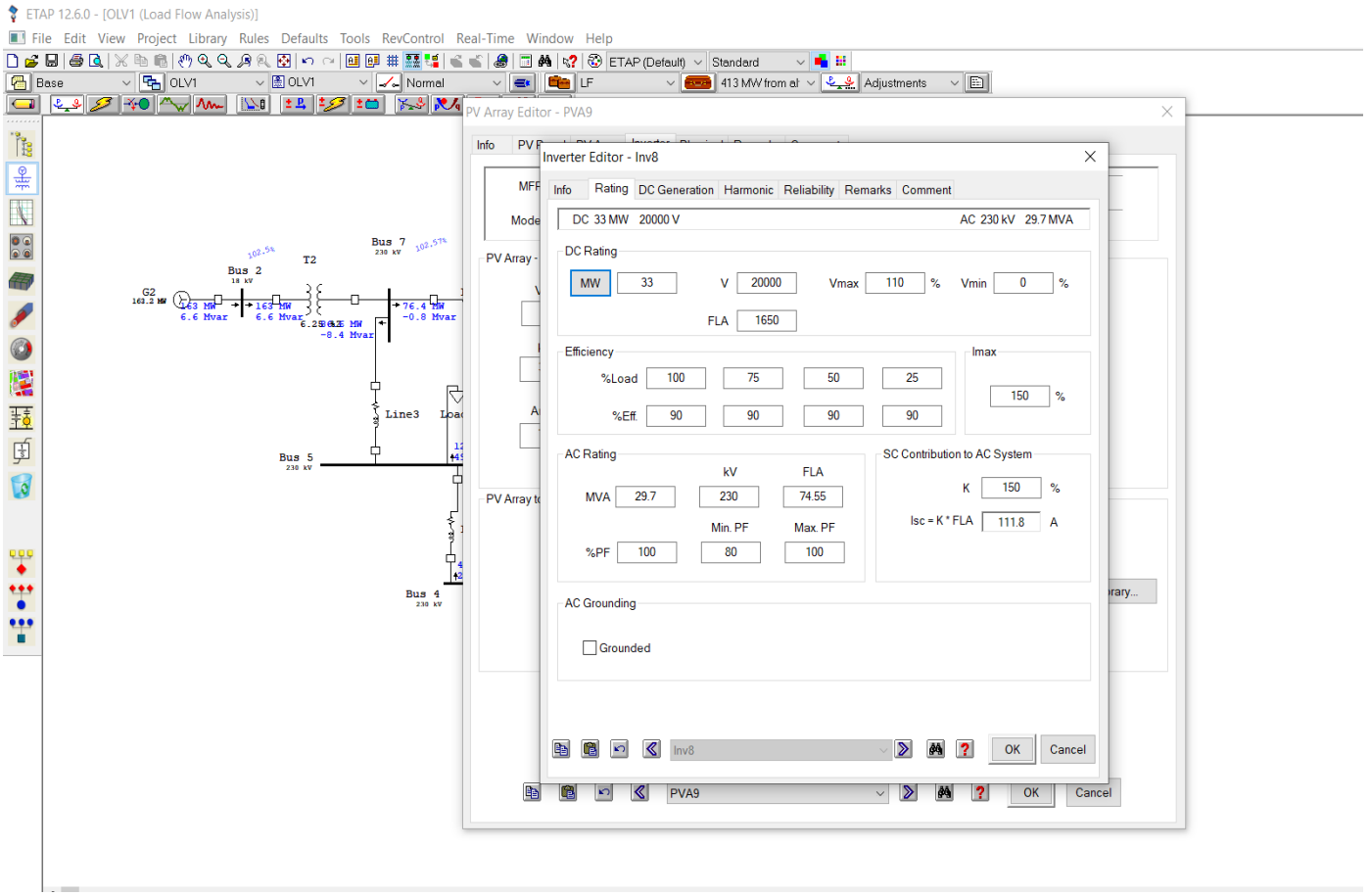

Fig 20: Rating of Inverter

4.5. HARMONIC ANALYSIS:

A power system's output of voltage and current is not a pure sine wave. There is some distortion present, including harmonics at the fundamental frequency and some distortion itself. The most often used index to gauge how much harmonic distortion there is in voltage and current is known as Total Harmonic Distortion (THD), also known as Harmonic Distortion Factor (DF). THD is calculated as the ratio between the RMS values of all harmonic components and the RMS value of the fundamental component, and it is often represented as a percentage (%).

Voltage and current waveforms are distorted, changing their typical features or shapes. It is often categorised as a severe power quality issue. As was already mentioned, the usage of inverters, converters, and other power electronic equipment in PV systems can result in the production of harmonics. In this regard, various distortion-producing power-electronic components are found in photovoltaic power plants. The high current and voltage harmonics' amplitudes also cause grid-side protection systems to malfunction and cause extra losses in the power system.

Total Harmonic Distortion (THD):

The number of harmonics on a line relative to the line fundamental frequency, such as 50Hz, is known as total harmonic distortion (THD). The THD takes into account every harmonic frequency on a line. Both current and voltage harmonics can be connected to THD.

Mathematically, it can be represented in equation 7 as

$$THD = \sqrt{\{(\frac{v_{or}}{v_{or1}})^2 - 1\}} \ldots\ldots\ldots\ldots(7)$$

Where v_{or} = rms output voltage and v_{or1} = fundamental rms output voltage

Voltage Distortion Factor (VDF):

VDF is the ratio of fundamental rms output voltage and rms output voltage.
Mathematically, it can be represented in equation 8 as

$$VDF = \frac{v_{or1}}{v_{or}} \ldots\ldots\ldots\ldots(8)$$

4.6. CONCLUSION:

I have read several thesis papers in order to obtain these ideas and these ideas have assisted me towards the completion of the project. Grid-connected home PV systems are typically modest to medium in size compared to the distribution grid's high short-circuit levels. Voltage distortion is thus minimal when a single PV system is connected to the grid.

Chapter 5: SYSTEM DESCRIPTION AND EXPERIMENTAL PROCEDURE:

5.1. INTRODUCTION:

In the previous section, present technologies and their applications has been discussed. In this section, system description and the flow chart will be discussed that means step by step process will be shown by flowchart. Below flowchart explains the steps involved in this project.

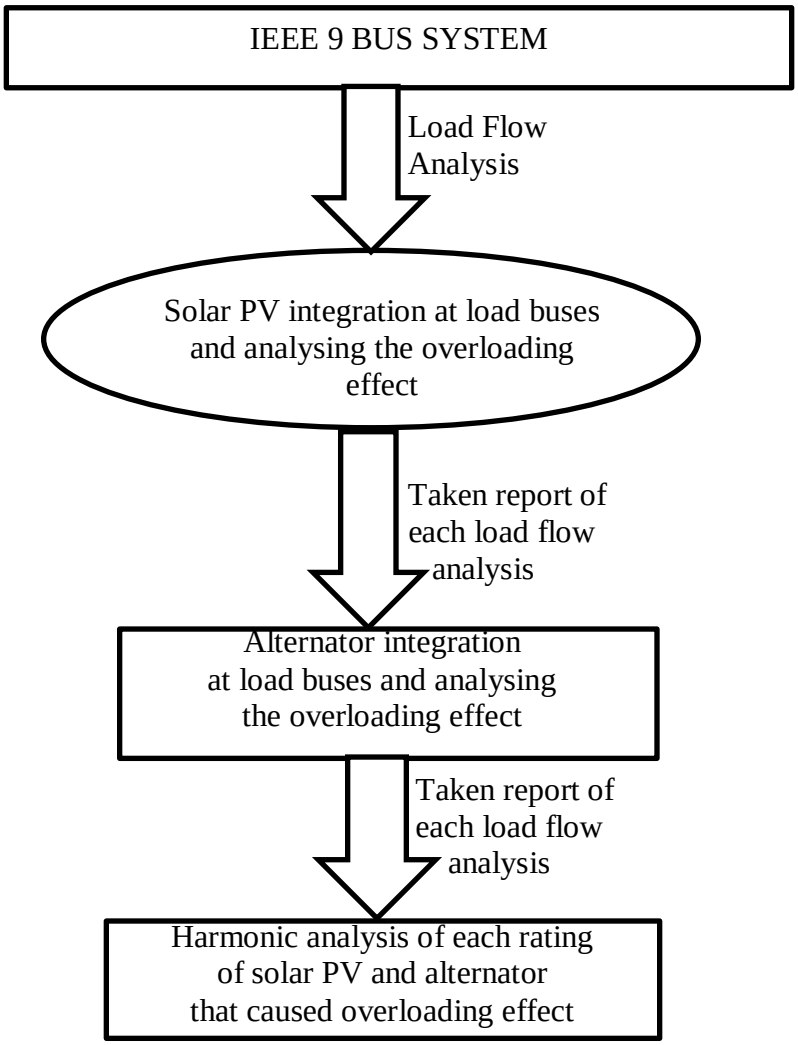

Fig. 21: Flowchart of the Experimental Procedure

5.2. SYSTEM DESCRIPTION:

Power systems experts utilise the Electrical Transient analyser Program (ETAP), a modelling and simulation tool for electrical networks, to build an "electrical digital twin" to examine the dynamics, transients, and protection of electrical power systems. A power system network model with system connections, topology, electrical device characteristics, historical system response, and real-time operations data is needed for power system simulation in order to make offline or online choices. Electrical engineers and operators can conduct numerous studies using ETAP power engineering software in offline or online mode by using an electrical digital twin.

5.3. EXPERIMENTAL PROCEDURE:

There are several steps that has been taken to proceed this experiment.

1. At first, a standard IEEE 9 BUS system has been taken by using standard IEEE 9 BUS system rating. This 9 BUS system consists of following elements like:
    - 3 synchronous generators of ratings 247.5 MW, 108.8 MW and 163.2 MW.
    - 3 two winding transformers of ratings 100 MVA and per unit impedances of 5.76 pu, 5.86 pu and 6.25 pu.
    - 6 transmission lines of various impedances according to the standard values of IEEE system.
    - 3 static loads of ratings 135.532 MVA, 92.45 MVA, 102.64 MVA.

Figure 3.1 shows a standard 9 BUS system with the elements used to design the system.

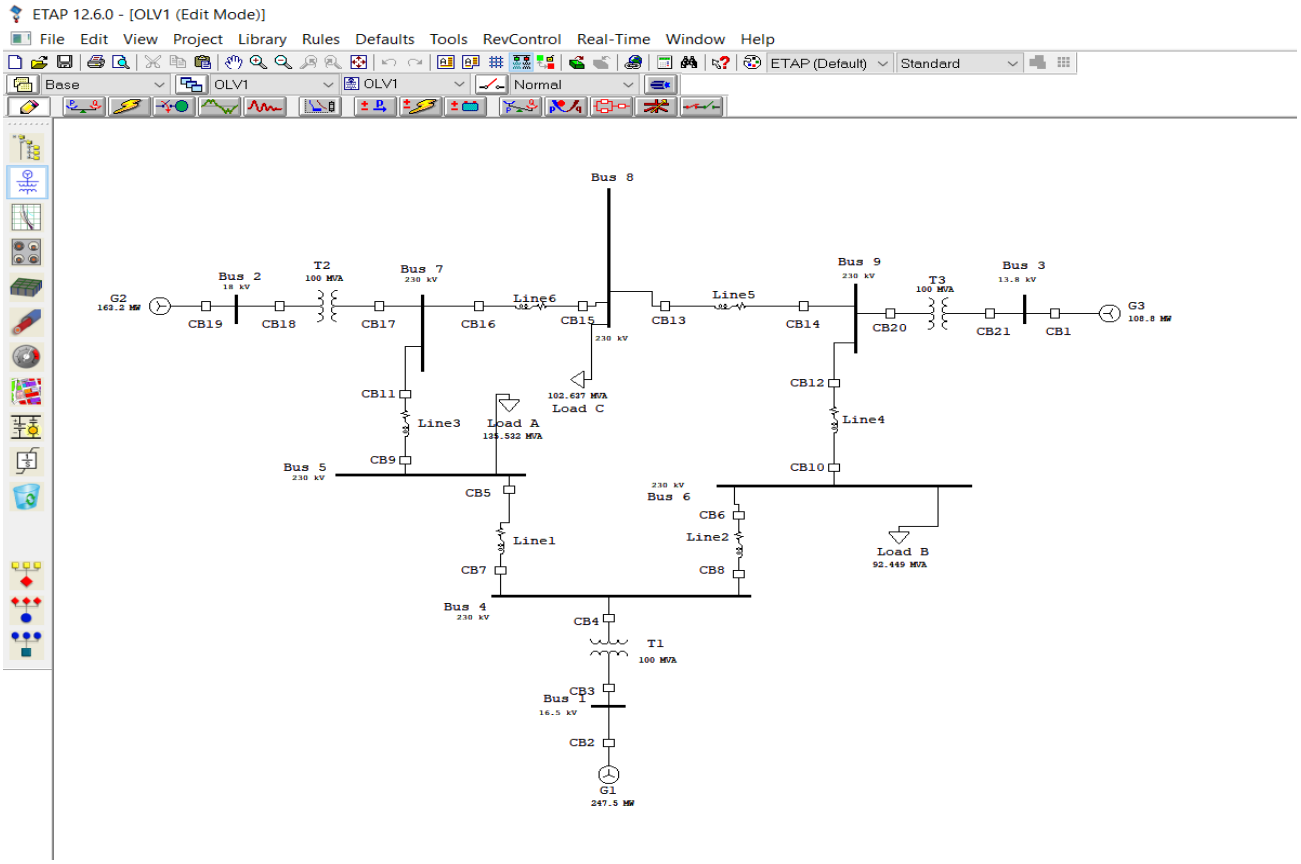

Fig 3.1: IEEE 9 BUS system

2. After that, load flow studies by using adaptive Newton Raphson method has been used. In the Load Flow Analysis mode of ETAP, study case has been edited and iterative method was selected as adaptive Newton Raphson method where maximum iteration is 9999 and precision was taken as 0.0001. Then load flow analysis has been done by using NR method.

Figure 18.1 are represented to simplify step two of the experimental procedure.

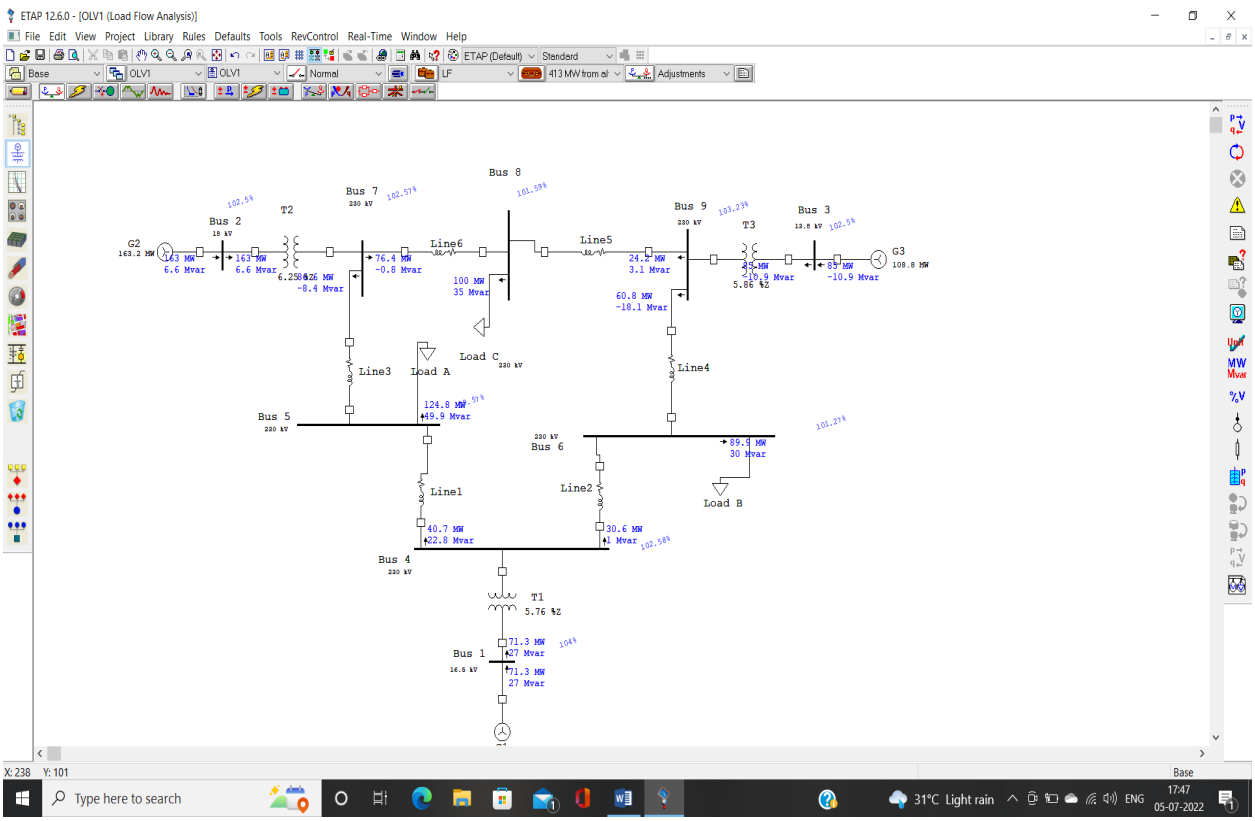

Fig 18.1: Load Flow Analysis

3. Then, a PV system has been selected. The minimum rating of the system is 10% of the total load that means three static loads has been used and combined load of the system is approximately 330 MW. So, minimum rating of PV system is taken as 33 MW.

Figure 22 shows the minimum rating of the PV system.

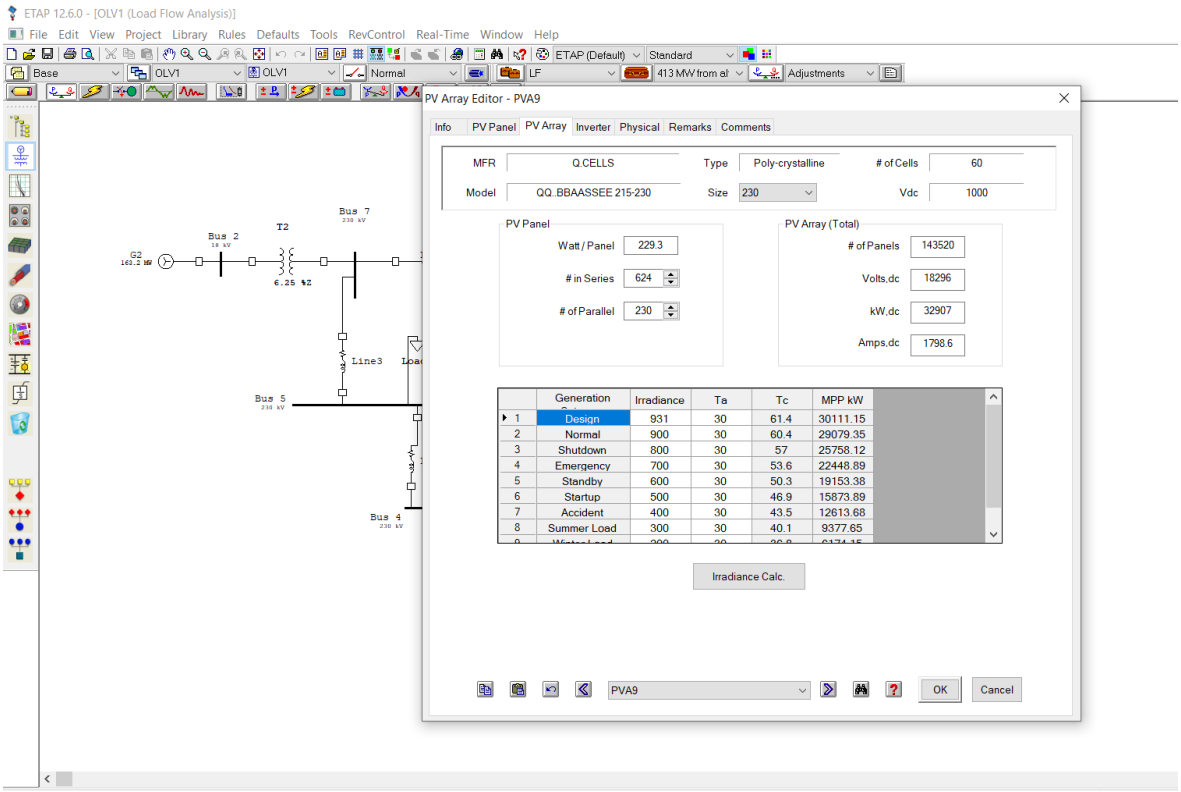

Fig 22: Rating of 33 MW PV system

4. After that, in each step 10% increment has been done and load flow analysis has been performed in each cases by integrating solar PV system in each load buses. Here PV system rating from 33 MW to 496 MW has been used and all PV systems between the ranges has been integrated at all 3 load buses.

Figure 23 shows the analysis of load flow by integrating 33 MW PV system at BUS 8.

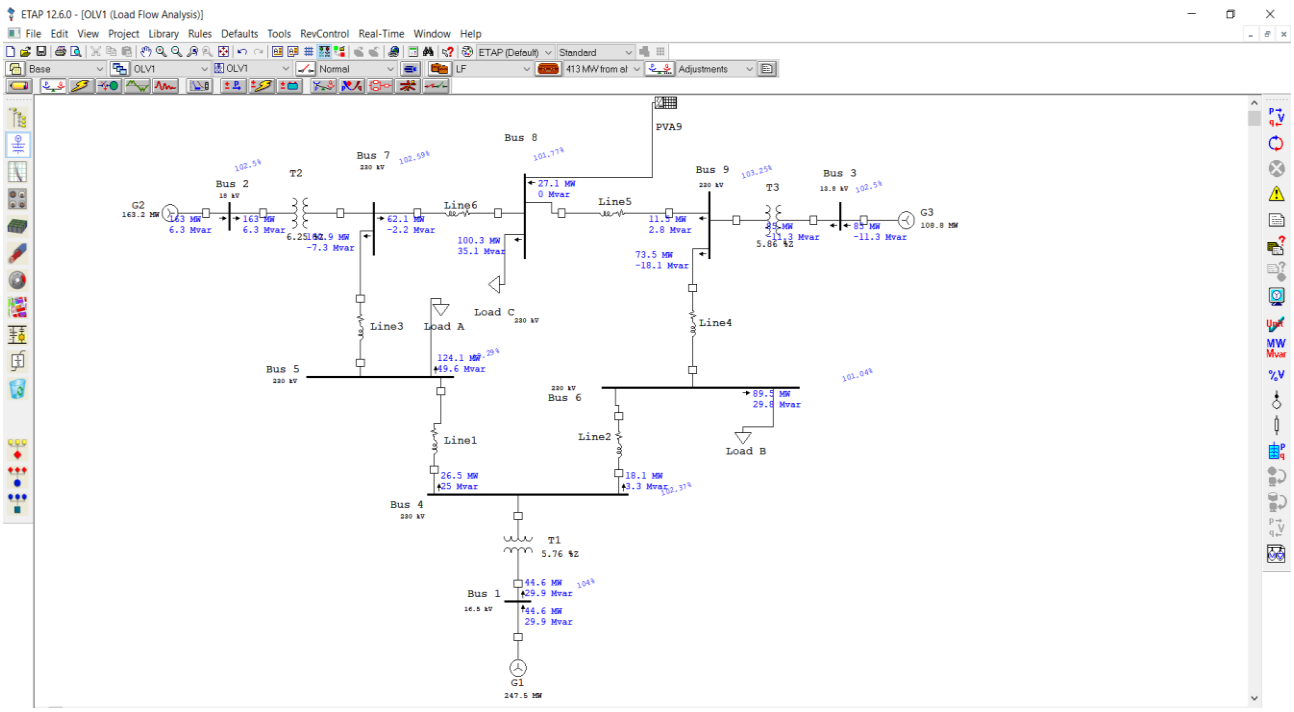

Fig 23: Load Flow Analysis by integrating Solar PV

5. Then, by integrating solar PV with each buses overloading effect has been analysed that means first BUS 8 has been taken and rating used is between 33 MW to 413 MW. For each cases, overloading effect of each buses has been analysed. After that, BUS 5 and BUS 6 are also taken and has been analysed accordingly.

Each cases has been taken for each buses. Power flow has been considered at each BUS and corresponding overloading effect has also been considered. Here, in each cases, every buses flows power to two transmission lines and one static load. Three cases has been discussed and each case describes the overloading effect of other buses.
Synchronous generator was also used to analyse the overloading effect of the system as alternator was delivering reactive power too with the real power but PV system was delivering only real power as we have considered unity power factor for solar PV inverter. Following tables are used to compare the overloading effect of the 9 BUS system after integrating solar PV and alternator.

Table 5.1: Effect of PV system and alternator integration at BUS 8

Supplied by PV system	Supplied by Alternator System	Supplied to line 5 By PV system	Supplied to line 5 by alternator	Supplied to line 6 by PV system	Supplied to line 6 by alternator	Supplied to load C by PV system	Supplied to load C by alternator
217.5 MW (BUS5 and GEN1 is overloaded)	132 MW + 9 MVAr(GEN1 is overloaded)	80.2 MW – 24.7 MVAr	37.7 MW – 20.9 MVAr	38.1 MW – 10 MVAr	– (7.5 MW – 9.9 MVAr)	99.3 MW + 34.7 MVAr	101 MW + 35.6 MVAr
245.5 MW (BUS5 and GEN1 is overloaded)	230 MW + 21 MVAr(BUS5 and GEN1 is overloaded)	94.2 MW – 24.6 MVAr	84.9 MW – 15.8 MVAr	52.9 MW – 9.8 MVAr	43.3 MW + 1.1 MVAr	98.4 MW + 34.4 MVAr	101.8 MW + 35.6 MVAr
264.4 MW (BUS5 & BUS6 and GEN1 is overloaded)	300 MW + 39.2 MVAr(BUS5 ,BUS6 and GEN1 is overloaded)	103.8 MW – 24.5 MVAr	119.9 MW – 7.8 MVAr	62.9 MW – 9.7 MVAr	79.1 MW + 11.4 MVAr	97.7 MW + 34.2 MVAr	101.8 MW + 35.6 MVAr
311.6 MW (BUS4,BUS5 & BUS6 is overloaded)	380 MW + 74 MVAr(BUS4 ,BUS5,BUS6 and GEN1 is overloaded)	128.4 MW – 24.1 MVAr	159.1 MW + 7.5 MVAr	87.8 MW – 9.2 MVAr	119.1 MW + 30.8 MVAr	95.4 MW + 33.4 MVAr	101.8 MW + 35.6 MVAr
339.9 MW (BUS4,BUS5 & BUS6 is overloaded)	430 MW + 100 MVAr(BUS4 ,BUS5,BUS6 and GEN1 is overloaded)	143.6 MW – 23.8 MVAr	186.1 MW + 19.3 MVAr	102.8 MW – 8.9 MVAr	143.6 MW + 45.6 MVAr	93.5 MW + 32.7 MVAr	100.3 MW + 35.1 MVAr

Table 5.2: Effect of PV system and alternator integration at BUS 5

Supplied by PV system	Supplied by Alternator system	Supplied from line 3 by PV system	Supplied to line 3 by alternator	Supplied to line 1 by PV system	Supplied to line 1 by alternator	Supplied to load A by PV system	Supplied to load A by alternator
108.5 MW (GEN1 is overloaded)	132 MW +26.6 MVAr(GEN1 is overloaded)	73.1 MW – 11.3 MVAr	– (70.6 MW – 21.7 MVAr)	53.2 MW – 38.6 MVAr	68.9 MW – 23.1 MVAr	126.7 MW + 50.7 MVAr	132.2 MW + 52.9 MVAr
162.4 MW (GEN1 is overloaded)	265 MW + 35.4 MVAr(GEN1 is overloaded)	66.4 MW – 10.8 MVAr	– (54.4 MW – 20.7 MVAr)	100.8 MW – 36.7 MVAr	186.2 MW – 10.3 MVAr	126.6 MW + 50.6 MVAr	132.2 MW + 52.9 MVAr
189.6 MW(GEN1 is overloaded)	380 MW + 59.9 MVAr(GEN1 is overloaded)	63 MW – 10.0 MVAr	– (40.2 MW – 19.8 MVAr)	125.1 MW – 35.2 MVAr	287.5 MW – 17 MVAr	126.3 MW + 50.5 MVAr	132.2 MW + 52.9 MVAr

Table 5.3: Effect of PV system and alternator integration at BUS 6

Supplied by PV system	Supplied by Alternator system	Supplied from line 4 by PV system	Supplied to line 4 by alternator	Supplied to line 2 by PV system	Supplied to line 2 by alternator	Supplied to load B by PV system	Supplied to load B by alternator
108.5 MW(GEN1 is overloaded)	132 MW + 0.8 MVAr(GEN1 is overloaded)	46.5 MW – 21.5 MVAr	– (43.4 MW – 21.8 MVAr)	62.3 MW – 17.6 MVAr	82.6 MW – 16.8 MVAr	91.9 MW + 30.6 MVAr	92.1 MW + 30.7 MVAr
162.4 MW(GEN1 is overloaded)	230 MW + 3.6 MVAr(GEN1 is overloaded)	39.4 MW – 21.2 MVAr	– (30.7 MW – 20.2 MVAr)	109.2 MW – 16.4 MVAr	168.2 MW – 11 MVAr	92.1 MW + 30.7 MVAr	92.1 MW + 30.7 MVAr
217.5 MW(GEN1 is overloaded)	265 MW + 7.3 MVAr(GEN1 is overloaded)	32.3 MW – 19.4 MVAr	– (26.2 MW – 19.7 MVAr)	157.7 MW – 13.8 MVAr	198.8 MW – 6.2 MVAr	91.7 MW + 30.6 MVAr	92.1 MW + 30.7 MVAr

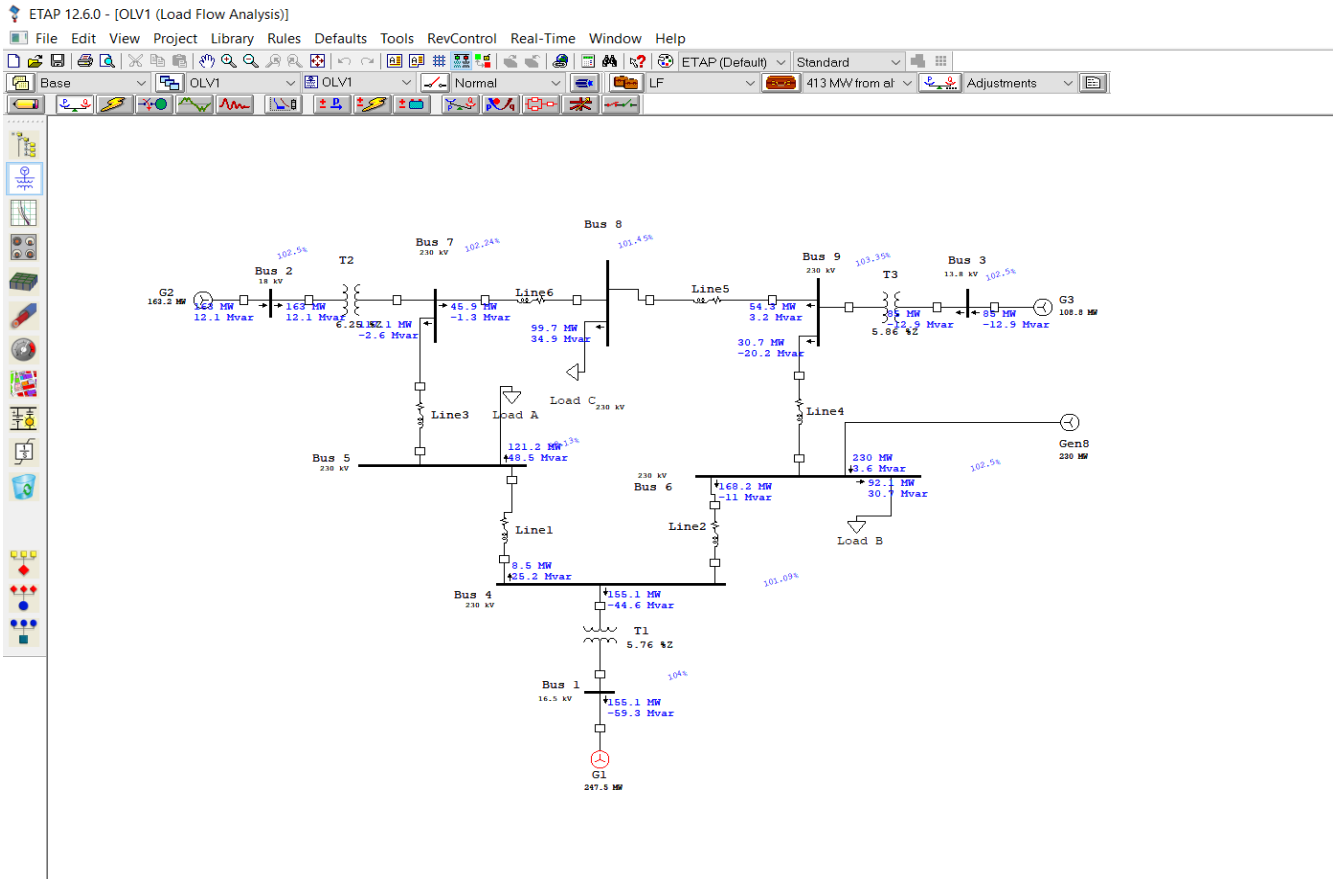

Fig 24: Load Flow Analysis by integrating synchronous generator

6. After that, minimum and maximum ratings of alternator and solar PV has been taken and by integrating PV and alternator in each buses harmonic spectrum and distorted waveforms has been observed.

Following figures has shown the harmonic load flow of the system by integrating minimum ratings of solar PV and alternator given that two winding transformers and static loads consists of harmonics in their systems.

Figure 15 represents two winding transformer harmonics and Figure 25 represents the harmonics present in the static loads.

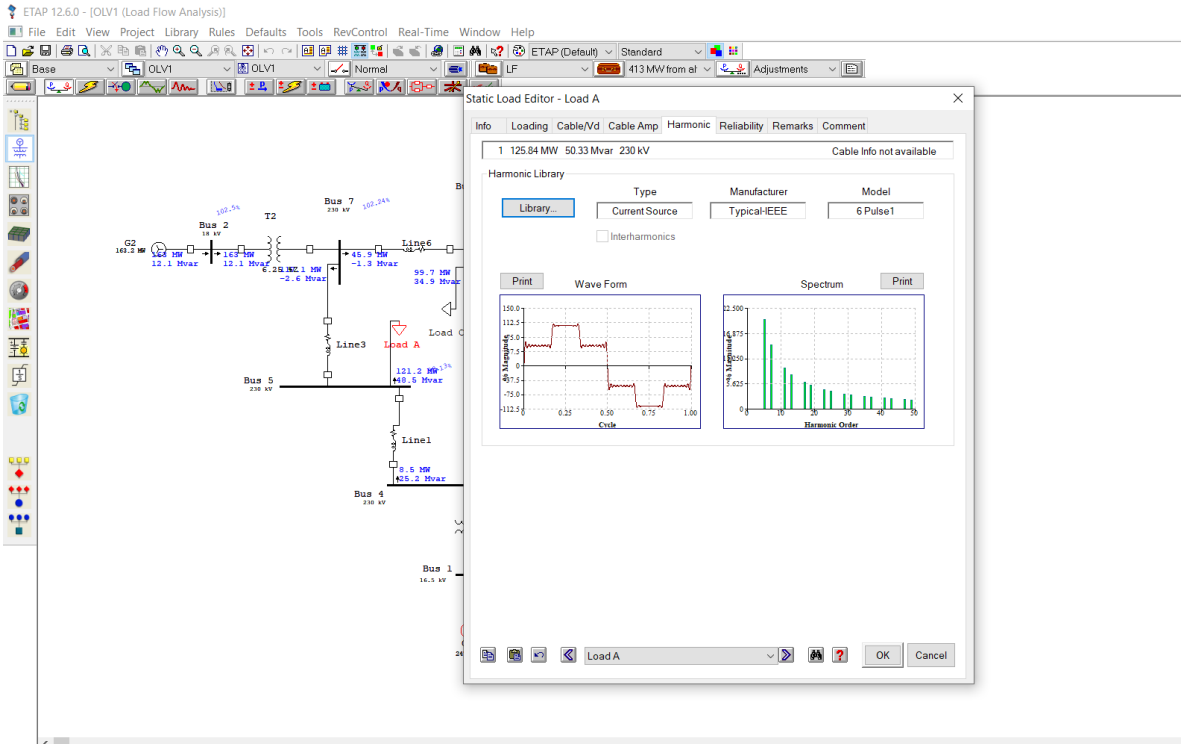

Fig 25: Harmonics present in static loads

For example, Minimum rating of PV and alternator has been integrated to BUS 8 and corresponding spectrum and waveform has been shown below.

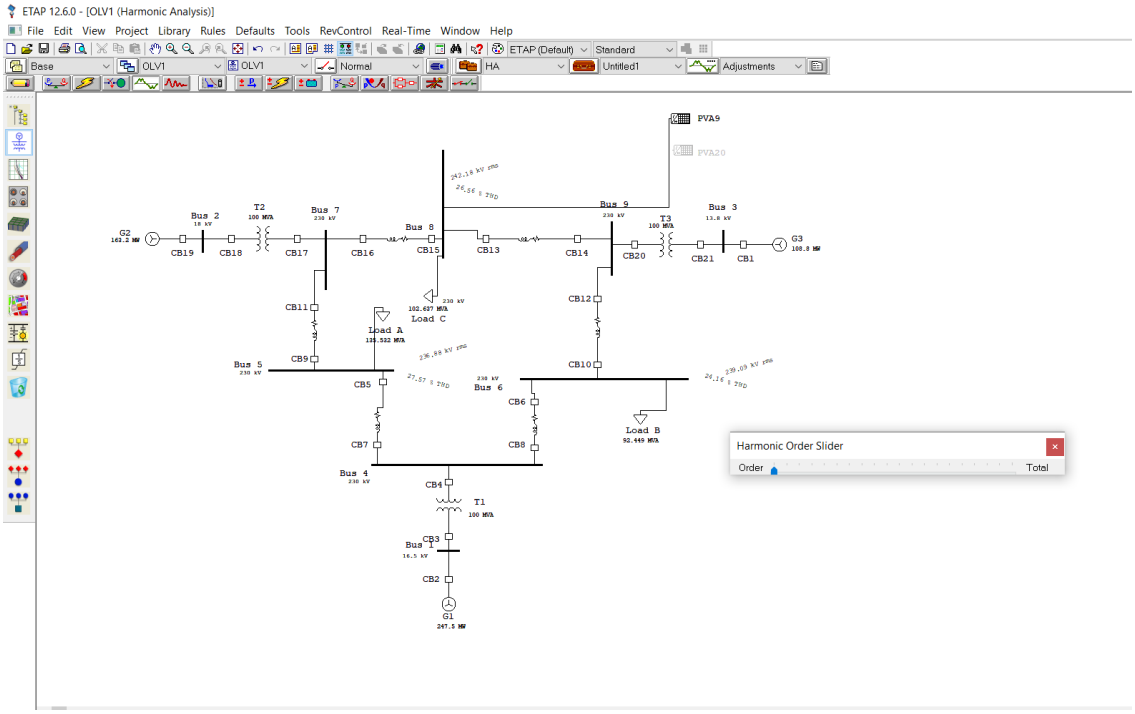

Fig 26: Harmonic load flow by integrating solar PV

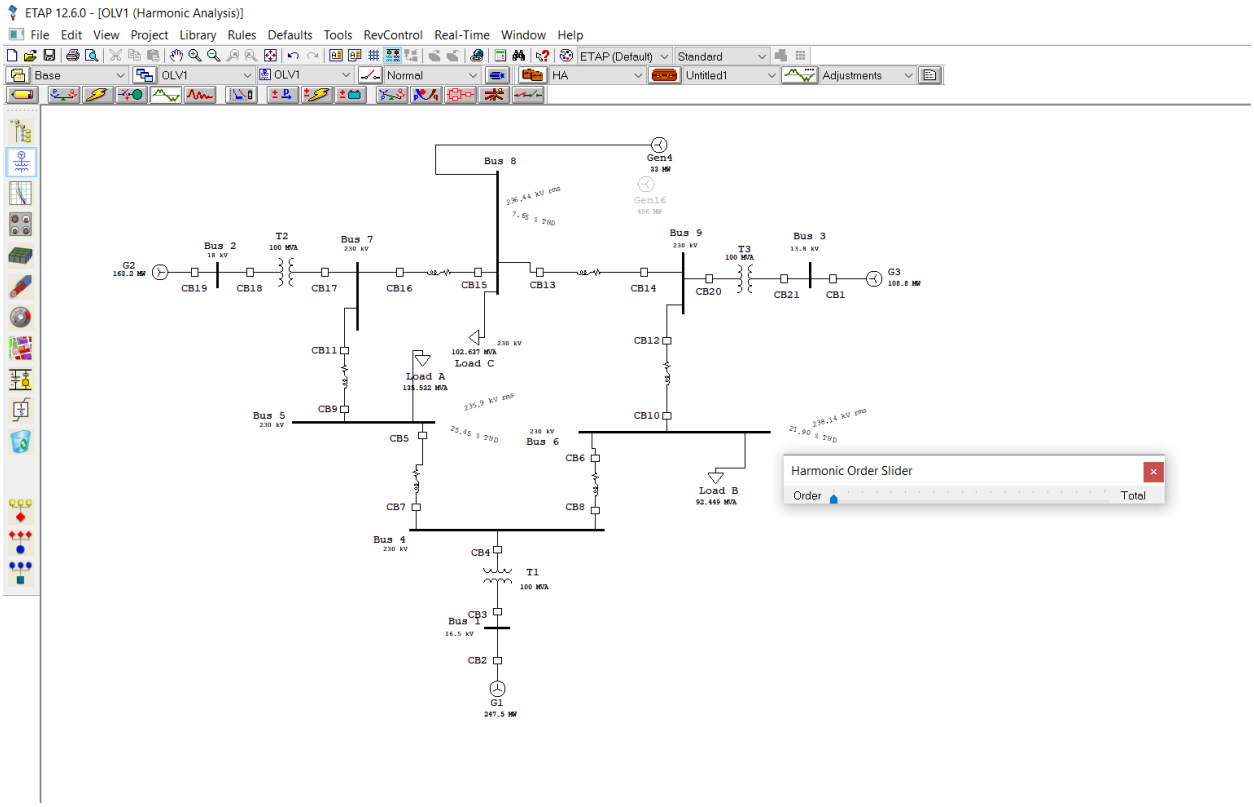

Fig 27: Harmonic load flow by integrating alternator

5.4. CONCLUSION:

These concepts, which I discussed in-depth in the previous sections, are crucial components that are aiding in building the framework for this project. I have discussed the steps which I have done to complete this project. So, in these project I have done a comparison of the overloading effect of an IEEE 9 BUS system by integrating solar PV and alternator. Then, I have done the harmonic analysis for each cases considering the presence of harmonics in the two winding transformers and the static loads.
In the next chapter, I will present the results of analysis and also give a discussion about the results.

Chapter 6: RESULTS AND DISCUSSION

6.1. INTRODUCTION:

In the previous section, system description and procedure to experiment of the project has been discussed. In this section, load flow analysis reports and corresponding harmonic analysis that includes voltage spectrum report and harmonic waveform report has been discussed.

6.2. RESULTS DURING EACH STEP:

At first step, I have done the load flow analysis by integrating solar PV and alternator and power rating used was in between 33 MW and 413 MW.
For each cases, load flow report has been taken and reports will be attached for each overloading cases according to Table 5.1, Table 5.2 and Table 5.3.
Following reports has been generated by integrating solar PV and alternator at BUS 8.

LOAD FLOW REPORT

Bus		Voltage		Generation		Load		Load Flow					XFMR
ID	kV	% Mag.	Ang.	MW	Mvar	MW	Mvar	ID	MW	Mvar	Amp	%PF	%Tap
* Bus 1	16.500	104.000	0.0	-145.801	100.698	0	0	Bus 4	-145.801	100.698	5961.7	-82.3	
* Bus 2	18.000	102.500	33.8	163.000	31.232	0	0	Bus 7	163.000	31.232	5193.5	98.2	
* Bus 3	13.800	102.500	27.8	85.000	11.370	0	0	Bus 9	85.000	11.370	3500.3	99.1	
Bus 4	230.000	98.762	4.7	0	0	0	0	Bus 5	-74.850	53.992	234.6	-81.1	
								Bus 6	-70.968	29.985	195.8	-92.1	
								Bus 1	145.818	-83.977	427.7	-86.7	
Bus 5	230.000	94.400	9.0	0	0	112.142	44.848	Bus 4	75.825	-62.123	260.7	-77.4	
								Bus 7	-187.967	17.274	501.9	-99.6	
Bus 6	230.000	96.745	9.0	0	0	82.089	27.363	Bus 4	72.094	-38.996	212.7	-88.0	
								Bus 9	-154.183	11.633	401.2	-99.7	
Bus 7	230.000	101.075	28.1	0	0	0	0	Bus 5	200.997	19.017	501.4	99.6	
								Bus 8	-38.014	-4.171	95.0	99.4	
								Bus 2	-162.984	-14.846	406.4	99.6	
Bus 8	230.000	101.187	29.7	217.525	0.000	99.192	34.703	Bus 9	80.198	-24.660	208.1	-95.6	
								Bus 7	38.135	-10.043	97.8	-96.7	
Bus 9	230.000	101.961	25.1	0	0	0	0	Bus 6	164.424	-2.352	404.8	-100.0	
								Bus 8	-79.428	9.620	197.0	-99.3	
								Bus 3	-84.996	-7.268	210.0	99.6	

Figure 28.1: 217.5 MW supply from PV system to BUS 8

LOAD FLOW REPORT

Bus		Voltage		Generation		Load		Load Flow					XFMR
ID	kV	% Mag.	Ang.	MW	Mvar	MW	Mvar	ID	MW	Mvar	Amp	%PF	%Tap
* Bus 1	16.500	104.000	0.0	-58.052	54.811	0	0	Bus 4	-58.052	54.811	2686.2	-72.7	
* Bus 2	18.000	102.500	23.2	163.000	9.164	0	0	Bus 7	163.000	9.164	5108.8	99.8	
* Bus 3	13.800	102.500	17.9	85.000	-8.679	0	0	Bus 9	85.000	-8.679	3487.4	-99.5	
Bus 4	230.000	101.019	1.8	0	0	0	0	Bus 5	-28.087	36.754	114.9	-60.7	
								Bus 6	-29.969	14.663	82.9	-89.8	
								Bus 1	58.056	-51.417	192.7	-74.9	
Bus 5	230.000	97.489	3.5	0	0	119.602	47.832	Bus 4	28.369	-51.698	151.8	-48.1	
								Bus 7	-147.970	3.866	381.1	-100.0	
Bus 6	230.000	99.502	3.6	0	0	86.834	28.945	Bus 4	30.205	-29.272	106.1	-71.8	
								Bus 9	-117.038	0.327	295.3	100.0	
Bus 7	230.000	102.415	17.6	0	0	0	0	Bus 5	155.457	3.206	381.1	100.0	
								Bus 8	7.527	-9.897	30.5	-60.5	
								Bus 2	-162.984	6.691	399.8	-99.9	
* Bus 8	230.000	102.500	17.3	132.000	9.032	101.784	35.610	Bus 9	37.739	-20.874	105.6	-87.5	
								Bus 7	-7.523	-5.704	23.1	79.7	
Bus 9	230.000	103.106	15.2	0	0	0	0	Bus 6	122.563	-12.997	300.1	-99.4	
								Bus 8	-37.567	0.246	91.5	100.0	
								Bus 3	-84.996	12.751	209.2	-98.9	

Figure 28.2: 132 MW supply from alternator to BUS 8

Following reports has been generated by integrating solar PV and alternator at BUS 5.

LOAD FLOW REPORT

Bus		Voltage		Generation		Load		Load Flow					XFMR
ID	kV	% Mag.	Ang.	MW	Mvar	MW	Mvar	ID	MW	Mvar	Amp	%PF	%Tap
* Bus 1	16.500	104.000	0.0	-35.319	28.620	0	0	Bus 4	-35.319	28.620	1529.5	-77.7	
* Bus 2	18.000	102.500	15.8	163.000	4.115	0	0	Bus 7	163.000	4.115	5102.3	100.0	
* Bus 3	13.800	102.500	9.9	85.000	-10.662	0	0	Bus 9	85.000	-10.662	3496.6	-99.2	
Bus 4	230.000	102.436	1.1	0	0	0	0	Bus 5	-52.880	23.691	142.0	-91.3	
								Bus 6	17.560	3.828	44.0	97.7	
								Bus 1	35.320	-27.520	109.7	-78.9	
Bus 5	230.000	100.330	3.8	108.461	0.000	126.674	50.660	Bus 4	53.250	-38.640	164.6	-80.9	
								Bus 7	-71.463	-12.020	181.3	98.6	
Bus 6	230.000	101.065	0.3	0	0	89.583	29.861	Bus 4	-17.486	-19.789	65.6	66.2	
								Bus 9	-72.097	-10.072	180.8	99.0	
Bus 7	230.000	102.721	10.3	0	0	0	0	Bus 5	73.090	-11.341	180.7	-98.8	
								Bus 8	89.894	-0.360	219.7	100.0	
								Bus 2	-162.984	11.701	399.3	-99.7	
Bus 8	230.000	101.643	6.7	0	0	100.089	35.017	Bus 9	-10.850	-25.369	68.1	39.3	
								Bus 7	-89.238	-9.648	221.7	99.4	
Bus 9	230.000	103.219	7.2	0	0	0	0	Bus 6	74.108	-18.516	185.8	-97.0	
								Bus 8	10.888	3.761	28.0	94.5	
								Bus 3	-84.996	14.756	209.8	-98.5	

Figure 29.1: 108.5 MW supply from solar PV to BUS 5

LOAD FLOW REPORT

Bus		Voltage		Generation		Load		Load Flow					XFMR
ID	kV	% Mag.	Ang.	MW	Mvar	MW	Mvar	ID	MW	Mvar	Amp	%PF	%Tap
* Bus 1	16.500	104.000	0.0	-51.565	16.207	0	0	Bus 4	-51.565	16.207	1818.6	-95.4	
* Bus 2	18.000	102.500	16.6	163.000	-4.426	0	0	Bus 7	163.000	-4.426	5102.6	-100.0	
* Bus 3	13.800	102.500	10.6	85.000	-14.285	0	0	Bus 9	85.000	-14.285	3518.1	-98.6	
Bus 4	230.000	103.145	1.6	0	0	0	0	Bus 5	-68.458	8.519	167.9	-99.2	
								Bus 6	16.891	6.132	43.7	94.0	
								Bus 1	51.567	-14.651	130.5	-96.2	
* Bus 5	230.000	102.500	4.8	132.000	26.631	132.212	52.875	Bus 4	68.928	-23.127	178.1	-94.8	
								Bus 7	-69.140	-3.118	169.5	99.9	
Bus 6	230.000	101.578	0.9	0	0	90.494	30.165	Bus 4	-16.811	-22.260	68.9	60.3	
								Bus 9	-73.683	-7.905	183.1	99.4	
Bus 7	230.000	103.240	11.1	0	0	0	0	Bus 5	70.647	-21.684	179.7	-95.6	
								Bus 8	92.337	1.441	224.5	100.0	
								Bus 2	-162.984	20.243	399.3	-99.2	
Bus 8	230.000	102.024	7.5	0	0	100.840	35.280	Bus 9	-9.190	-23.961	63.1	35.8	
								Bus 7	-91.650	-11.319	227.2	99.2	
Bus 9	230.000	103.426	7.9	0	0	0	0	Bus 6	75.777	-20.580	190.6	-96.5	
								Bus 8	9.219	2.152	23.0	97.4	
								Bus 3	-84.996	18.429	211.1	-97.7	

* Indicates a voltage regulated bus (voltage controlled or swing type machine connected to it)

# Indicates a bus with a load mismatch of more than 0.1 MVA

Figure 29.2: 132 MW supply from alternator to BUS 5

Following reports has been generated by integrating solar PV and alternator at BUS 6.

LOAD FLOW REPORT

Bus		Voltage		Generation		Load		Load Flow					XFMR
ID	kV	% Mag.	Ang.	MW	Mvar	MW	Mvar	ID	MW	Mvar	Amp	%PF	%Tap
* Bus 1	16.500	104.000	0.0	-35.317	30.788	0	0	Bus 4	-35.317	30.788	1576.4	-75.4	
* Bus 2	18.000	102.500	14.6	163.000	7.225	0	0	Bus 7	163.000	7.225	5105.7	99.9	
* Bus 3	13.800	102.500	11.3	85.000	-14.233	0	0	Bus 9	85.000	-14.233	3517.7	-98.6	
Bus 4	230.000	102.315	1.1	0	0	0	0	Bus 5	26.316	25.035	89.1	72.5	
								Bus 6	-61.634	4.583	151.6	-99.7	
								Bus 1	35.318	-29.619	113.1	-76.6	
Bus 5	230.000	99.230	0.0	0	0	123.912	49.556	Bus 4	-26.138	-41.398	123.9	53.4	
								Bus 7	-97.774	-8.158	248.2	99.7	
Bus 6	230.000	102.346	4.3	108.461	0.000	91.868	30.623	Bus 4	62.278	-17.646	158.8	-96.2	
								Bus 9	-45.685	-12.977	116.5	96.2	
Bus 7	230.000	102.532	9.1	0	0	0	0	Bus 5	100.897	-7.286	247.7	-99.7	
								Bus 8	62.087	-1.325	152.0	-100.0	
								Bus 2	-162.984	8.611	399.6	-99.9	
Bus 8	230.000	101.652	6.6	0	0	100.106	35.023	Bus 9	-38.334	-23.485	111.0	85.3	
								Bus 7	-61.772	-11.538	155.2	98.3	
Bus 9	230.000	103.423	8.7	0	0	0	0	Bus 6	46.474	-21.475	124.3	-90.8	
								Bus 8	38.522	3.099	93.8	99.7	
								Bus 3	-84.996	18.376	211.1	-97.7	

* Indicates a voltage regulated bus (voltage controlled or swing type machine connected to it)

# Indicates a bus with a load mismatch of more than 0.1 MVA

Figure 30.1: 108.46 MW supply from solar PV to BUS 6

LOAD FLOW REPORT

Bus		Voltage		Generation		Load		Load Flow					XFMR
ID	kV	% Mag.	Ang.	MW	Mvar	MW	Mvar	ID	MW	Mvar	Amp	%PF	%Tap
* Bus 1	16.500	104.000	0.0	-58.398	34.000	0	0	Bus 4	-58.398	34.000	2273.6	-86.4	
* Bus 2	18.000	102.500	15.8	163.000	7.747	0	0	Bus 7	163.000	7.747	5106.5	99.9	
* Bus 3	13.800	102.500	12.8	85.000	-14.544	0	0	Bus 9	85.000	-14.544	3519.8	-98.6	
Bus 4	230.000	102.171	1.8	0	0	0	0	Bus 5	23.061	25.299	84.1	67.4	
								Bus 6	-81.461	6.270	200.7	-99.7	
								Bus 1	58.400	-31.569	163.1	-88.0	
Bus 5	230.000	99.089	0.9	0	0	123.560	49.415	Bus 4	-22.896	-41.724	120.6	48.1	
								Bus 7	-100.664	-7.691	255.8	99.7	
* Bus 6	230.000	102.500	6.1	132.000	0.810	92.145	30.715	Bus 4	82.576	-16.784	206.4	-98.0	
								Bus 9	-42.721	-13.121	109.4	95.6	
Bus 7	230.000	102.501	10.2	0	0	0	0	Bus 5	103.984	-6.705	255.2	-99.8	
								Bus 8	59.001	-1.390	144.5	-100.0	
								Bus 2	-162.984	8.095	399.6	-99.9	
Bus 8	230.000	101.641	7.9	0	0	100.086	35.016	Bus 9	-41.370	-23.293	117.3	87.1	
								Bus 7	-58.716	-11.722	147.9	98.1	
Bus 9	230.000	103.441	10.1	0	0	0	0	Bus 6	43.411	-21.830	117.9	-89.3	
								Bus 8	41.585	3.137	101.2	99.7	
								Bus 3	-84.996	18.692	211.2	-97.7	

Figure 30.2: 132 MW supply from alternator to BUS 6

After that, harmonic load flow has been done and corresponding spectrums and waveforms has been observed. Minimum and maximum rating of solar PV and alternator has been integrated to each buses.
Following spectrums and waveforms has been attached for the reference of bus 8.

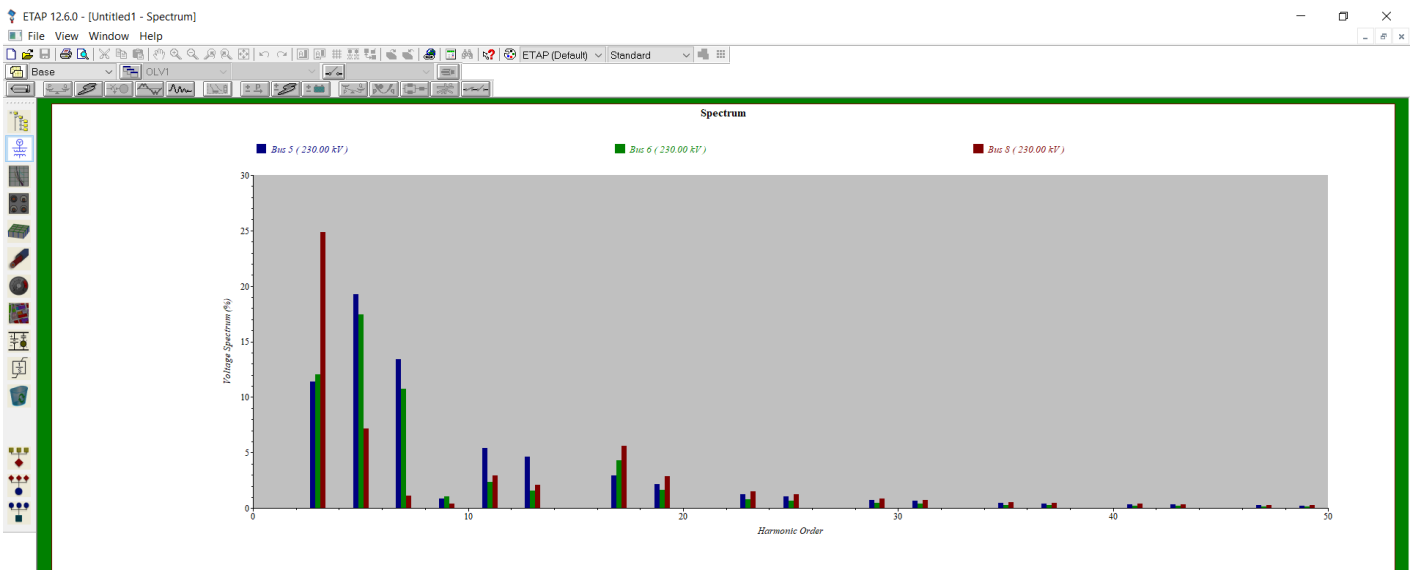

Figure 28.3: Voltage Spectrum for 33 MW PV integration at BUS 8

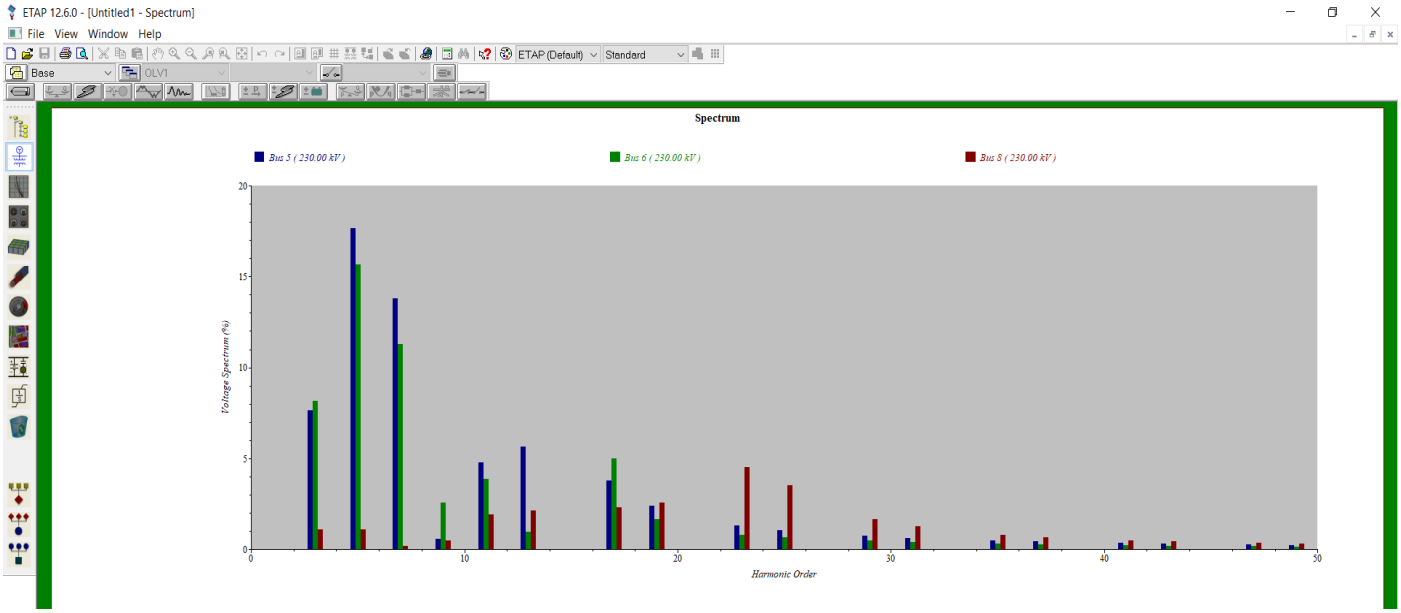

Figure 28.4: Voltage Spectrum for 33 MW alternator integration at BUS 8

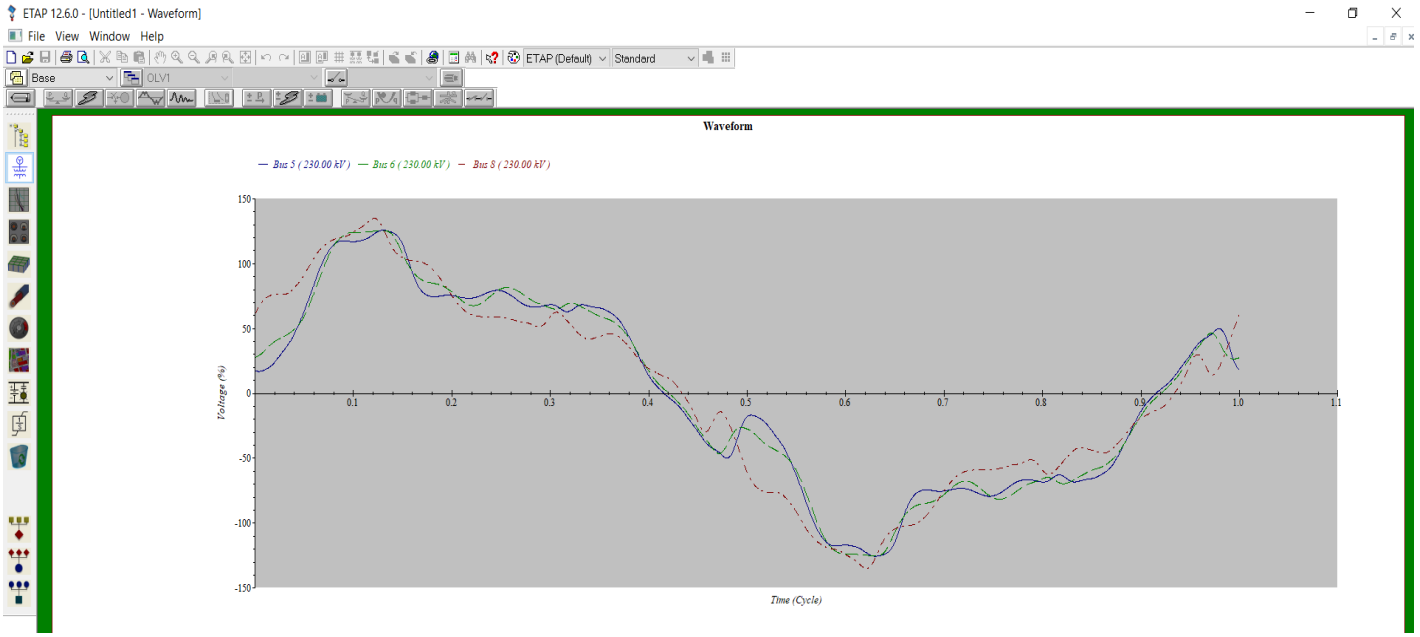

Figure 28.5: Harmonic waveforms for 33 MW solar PV integration at BUS 8

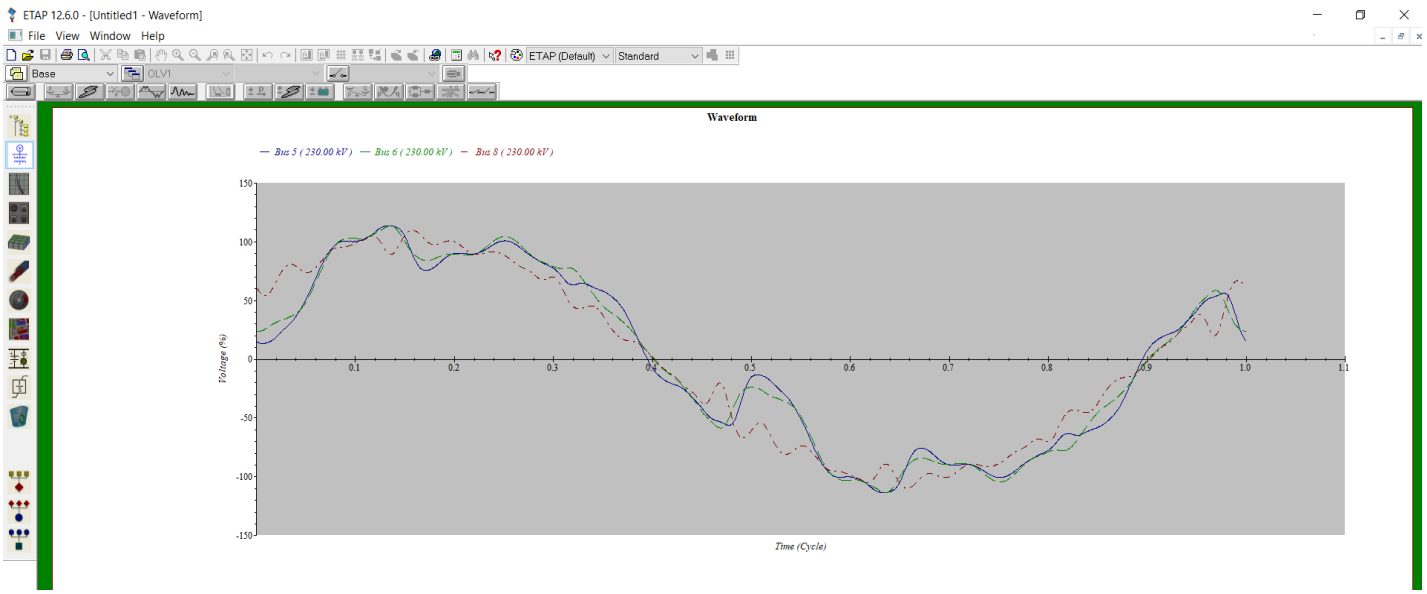

Figure 28.6: Harmonic waveforms for 33 MW alternator integration at BUS 8

Following spectrums and waveforms has been attached for the reference of bus 5.

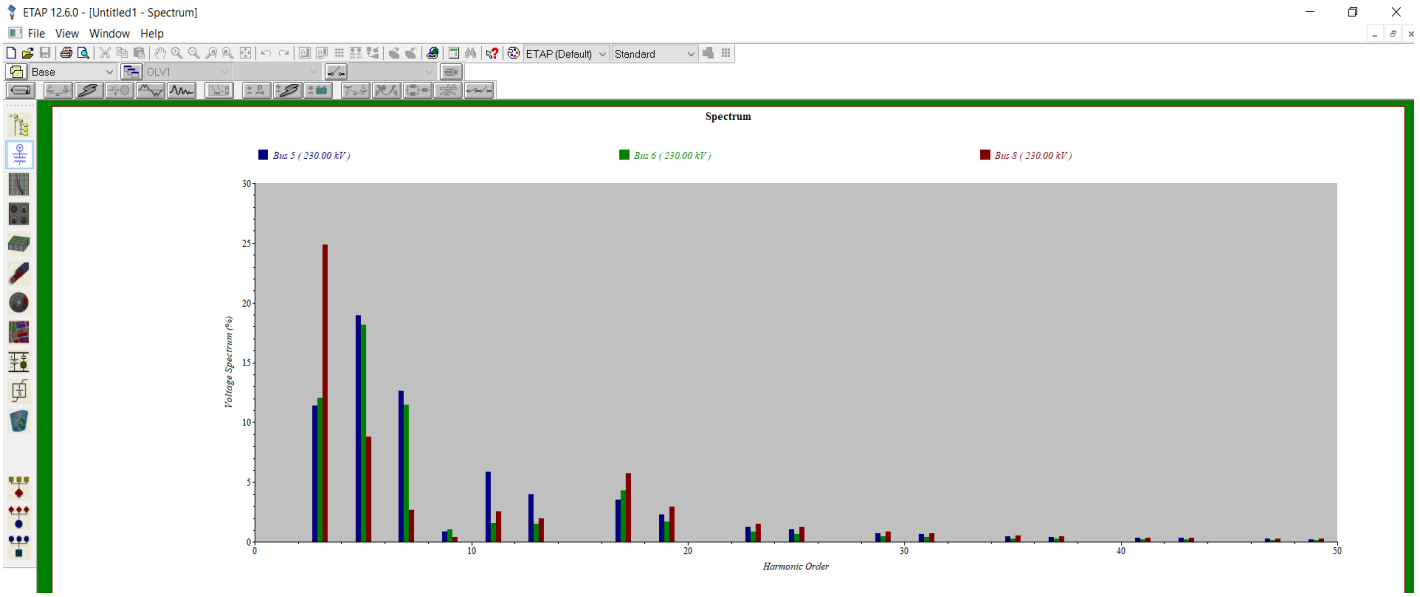

Figure 29.3: Voltage Spectrums for 33 MW solar PV integration at BUS 5

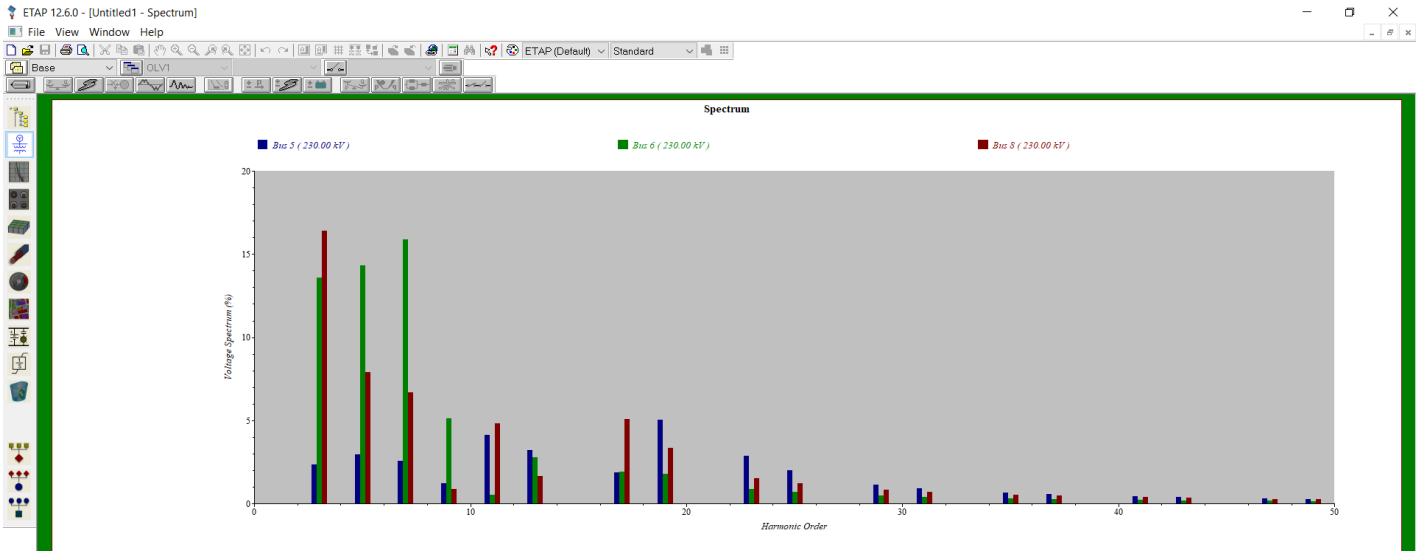

Figure 29.4: Voltage Spectrums for 33 MW alternator integration at BUS 5

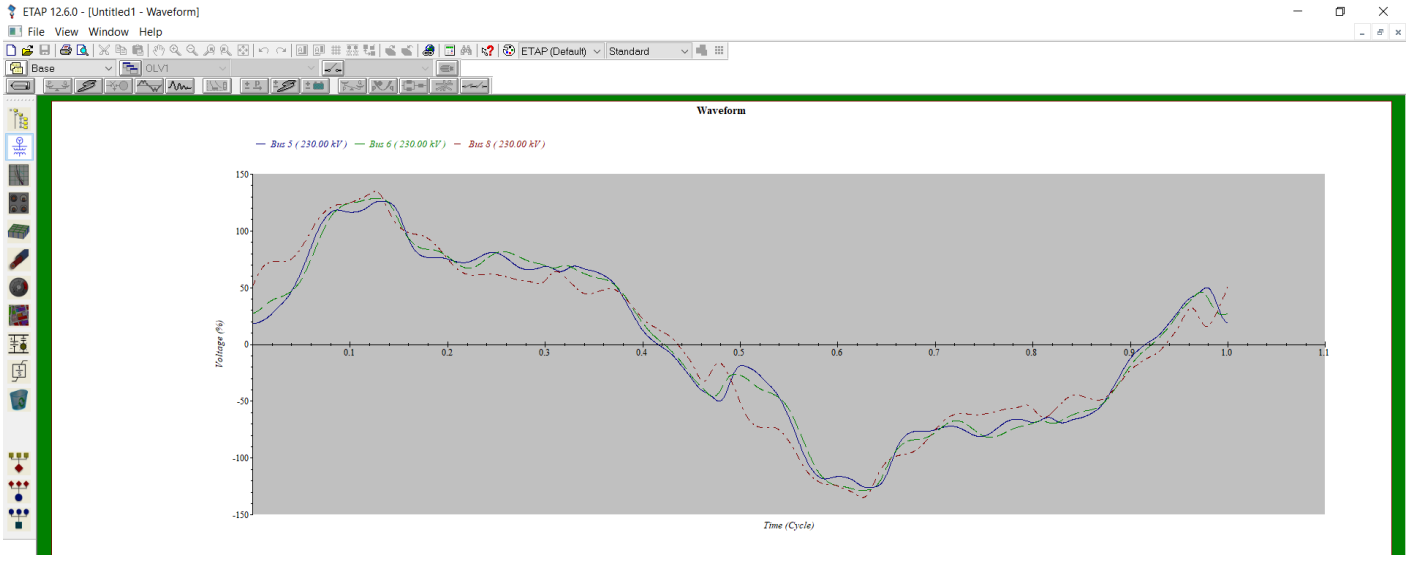

Figure 29.5: Harmonic waveforms for 33 MW solar PV integration at BUS 5

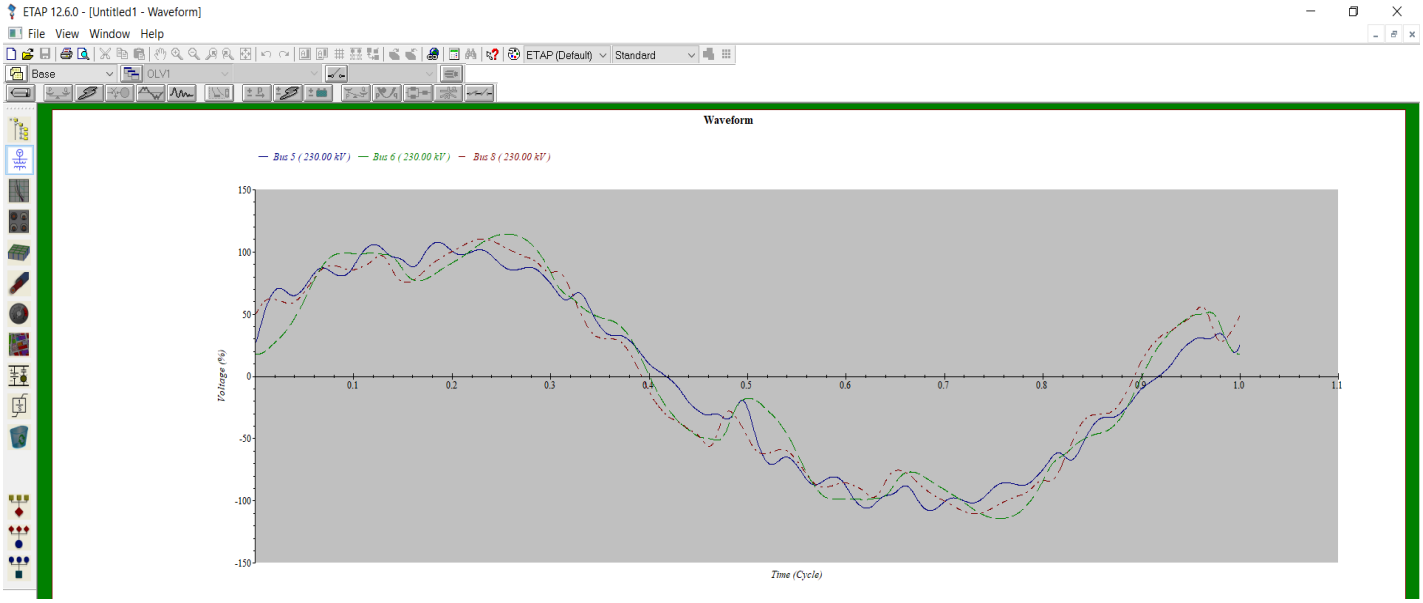

Figure 29.6: Harmonic waveforms for 33 MW alternator integration at BUS 5

Following spectrums and waveforms has been attached for the reference of bus 6.

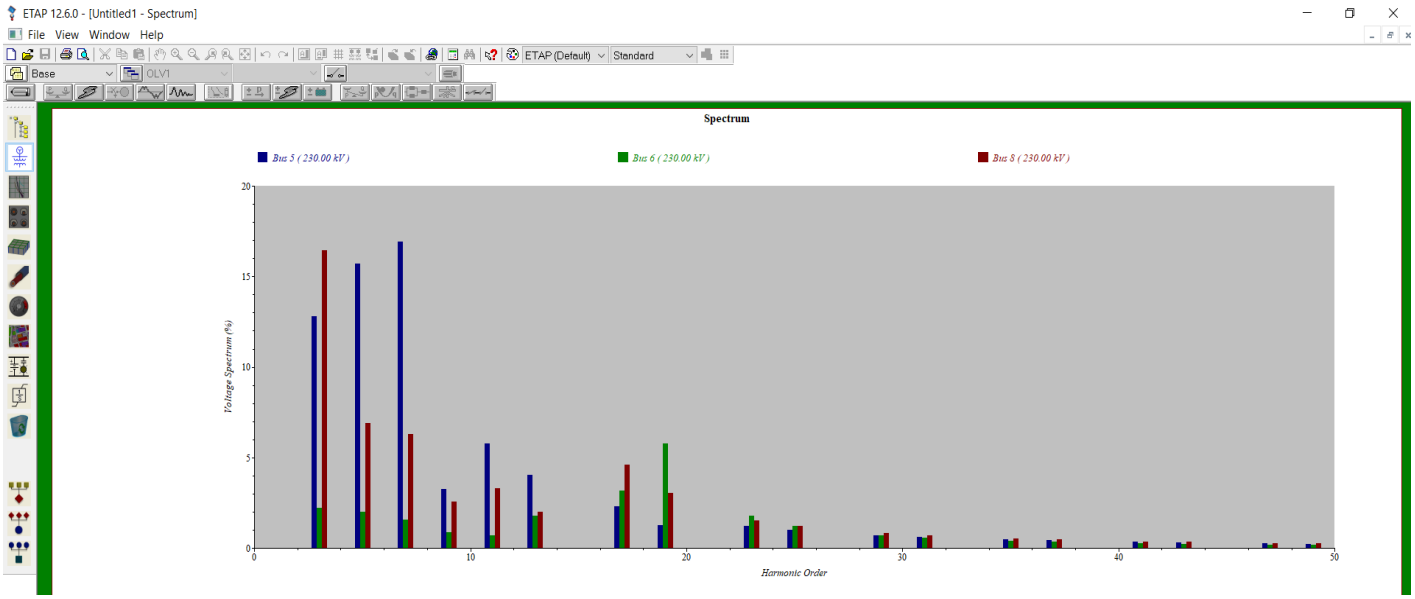

Figure 30.3: Voltage spectrum for 33 MW solar PV integration at BUS 6

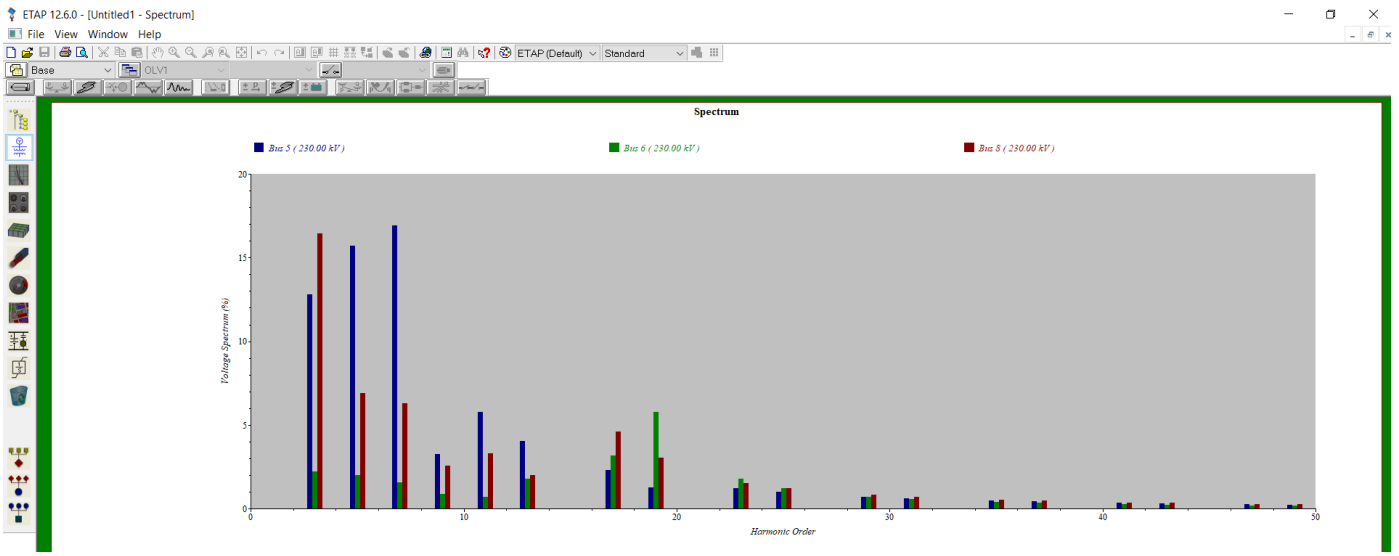

Figure 30.4: Voltage spectrum for 33 MW alternator integration at BUS 6

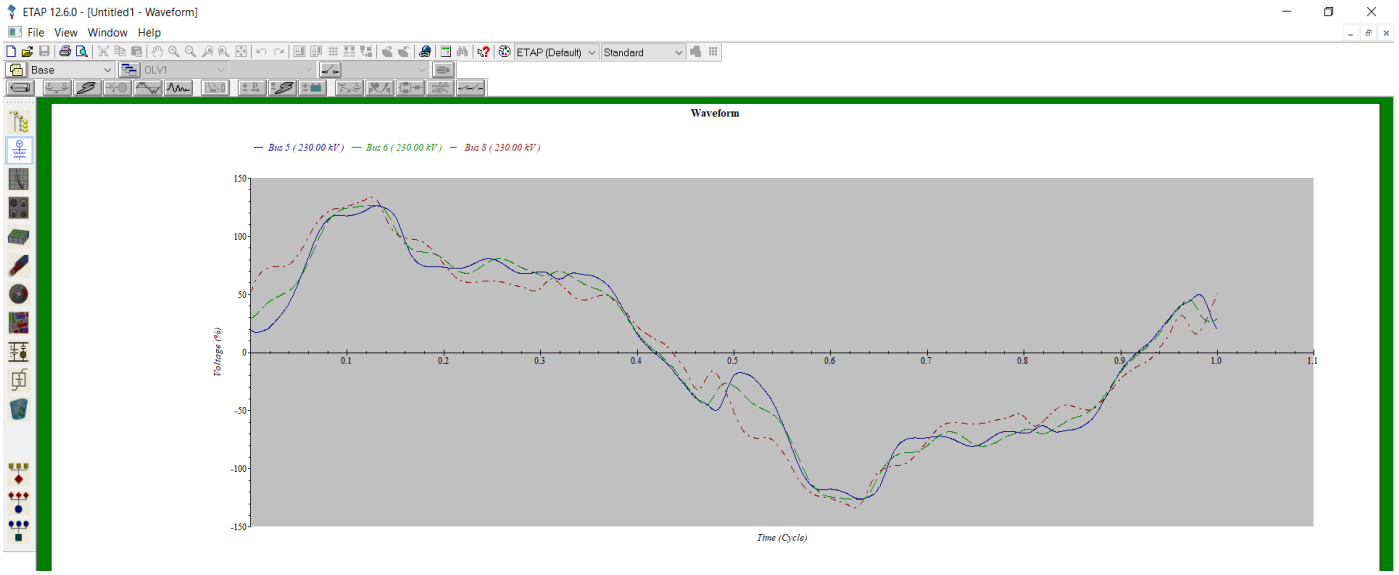

Figure 30.5: Harmonic waveforms for 33 MW solar PV integration at BUS 6

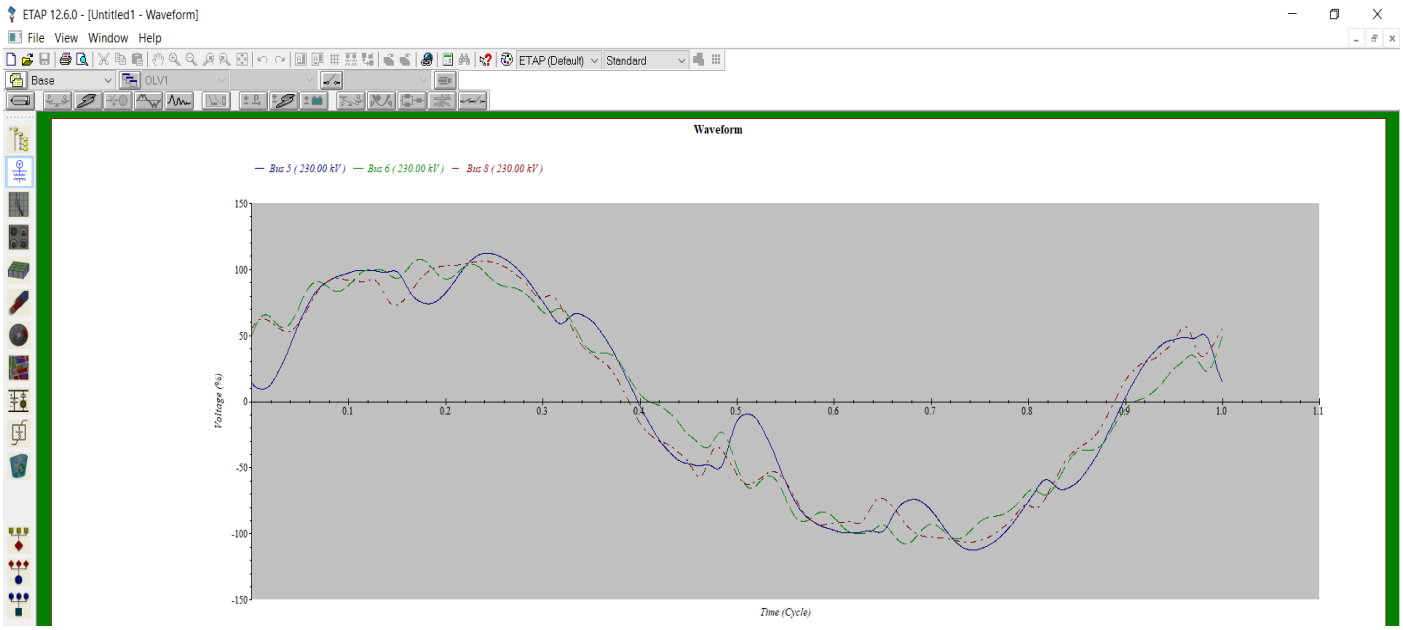

Figure 30.6: Harmonic waveforms for 33 MW alternator integration at BUS 6

6.3. DISCUSSION:

As it is discusses in the previous sections, table 5.1 ,5.2 and 5.3 describes the overloading effect by integrating solar PV and alternator and compares it with various power ratings for solar PV or alternator for bus 5, 6 and 8.

Figure 28.1 to 28.2 shows the reports for 217.5 MW supply from Solar PV integration and 132 MW supply from alternator integration which caused an overloading effect by integrating solar PV and alternator simultaneously at bus 8. Voltage spectrum magnitude with respect to fundamental voltage source and harmonic waveforms are also shown in the figure 28.3 to 28.6 by taking 33 MW for Solar PV and alternator both type of integration.

Figure 29.1 to 29.2 shows the reports for 108.5 MW supply from Solar PV integration and 132 MW supply from alternator integration which caused an overloading effect by integrating solar PV and alternator simultaneously at bus 5. Voltage spectrum magnitude with respect to fundamental voltage source and harmonic waveforms are also shown in the figure 29.3 to 29.6 by taking 33 MW for Solar PV and alternator both type of integration..

Figure 30.1 to 30.2 shows the reports for 108.46 MW supply from Solar PV integration and 132 MW supply from alternator integration which caused an overloading effect by integrating solar PV and alternator simultaneously at bus 6. Voltage spectrum magnitude with respect to fundamental voltage source and harmonic waveforms are also shown in the figure 30.3 to 30.6 by taking 33 MW for Solar PV and alternator both type of integration.

Other ratings can also be done by following the same process. Voltage spectrum is showing the magnitude of voltage for each harmonic orders represented in horizontal axis. Harmonic waveforms are showing that magnitude of voltage for each time cycle represented in horizontal axis.

6.4. CONCLUSION:

So, in this section all the reports related to this thesis work that includes load flow reports of the ratings which have done overloading effect on all the load buses that is bus 5, 6 and 8. It also includes voltage spectrums with respect to harmonic orders and harmonic waveforms with respect to time for each load buses.

These figures and reports in this chapter explain our analysis by various aspects and it can guide us for further improvement of our work. In the next section, summary of the current work and avenues of the future work will be discussed.

Chapter 7: CONCLUSION

7.1. SUMMARY OF THE WORK:

At first, a standard IEEE 9 BUS system is created by using standard ratings of 9 bus system. Here total static load is distributed in 3 buses that is bus 5, bus 6 and bus 8. Combined load is approximately 330 MW. Minimum PV rating has been taken as 10% of total load that is 33 MW. Now, rating from 33 MW to 496 MW has been used for PV system and alternators and each system has been integrated to each of the three load buses to observe the overloading effect of the system. After that, minimum and maximum rating PV systems and alternators has been taken and voltage spectrum with respect to harmonic orders and harmonic waveforms with respect to time has been analysed.

7.2. AVENUES OF THE FUTURE WORK:

As it has been discussed earlier, harmonic analysis has been done by integrating solar PV and alternator in each of the load buses. For further improvement of this work, it can be implemented in large systems that means 33 buses or 66 buses can be used instead of 9 bus system. Various types of other renewable energies like wind energy, biomass etc. can be integrated to this system by analysing performance and quality of the power to meet the load requirements based on their positions and capacity in the bus system.

7.3. CONCLUDING REMARKS:

Author has studied a number of research papers to get these ideas, and these ideas have helped him finish the research. In contrast to the distribution grid's high short-circuit levels, grid-connected house PV systems are generally small to medium in size. Thus, when just one PV system is linked to the grid, voltage distortion is not noticeable.
Hybrid system which is used here for the analysis purpose has many aspects of further work. In Many ways it can be upgraded for the advancement of its purpose.

REFERENCES:

[1] Nwaigwe, K.N., Mutabilwa, P. and Dintwa, E., 2019. An overview of solar power (PV systems) integration into electricity grids. *Materials Science for Energy Technologies*, *2*(3), pp.629-633.

[2] Allouhi, A., 2021. A novel grid-connected solar PV-thermal/wind integrated system for simultaneous electricity and heat generation in single family buildings. *Journal of Cleaner Production*, *320*, p.128518.

[3] Kumar, S.R., Gafaro, F., Daka, A. and Raturi, A., 2017. Modelling and analysis of grid integration for high shares of solar PV in small isolated systems–A case of Kiribati. *Renewable energy*, *108*, pp.589-597.

[4] Wang, F., Zhu, Y. and Yan, J., 2018. Performance of solar PV micro-grid systems: A comparison study. *Energy Procedia*, *145*, pp.570-575.

[5] Alanazi, M., Mahoor, M. and Khodaei, A., 2020. Co-optimization generation and transmission planning for maximizing large-scale solar PV integration. *International Journal of Electrical Power & Energy Systems*, *118*, p.105723.

[6] Sarkar, S., Bhaskar, M.S., Rao, K.U., Prema, V., Almakhles, D. and Subramaniam, U., 2022. Solar PV network installation standards and cost estimation guidelines for smart cities. *Alexandria Engineering Journal*, *61*(2), pp.1277-1287.

[7] Balcombe, P., Rigby, D. and Azapagic, A., 2015. Energy self-sufficiency, grid demand variability and consumer costs: Integrating solar PV, Stirling engine CHP and battery storage. *Applied Energy*, *155*, pp.393-408.

[8] Yang, D., Li, W., Yagli, G.M. and Srinivasan, D., 2021. Operational solar forecasting for grid integration: Standards, challenges, and outlook. *Solar Energy*, *224*, pp.930-937.

[9] Tu, Q., Mo, J., Betz, R., Cui, L., Fan, Y. and Liu, Y., 2020. Achieving grid parity of solar PV power in China-The role of Tradable Green Certificate. *Energy Policy*, *144*, p.111681.

[10] Hou, S., Yi, B.W. and Zhu, X., 2021. Potential economic value of integrating concentrating solar power into power grids. *Computers & Industrial Engineering*, *160*, p.107554.

[11] Komiyama, R. and Fujii, Y., 2019. Optimal integration assessment of solar PV in Japan's electric power grid. *Renewable Energy*, *139*, pp.1012-1028.

[12] Liao, J.T., Chuang, Y.S., Yang, H.T. and Tsai, M.S., 2018. BESS-sizing optimization for solar PV system integration in distribution grid. *IFAC-PapersOnLine*, *51*(28), pp.85-90.

[13] Behura, A.K., Kumar, A., Rajak, D.K., Pruncu, C.I. and Lamberti, L., 2021. Towards better performances for a novel rooftop solar PV system. *Solar Energy*, *216*, pp.518-529.

[14] Pan, Z., Wang, X., Guan, Q., Chen, Y. and Tian, L., 2021. Adaptive current harmonics suppression strategy for grid-tie inverters. *ISA transactions*.

[15] Zhang, Y., Roes, M.G.L., Hendrix, M.A.M. and Duarte, J.L., 2020. Symmetric-component decoupled control of grid-connected inverters for voltage unbalance correction and harmonic compensation. *International Journal of Electrical Power & Energy Systems*, *115*, p.105490.

[16] Rivas, A.E.L., da Silva, N. and Abrão, T., 2020. Adaptive current harmonic estimation under fault conditions for smart grid systems. *Electric Power Systems Research*, *183*, p.106276.

[17] EEEGUIDE, *Newton Raphson Method for Load Flow Analysis*. Available at (https://www.eeeguide.com/newton-raphson-method-for-load-flow-analysis/)

[18] Electronicsandyou, *PV cell working principle*. Available at (http://www.electronicsandyou.com/pv-cell-working-principle-how-solar-photovoltaic-cells-work.html)
[19] Electricalbaba, *Three phase full bridge inverter*. Available at (https://electricalbaba.com/three-phase-bridge-inverter/)
[20] Statista, *Energy Consumption by top 10 Energy consuming countries.* Available at (https://www.statista.com/statistics/268151/per-capita-energy-consumption-in-selected-countries/)